GEOPHYSICAL SITE INVESTIGATION AND GROUND RESPONSE ANALYSIS OF BANGKOK SUBSOIL DUE TO EARTHQUAKE
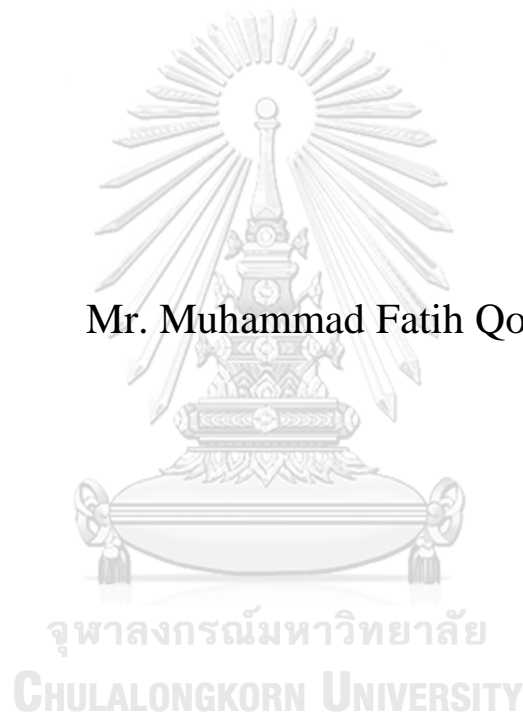
Mr. Muhammad Fatih Qodri

จุฬาลงกรณ์มหาวิทยาลัย
CHULALONGKORN UNIVERSITY

A Thesis Submitted in Partial Fulfillment of the Requirements
for the Degree of Master of Engineering in Civil Engineering
Department of Civil Engineering
Faculty of Engineering
Chulalongkorn University
Academic Year 2018
Copyright of Chulalongkorn University

การสำรวจทางธรณีฟิสิกส์และการวิเคราะห์ผลตอบสนองของชั้นดินกรุงเทพจากการกระทำของแผ่นดินไหว

นายมูฮัมหมัด ฟาตี โควดรี้

Thesis Title   GEOPHYSICAL SITE INVESTIGATION AND
GROUND RESPONSE ANALYSIS OF BANGKOK
SUBSOIL DUE TO EARTHQUAKE
By   Mr. Muhammad Fatih Qodri
Field of Study   Civil Engineering
Thesis Advisor   Professor SUCHED LIKITLERSUANG, Ph.D.

Accepted by the Faculty of Engineering, Chulalongkorn University in Partial
Fulfillment of the Requirement for the Master of Engineering

                                     Dean of the Faculty of Engineering
              (Professor SUPOT TEACHAVORASINSKUN, D.Eng.)

THESIS COMMITTEE

                                     Chairman
              (Associate Professor TIRAWAT BOONYATEE, D.Eng.)
                                     Thesis Advisor
              (Professor SUCHED LIKITLERSUANG, Ph.D.)
                                     Examiner
              (Dr. Veerayut Komolvillas)
                                     External Examiner
              (Dr. Susit Chaiprakaikeow)

จุฬาลงกรณ์มหาวิทยาลัย

CHULALONGKORN UNIVERSITY

มูฮัมหมัด ฟาตี โควดรี้ : การสำรวจทางธรณีฟิสิกส์และการวิเคราะห์ผลตอบสนองของชั้นดินกรุงเทพจากการกระทำของแผ่นดินไหว. (GEOPHYSICAL SITE INVESTIGATION AND GROUND RESPONSE ANALYSIS OF BANGKOK SUBSOIL DUE TO EARTHQUAKE) อ.ที่ปรึกษาหลัก : สุเชษฐ์ ลิขิตเลอสรวง

ความเสียหายต่ออาคารและสาธารณูปโภคอาจเกิดขึ้นจากแผ่นดินไหวทางไกล เนื่องจากการสั่นสะเทือนอาจขยายการเคลื่อนที่ของพื้นดินในระหว่างการแผ่ขยายคลื่น กรุงเทพมหานครตั้งอยู่ห่างจากจุดศูนย์กลางแผ่นดินไหวเป็นระยะทางหลายร้อยกิโลเมตร อย่างไรก็ตามบางคนในกรุงเทพฯอาจรู้สึกถึงการสั่นสะเทือนเมื่อเกิดแผ่นดินไหวได้ ซึ่งบ่งบอกว่าการสั่นไหวในช่วงคาบยาวอาจเกิดขึ้นในระหว่างเกิดแผ่นดินไหว ด้วยเหตุการณ์ในลักษณะนี้ การศึกษานี้จึงมีวัตถุประสงค์เพื่อแปลผลของแฟกเตอร์กำลังขยายและความเร่งเชิงสเปคตรัมของชั้นดินในพื้นที่กรุงเทพมหานครจากการเกิดแผ่นดินไหวระยะไกล ดำเนินการวัดการสั่นของคลื่นผิวดินจากการทดสอบในพื้นที่กรุงเทพมหานครสี่ตำแหน่ง เพื่อทราบข้อมูลความถี่ธรรมชาติของชั้นดินพร้อมทั้งตรวจสอบข้อมูลด้วยเจาะสำรวจดินและข้อมูลทางธรณีวิทยา วิธีอัตราส่วนสเปกตรัมแนวนอนต่อแนวตั้งถูกนำมาใช้เพื่อการประมาณค่าความหนาของชั้นดินและความเร็วคลื่นแบบเฉือน แบบจำลองลดทอนพลังงานคลื่นรุ่นใหม่ได้ถูกนำมาใช้เพื่อการจำลองคลื่นแผ่นดินไหว โดยจำลองการเกิดแผ่นดินไหวที่บริเวณรอยเลื่อนด่านเจดีย์สามองค์ ซึ่งเป็นรอยเลื่อนที่ยังมีการเคลื่อนตัวอยู่และอยู่ใกล้พื้นที่กรุงเทพมหานครมากที่สุด การจำลองการตอบสนองต่อคลื่นแผ่นดินไหวด้วยวิธีเชิงเส้นหนึ่งมิติได้ถูกนำมาใช้เพื่อสังเกตพฤติกรรมและคุณสมบัติการเคลื่อนที่ของพื้นดินในพื้นที่ศึกษาที่กำหนด โดยผลลัพธ์จากการศึกษาใช้สามารถอธิบายผลกระทบในพื้นที่จากแผ่นดินไหวในชั้นดินกรุงเทพมหานคร นอกจากนี้ในผลการศึกษานี้ได้ทำการเปรียบเทียบความเร่งเชิงสเปคตรัมที่ได้มากับมาตรฐานการออกแบบอาคารต้านทาน การสั่นสะเทือนของแผ่นดินไหว (มยพ. 1302) โดยหวังว่าผลการศึกษาจะสามารถสร้างความตระหนักในเรื่องแผ่นดินไหวสำหรับประชาชนในพื้นที่ได้

จุฬาลงกรณ์มหาวิทยาลัย

CHULALONGKORN UNIVERSITY

สาขาวิชา	วิศวกรรมโยธา	ลายมือชื่อนิสิต ....
ปีการศึกษา	2561	ลายมือชื่อ อ.ที่ปรึกษาหลัก ....

           Muhammad Fatih Qodri : GEOPHYSICAL SITE INVESTIGATION
           AND GROUND RESPONSE ANALYSIS OF BANGKOK SUBSOIL
           DUE TO EARTHQUAKE. Advisor: Prof. SUCHED LIKITLERSUANG,
           Ph.D.

          The potential damages on building and infrastructure could be affected by
long-distance earthquakes since the vibrations can appear ground motion
amplification during the wave propagation. Bangkok urban area is located a
hundred kilometers away from the potential area of the earthquake
epicenter. However, some people in Bangkok could feel the shaking during the
earthquake. It indicates that the long-period shaking could happen during the
earthquake. In line with this phenomenon, this study aims to interpret the
amplification effect and spectral acceleration in the local site of Bangkok due to
remoted earthquakes. The microtremor measurement was conducted at four
locations in Bangkok to obtain the information of the natural frequency of subsoil
and verified with boring log and geological data. The horizontal-to-vertical spectral
ratio (HVSR) method was applied to estimate ground thickness and shear wave
velocity. The next generation attenuation (NGA) models were implemented to
generate ground motion at Three Pagoda Fault as the closest active fault from
Bangkok. Equivalent linear one-dimensional seismic ground response analysis was
then performed to observe the soil behavior and ground motion parameters on the
investigated sites. The results could describe the site effect due to earthquake on
Bangkok subsoils. In addition, this research assesses spectral acceleration result
compared to spectral acceleration design for Bangkok from seismic resistant design
of buildings and structures of Thailand. In general, the results are also addressed to
make awareness of the earthquakes for the local people.

จุฬาลงกรณ์มหาวิทยาลัย
CHULALONGKORN UNIVERSITY

Field of Study:	Civil Engineering	Student's Signature	
		....	
Academic Year:	2018	Advisor's Signature	
		....	

ACKNOWLEDGEMENTS

TABLE OF CONTENTS

Page

LIST OF TABLES

จุฬาลงกรณ์มหาวิทยาลัย

CHULALONGKORN UNIVERSITY

LIST OF FIGURES

CHAPTER 1

INTRODUCTION

1.1. Background

Bangkok is a main city as business, tourism, education, and many vital activities of Thailand. The infrastructure of this city grows rapidly. Many constructions of skyscraper buildings are increased. In last couple decades, there are two big earthquakes in Thailand. The epicenter of that earthquake were located Tarlay, Myanmar and Mae Lao, North of Thailand (Mase et al., 2018). The Tarlay earthquake was happened in 2011 as shown in Figure 1.1. It had magnitude of M_w 6.8 that recorded by United Stated Geological Survey (USGS). The maximum peak ground acceleration of Tarlay earthquake is 0.207g (Observation station is at Mae Sai Station (MSAA)).
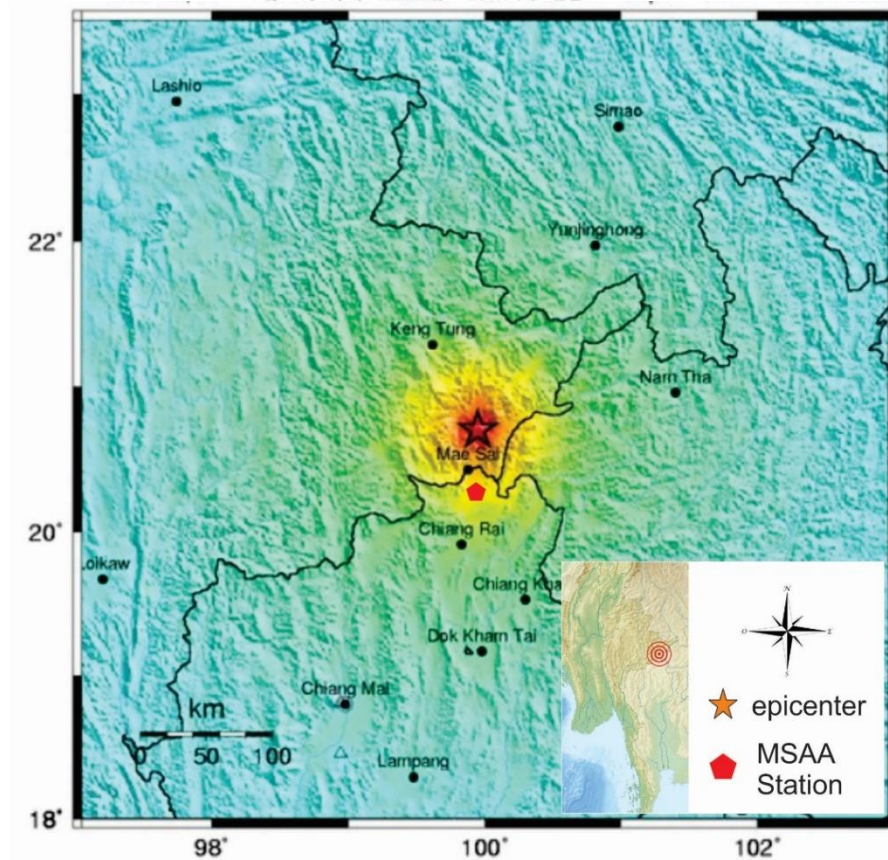
Figure 1.1. The epicenter of Tarlay earthquake in 2011 and Mae Sai Station (USGS, 2011; TMD, 2015)

The Mae Lao earthquake was happened in 2014. It had magnitude of 6.1 M_w that recorded by United Stated Geological Survey (USGS) as presented in Figure 1.2. The maximum peak ground acceleration of Tarlay earthquake is 0.3g (Observation station is at Mae Suai Dam Station).
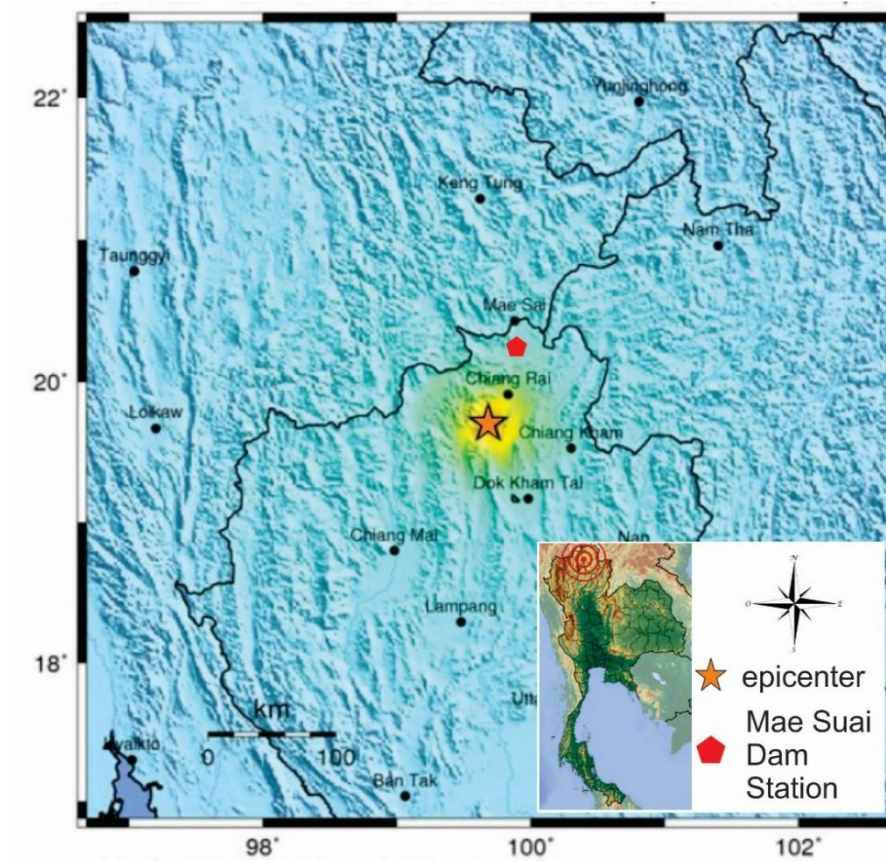
Figure 1.2. The epicenter of Mae Lao earthquake in 2014 and Mae Sai Station *(USGS, 2014; TMD, 2015)*

Tarlay and Mae Lao earthquakes occurred hundred kilometers away from the Bangkok, the capital city of Thailand. However, those vibration of earthquakes could reach the city. Basically, the Bangkok subsoil is predicted to amplify due to the long period earthquake. The anticipation of earthquake can be prepared using site response analysis. It is important to create disaster risk assessment and reduce the damage impact that may occur in the future. The most influential factors in earthquake disaster are geological conditions which include soil and rock profile and vibration intensity of the ground. An investigation is necessary to find out the site characteristics. Bangkok region is covered by soft clay layers, where the thickness is about 15 to 20 m. It may appear the amplification that induced by sediment (Poovarodom & Jirasakjamroonsri,

2016). Hopefully, the site response analysis can be used as a reference for the infrastructure development in Bangkok in the future. Earthquake that affected to Bangkok City is very essential to quantify the potential consequences such as structural damage.

Assessing site response from the earthquake, the motion magnitude and the intensity of the earthquake that may occur in the future must be defined first. Last couple decades, research about earthquake always be conducted since the victim and the impact of the earthquake increased. One of the highlight research about earthquake is seismic hazard analysis. This research is about the prediction of acceleration due to magnitude, distance, intensity, and soil properties. As mentioned before, Bangkok is relatively far from the earthquake source, so attenuation model is important to estimate the magnitude that will be happen in Bangkok compared to the real magnitude from the source. With this research, the actual motion can be defined to get the appropriate result of site response.

Thailand has several active faults (Palasri & Ruangrassamee, 2010). One of those faults is Three Pagodas Fault witch close to Bangkok city around 130 km away that may cause earthquake to occur in the future. Earthquake that affected to Bangkok City is calculated to quantify the potential consequences such as structure damage. Assessing site response from earthquake, the motion magnitude and the intensity of the earthquake that may occur in the future must be defined first.

The study to perform shear wave vertical propagation of the soil is one-dimensional site response analysis. This analysis is required to understand and measure wave propagation from the earthquake motion (Hashash et al., 2010). This analysis is also dealing with the ground propagation trough the soil layers. Furthermore, equivalent linear site response research has been demonstrated. Some researchers i.e. Poovarodom et al. (2013), Warnichai et al (2000), Ashford et al. (2000), etc. have done many studies about Bangkok subsoil related to seismic response. In the previous studies, the observations were conducted using the boring log and spectral analysis of surface wave (SASW) to get shear wave velocity and Bangkok subsoil strata.

In this research, the microtremor as one of the latest equipment is conducted to get the soil profile data. It is one of geophysical methods and always be considered to

estimate the ground motion accurately. This tool can calculate the motion that reflects mechanical properties of subsoil and also confirm the subsoil characteristic. The results from microtremor is presented as shear wave velocity (V_s) profiles and depth of bedrock (Poovarodom & Plalinyot, 2015).

This study develops site response during the earthquake in specific area of Bangkok using the soil data from geophysical microtremor observation due to earthquake triggered by Three Pagodas Fault, such as peak ground acceleration (PGA) and spectral acceleration (SA). The author is interested to conduct this research with title "Geophysical Site Investigation and Ground Response Analysis of Bangkok Subsoil Due to Earthquake".

1.2. Research Objectives

Based on the background described in Section 1.1, the several research objectives can be pointed in the following points below.

1. To investigate and examine the shear wave velocity in the local site of Bangkok using microtremor.
2. To analyze the site response in the specific area of Bangkok using one-dimensional equivalent linear model during the earthquakes triggered by Three Pagodas Fault.
3. To estimate the assessment between spectral acceleration result and spectral acceleration design for Bangkok from seismic resistant design of buildings and structures of Thailand (TDS, 2019)

1.3. Expected Outcomes

This research is expected to provide the benefits from the result. The expected outcomes are:

1. The application of the microtremor can be used as additional method to complete boring log to determine shear wave velocity in Thailand
2. The site investigation can be used as guide for the development of infrastructure related the earthquake prevention in Bangkok area.
3. The site response characteristic can be used as parameter for engineers to create proper measurement for designing earthquake resilient.

1.4. Research Scope

The scope of this study are listed in the following points below.

1. The microtremor is performed at four locations of the specific area of Bangkok.

2. This research is using the previous investigation, such as boring log as verification and validation.

3. Tarlay earthquake ground motions that obtained by Thai Meteorological Department and some ground motion from The Pacific Earthquake Engineering Research Center (PEER) database are used to seismic hazard analysis earthquakes triggered by Three Pagodas Fault (PEER, 2011).

4. Abrahamson et al (2014) of Next Generation Attenuation Model (NGA-West2) 2014 is used to determine peak ground acceleration of the earthquake.

5. Site response study is conducted by using one-dimensional equivalent linear (Hashash, 2015).

จุฬาลงกรณ์มหาวิทยาลัย
CHULALONGKORN UNIVERSITY

CHAPTER 2
LITERATURE REVIEW

2.1. Seismicity and Earthquake History in Thailand

Thailand is the country in South East Asia Region. Basically, the tectonic setting in Thailand are controlled by the Indo-Australian plate, Eurasian Plate and West Pacific Plate That plates are undergone collision. The oblique subduction of Myanmar, Andaman thrust and Sunda Arc that influence the movement of this zone actively. Every year, about 60-70 mm is happened the movement of Australia plates toward South East Asia (Ornthammarath & Warnitchai, 2016). Based on seismotectonic by Thai Meteorological Department (2015), Thailand have seismic activity distribution of earthquakes. The epicenters of those potential earthquakes are in neighboring countries as well as inside Thailand. Those potential earthquakes are indicated by some active fault that exist as presented in Figure. 2.1. (TMD, 2015).

In the last decade, there are two strong earthquakes around Thailand, which also threated the people in Bangkok City. Those two earthquakes are Tarlay earthquake that happened on 24 March 2011 and Mae Lao earthquake that happened on 5 May 2014. The Tarlay earthquake epicenter was located around 10 km to Tarlay city, Myanmar with magnitude of the earthquake is M_w 6.8 with shallow focal depth, while Mae Lao earthquake as the second biggest earthquake in the Thailand history, the energy of the earthquake is M_w 6.1. Many wounded victims, structural damage, and landslide due to the earthquake are reported. Thai Metrological Department (TMD) was reported the largest horizontal PGA of Tarlay Earthquake is 0.207g that recorded at Mae Sai station and Mae Lao Earthquake is 0.33 g that recorded at Mae Suai Dam (NSAC). The Nam Ma fault was predicted as the main source which was generating the Tarlay Earthquake (Ornthammarath, 2013). Whereas, Mae Lao fault that placed in the northern part of the Phayao active fault zone, is predicted became source that generated Mae Lao earthquake. However, the fault is no observable clearly in the surface.
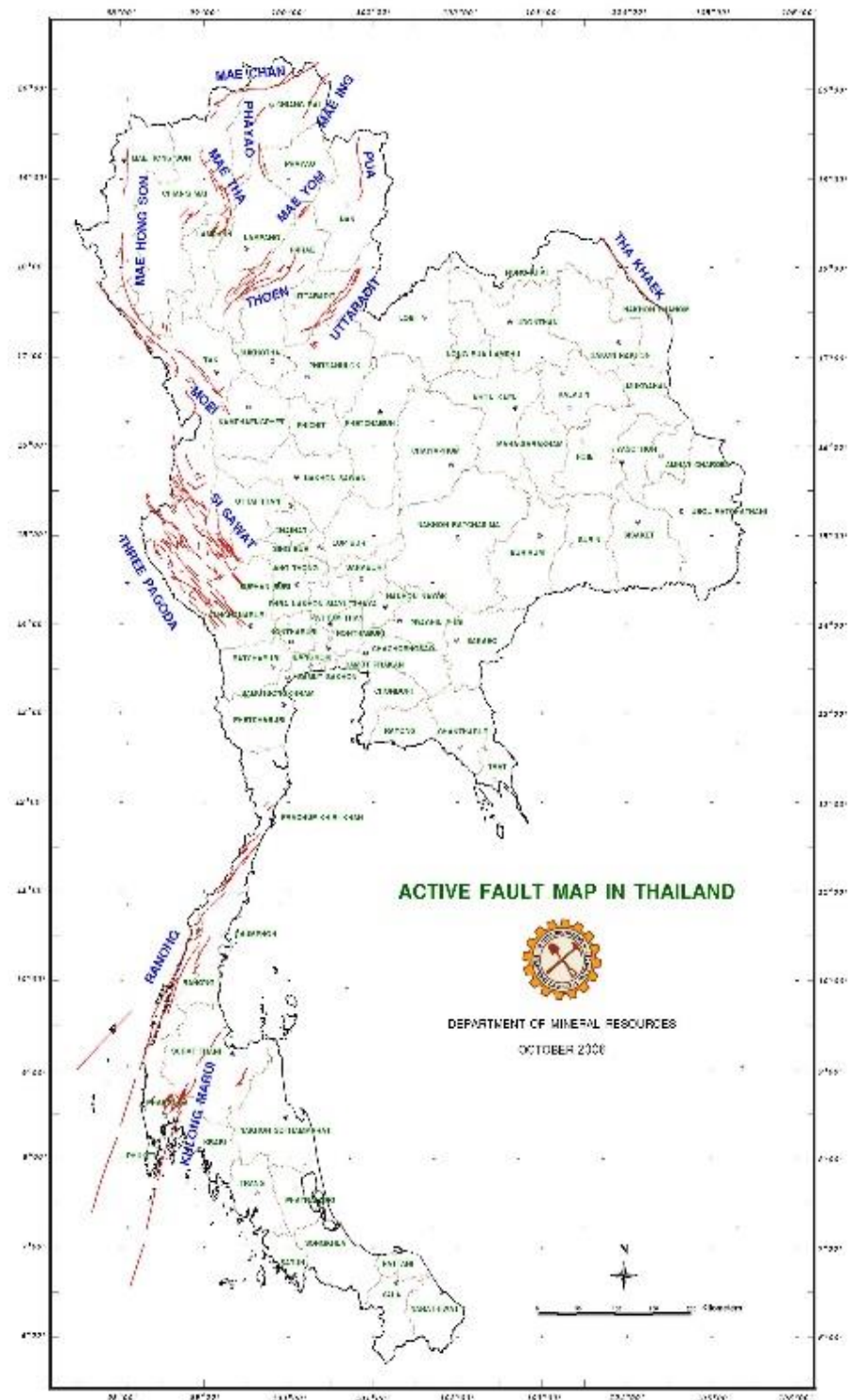
Figure 2.1. Active faults distribution map of Thailand (DMR, 2006)

Most of active faults that have an impact to the Bangkok city are in northern area and western area of Thailand. In the northern area, there are Mae Chan, Thoen and Phayao faults and in western area, there are Si Sawat and Three Pagodas faults. In

last few years, The Three Pagodas fault has been explored continuously (Palasri & Ruangrassamee, 2010). This strike slip fault type is the closest fault from Bangkok. According to the source to site distance, Three Pagodas Fault is more observed, especially related to the fault impact to Bangkok. The potential earthquake due to Three Pagodas fault is generated, and ground motion will be estimated.

2.2. Ground Motions Analysis

Identification of ground motion is necessary before determining site response analysis. In purpose to assess site response from earthquake shaking, the earthquake magnitude at the site and its intensity have do defined first. There are two equation models to identify the ground motion by using Deterministic Seismic Hazard Analysis (DSHA) or Probabilistic Seismic Hazard Analysis (PSHA). Both DSHA and PSHA are developed by considering the earthquake magnitudes by probability or rate of the exceedance at a site in variety ground motion intensity (Baker, 2013). PSHA is developed through the combination models from mathematic calculation from the location, magnitude of potential earthquake and prediction the intensity. Otherwise, DSHA is only considered to the one significant earthquake even which is maximum credible earthquake (MCE).

The ground motion parameters are obtained from the Ground Motion Prediction Equation (GMPEs). Those must be accurate and appropriate because it affects the result of peak ground acceleration (PGA) and spectral acceleration (SA). Warnitchai et al (2000) shows PGA and SA can be determined from earthquake magnitude, source to distance, and local site situation. Baker (2013) explains detailly about parameter that should be considered to compose seismic hazard.

1. Identification the earthquake source that have potential of ground motion.
2. Characterization the magnitude distribution that have potential to occur in the future.
3. Characterization the distribution of the distance from the source to site.
4. Prediction of distribution of ground motion intensity
5. Combination uncertainties of the earthquake magnitude, source situation and earthquake intensity by calculating the total probability theorem.

Basically, the seismic hazard analysis concern about the worse condition earthquake impact. For assessing that seismic hazard, parameters must be provided as following below.

1. Fault modelling

In this research, Three Pagodas Fault as strike-slip fault is taken as considered fault. This right-lateral fault is one of the known dynamic faults in the Western Thailand and the closest fault to Bangkok city.

2. Source-to-site distance

The distance among source must be defined because the type of the fault would affect the consideration of parameter. Area of the source, line source, and point source use the different parameter. There are several types of distance that was introduced by GMPEs that have different characteristic, i.e.

a. Rupture distance (R_{RUP}) as closest distance to co-seismic rupture (km)

b. Top of rupture distance (R_{TOR})

c. Joy Boore distance (R_{JB}) as closest distance to surface projection of co-seismic rupture (km)

d. Horizontal distance (R_X) as a horizontal distance from to if rupture measured perpendicular to fault strike

e. Horizontal distance off (R_{Y0}) as a horizontal off the end of the rupture measure parallel to strike (km)
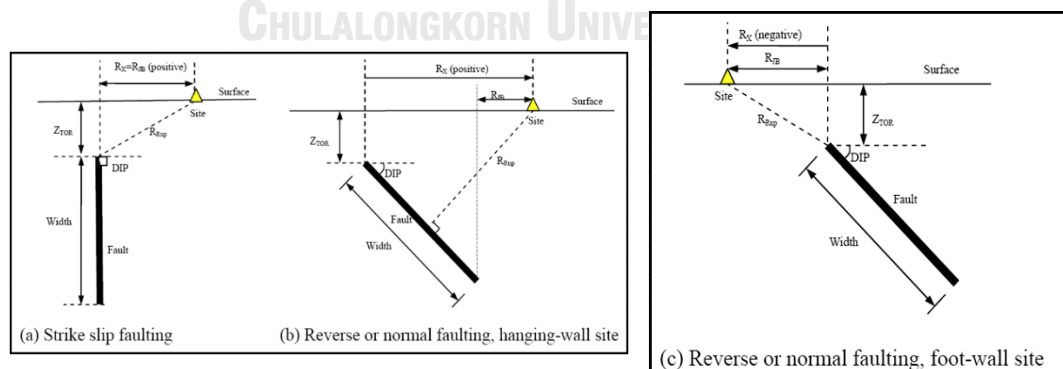
Figure 2.2. The different characteristic to define the source to site distance from NGA-West2 (2014).
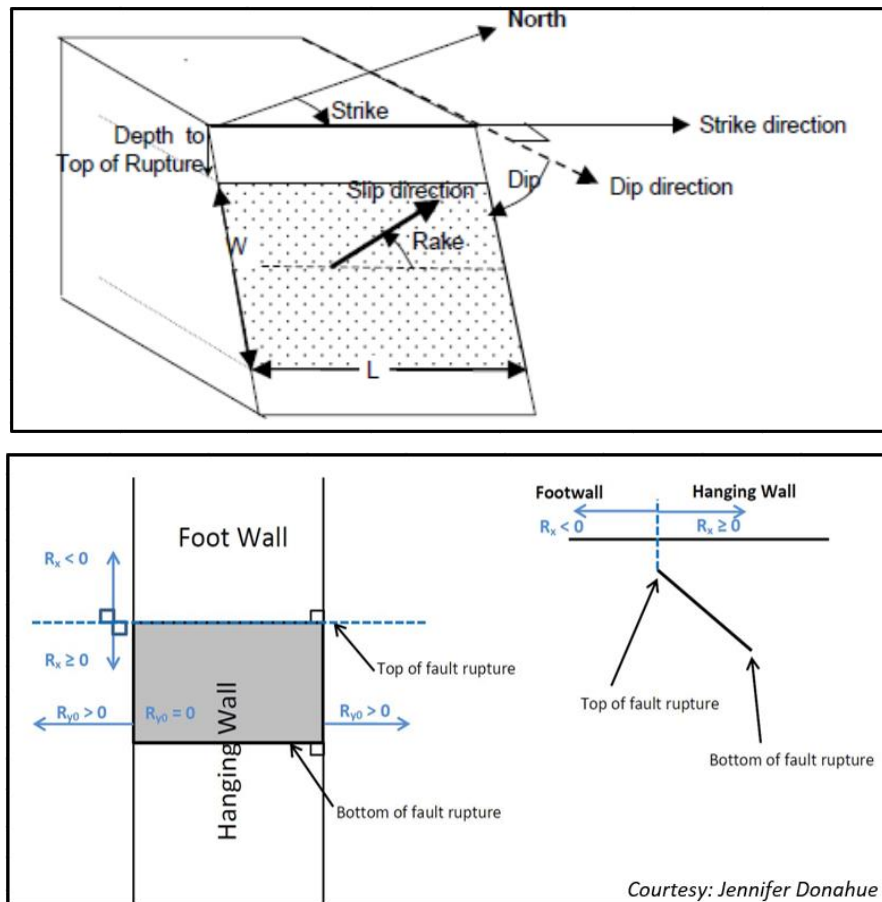
Figure 2.3. Faulting model and its mechanism NGA-West2 (2014).

3. Three Pagodas fault mean annual rate of exceedance

Mean annual rate of exceedance is calculated using Gutenberg-Richer law. It shown by the Equation 1 below

$$log\lambda_m = a - bm$$

Equation 1

Where λ_m is mean annual rate of exceedance, a is intercept between moment magnitude and log annual of earthquake, b is slope between moment magnitude and log annual, m is magnitude. The result of Three Pagodas fault mean annual rate of exceedance is shown in Table 2.1 below

Table 2.1. Zone of Three Pagodas Fault and seismicity factor in Thailand and its surrounding areas (adopted from Palasri & Ruangrassamee (2010))

Zone	Number of events	Parameter Guttenberg Richer Parameter		Maximum magnitude From Catalog	a-bm	Annual rate of exceedance
		a	b			
Zone Three Pagodas Fault	81	2.892	0.752	6.2 (7.5)	0.868	0.135518941

Palasri & Ruangrassamee (2010) have developed the seismic hazard map in Thailand especially in Kachanaburi Area where Three Pagodas Fault is located. This map considers the 2% and 10% probability of exceedance in 50 years One of the results of seismic hazard analysis is hazard curves that relates the rate of exceedance and peak horizontal acceleration every year. The seismic curve of Bangkok area is presented in Figure 2.4. This curve is important to acquire the contribution of source zones. For Bangkok seismic hazard, the most contributed earthquake is obviously in western Thailand (shown by the pink line and spot)
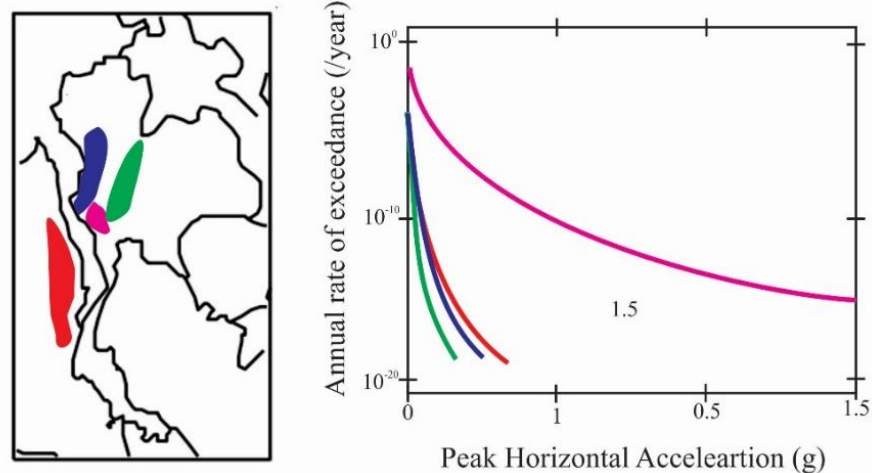
Figure 2.4. Seismic Hazard Curve at Bangkok Area (modified from Palasri & Ruangrassamee, 2010)

2.3. Attenuation Model

Considering the distance between the earthquake source and the sites, attenuation model is essential to estimate the ground motion acceleration. The attenuation model demonstrates about the relationship model between acceleration of the earthquake source and acceleration at the ground. For designing the motion, Next Generation Attenuation (NGA) was released as NGA-West1 in 2008 by Pacific Earthquake Engineering Research Center (PEER). In 2004, NGA-West2 is developed to update the NGA-West1. This NGA model is very important to design earthquake waves due to shallow earthquakes and applicable to all crustal earthquake for seismic hazard analysis. The NGA model is advance since it is built by seismological and geotechnical information as empirical data to acquire the models.

Recently, PEER leads designing of site motion by using the NGA-West2 2014 attenuation model. Several principal parameters were changed from NGA-West1 (Ancheta et al., 2014).

1. The number of sites increase with V_{S30} from measurement
2. 3D velocity models and shear wave velocity as basis to update and evaluate basin depth.
3. The estimation of V_{S30} is deepened by considering geology, geotechnical, geomorphology, and slope.
4. The estimation of V_{S30} method is updated by approaching the fit data for a given region.
5. The epistemic variability of mean V_{S30} is updated using appropriate measured V_S profiles.

There are several updated papers in 2014 that review about Ground Motion Prediction Equation (GMPEs) i.e.

1. Abrahamson et al. (ASK)
2. Boore et al. (BSSA)
3. Campbell and Bozorgnia (CB)
4. Chiou and Youngs (CY)
5. Idriss (IM)

ASK, BSSA, CB and CY models proposed peak ground acceleration (PGA) or pseudo-spectral acceleration (PSA) for equivalent linear site response parameter at

different site conditions. The parameters that were considered by each researcher are summarized in the Table 2.2. Every model of GMPEs is programmed by a s function of short distance and short period (Gregor et al., 2014).

The parameters of median ground motion from the NGA-West2 GMPEs have similar factor about 1.5–2.0 for 5–7 of magnitude and between 10–100 km of distances. Otherwise, median ground motion is increasing for large-magnitude (M > 8) earthquakes at long distances (R > 100–200 km) and short distances (R <10 km).

In this research, the model of Abrahamson et al. (2014) is used to estimate surface acceleration. The parameter from ASK is relevant to magnitudes 3.0–8.5, distances 0–300 km, and spectral periods of 0–10 s (Abrahamson et al., 2014). Considering the site condition, the V_{S30} in Bangkok city is very low and not applicable to this model basically. But NGA-West2 spreadsheet_5.7 has given the average that can be applicable to all site condition from PEER database (Gregor et al., 2014).

Table 2.2. Parameter Summary of five GMPEs models

Parameter	ASK	BSSA	CB	CY	IM
Moment magnitude	M	M	M	M	M
Depth to top of rupture (km)	Z_{TOR}, Z_{TOR}^b	-	Z_{TOR}	Z_{TOR}, Z_{TOR}^b	-
Hypocentral depth (km)	-	-	Z_{HYP}	-	-
Style of faulting	SS, RV, NM	SS, RV, NM, U	SS, RV, NM	SS, RV, NM	SS, RV
Class 2 event flag	F_{AS}	-	-	-	-
Dip (degrees)	δ^b	-	δ, δ^b	δ, δ^b	-
Down-dip rupture width (km)	W^b		W^b		
Closest distance to rupture plane (km)	R_{RUP}	-	R_{RUP}	R_{RUP}	R_{RUP}
Horizontal distance to surface project of rupture plane (km)	R_{JB}	R_{JB}	R_{JB}	R_{JB}	-
Horizontal distance to top edge of rupture plane measured perpendicular to strike (km)	R_X^b	-	R_X^b	R_X^b	-
Horizontal distance off the end of rupture plane measured parallel to strike (km)	R_{Y0}	-	-	-	-
Average shear-wave velocity in top 30 m (m/s)	V_{S30}	V_{S30}	V_{S30}	V_{S30}	V_{S30}
Depth to 1.0 km/s boundary (km)	$Z_{1.0}$	$\delta Z_{1.0}$	-	$Z_{1.0}$, $\Delta Z_{1.0}$	-
Depth to 2.5 km/s boundary (km)	-	-	$Z_{2.5}$	-	-
Rock motion PGA for nonlinear site response	-	PGAr	A_{1100}	-	-
Rock motion PSA for nonlinear site response	PSA_{1100}	-	-	$Y_{ref}(T)$	-
V_{S30} of rock motion used for nonlinear site response (m/s)	1,100	760	1,100	1,130	-
Regional adjustments	Taiwan, China, Japan	China/ Turkey, Italy/ Japan	China, Italy/ Japan	Italy/ Japan, Wenchuan	-

b is used for hanging-wall model, SS is strike-slip fault, RV is reverse fault, NM is normal fault, U is indefinite fault. According to site response analysis, shear wave velocity (V_{s30}) is used are the essential parameter in all five models. According to the V_{s30}, all models describe clearly the function of V_{s30} and the amplification result from all models is relatively similar. Figure 2.5 shows the prediction of five GMPEs regarding the ground motion, magnitude and the increasing distance. For $V_{s30} = 270$ m∕s with T = 1.0 s PSA got the relatively similar plotting.
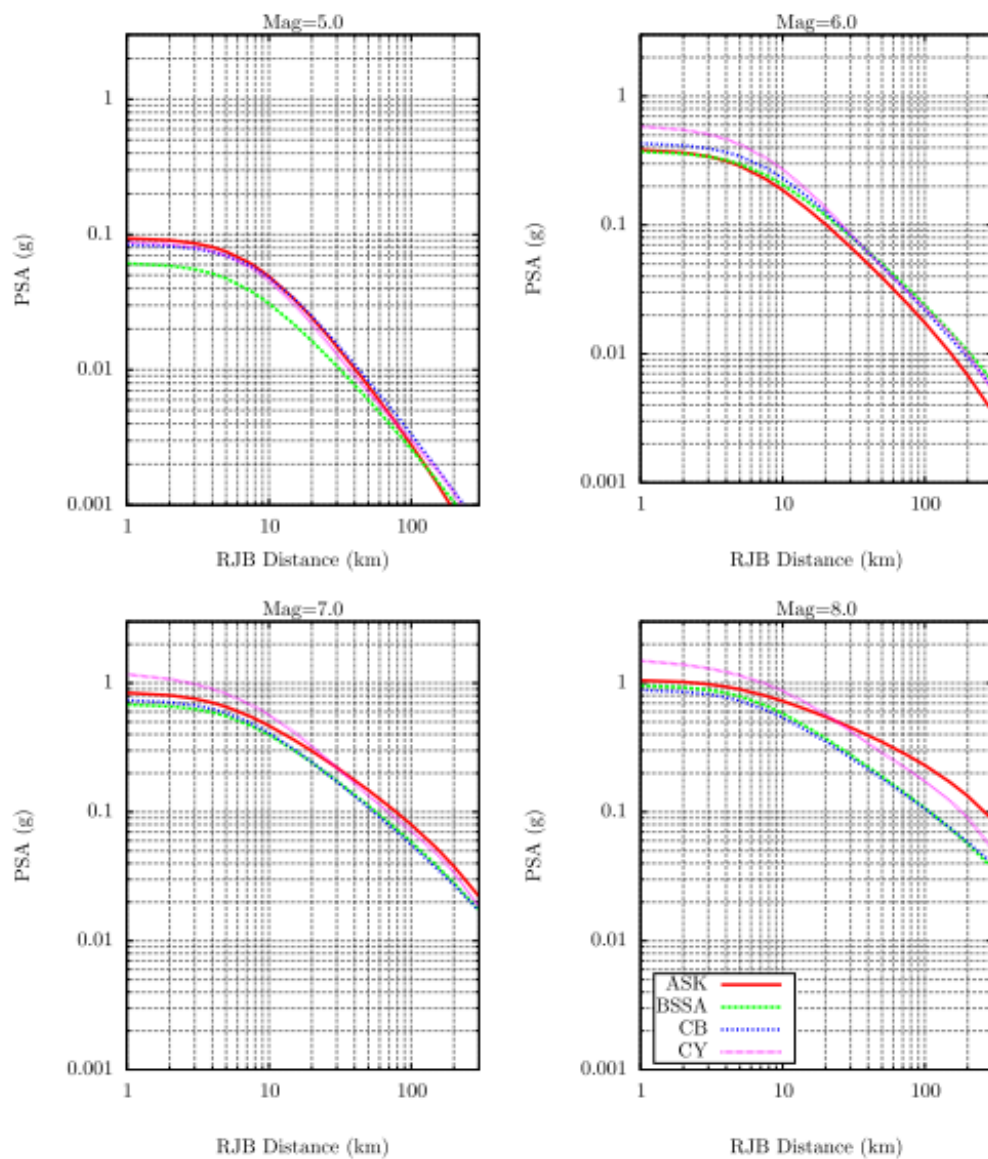
Figure 2.5. Pseudo spectral acceleration versus distance of strike-slip earthquakes from the five GMPEs for VS30 =270 m∕s (Gregor et al., 2014)

2.4. Bangkok Area and Geological Characteristic

Bangkok is composed by thick alluvial and deltaic sediments on large plain. The Bangkok subsoil consist of quaternary deposits and belongs the Lower Central Plain or Chao Phraya Plain basin (Shibuya et al., 2003). In general, geological of Lower Central Plain consist the basement rocks, pre-quaternary deposits and quaternary deposit that were deposited and built up the structural basin. This basin is formed by block faulting that developed horsts and grabens in Chao Phraya basement in Late Pliocene–Pleistocene. Basically, the Pleistocene delta is questionable, and the judgment was based on the Holocene depositional environment (Sinsakul, 2000).

The pre-quaternary geology in the Lower Central Plain consist of basement and Tertiary rock. Above this part is the unconsolidated sediment from the Quaternary period. The basement topography varies about 500 to 2000 below the ground surface. The rock making up the basement is igneous, sedimentary and metamorphic rocks from Paleozoic to Mesozoic period

Above basement of the pre-quaternary geology Lower Central Plain, there are thick of unconsolidated sediment from the quaternary deposits. But the subsurface information below 300 m depth is very lack and usually ignored. The depositional environment of these sediments was deposited alluvial, fluvial and deltaic environment about 2000 m of Pleistocene and Holocene. Considering the quaternary deposits, all information data about these deposits was collected from the drill log and electric log and the unconsolidated sediments are classified based on the material properties into 8 aquifers on upper 600 m of Pleistocene and Holocene as follows in Table 2.3. The geological profile of Bangkok is presented at Figure 2.6 by Shibuya et al. (2003).

Table 2.3. Aquifers of Quaternary Deposits of the Lower Central Plain (Adopted from Sinsakul, 2000)

Aquifers Name	Top Depth Range	Thickness	Lithology	Depositional Environment
Upper Bangkok	1-30	30	Soft clay (marine clay), clayey to fine sand, and fine to coarse sand with gravel	River channel point bar and flood plain
Lower Bangkok	30-50	60-80	Fine to coarse sand with gravel and clay layers	River channel point bar and flood plain
Phrapradang	60–80	20	Coarse sand and gravel with clay lenses	Fluvial
Nakorn Luang	100 to 140	50–70	Sand and gravel with clay layers	Terrace and floodplain
Nonthaburi	170–200	30–70	Sand and gravel	Distributary fluvial complex
Samkhok	240–250	40 - 80	Medium to coarse sand and gravel, clay lenses intercalated	Fluvio-deltaic
Phayathai	276–300	40–60	Medium to very coarse sand and gravel, clay layers intercalated	?
Thonburi	350–400	50–100	Coase sand and gravel interbedded with sandy and clay layers	?
Pak Nam	420–500	30	Sand and gravel with clay lenses, compact clay layers and carbonaceous matter.	?

The Bangkok elevation is about 4 to 5 m above the sea level. Bangkok soil or Bangkok soft clay belongs to Bangkok aquifer that has about 15 to 20 m thick as the result of sedimentation of Chaophraya River (Poovarodom & Plalinyot, 2015). Generally, in the top of Bangkok subsoil is very soft clay, and then following by stiff to hard clays and dense sands until reaching to bedrock. The deposition of the Chaophraya basin is lower deltaic area so marine can be found in the uppermost of clay layer. The deposits extend from 200 to 250 km in the East-West Direction and

200 to 300 km in the North-South direction. The Bangkok subsoil is recapped in Table 2.4 below
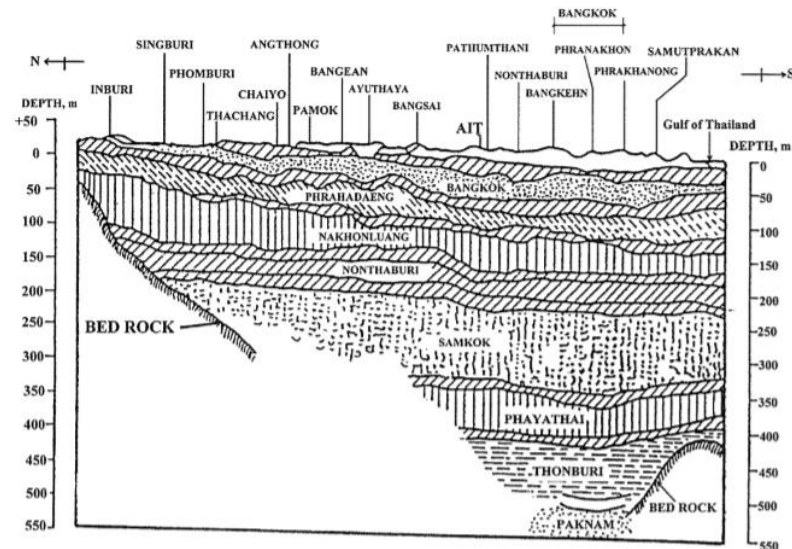
*Figure 2.6. G*eological stratigraphy of Chaopraya Basin *(Shibuya et al., 2003)*

Table 2.4. Bangkok subsoil characteristics (Shibuya et al., 2003)

Depth	Lithology	Characteristics
0-14	Bangkok soft clay	Dark grey highly compressible soft clay with 2 m weathered zone forming a hard crust
14-25	Stiff Clay	Light grey and brown fissured stiff clay
25-40	Sand Layer	Dense alluvial non-uniform sand, occasionally interbedded with stiff clay. Classified in parts as clayey sand
40-44	Stiff Clay	Light grey and brown, stiff often fissured silty clay
44->70	Sand Layer	Clean light grey silty sand

Horpibulsuk et al. (2007) explains detailed of soil type of Bangkok with the physical and engineering properties. Table 2.5 presents the soil type with their characteristics (soft clay until hard clay), thickness, liquid limit (LL) plastic limit (PL) and also presents natural water content (W_n), specific gravity (G_s) and undrained shear strength (S_u). The influence of plasticity index (PI) on cyclic loading is

changing in G/G_{max} and damping ratio of soil. Damping ratio is reduced (Vucetic & Dobry, 1991).

The basic result of laboratory testing is G with γ for Bangkok soils. For normalized relationship of G and γ as a function of plasticity index, Vucetic and Dobry (1991) model is used for clay and Seed and Idriss (1971) model is used for sand. Those models are used to estimate shear modulus and damping variation with shear strain of soil for purposes of site response analysis

Table 2.5. Soil Type and Engineering Properties of Bangkok Soil Class (Horpibulsuk et al., 2007)

Soil type	Thickness (m)	W_n (%)	LL (%)	PL (%)	S_u (kPa)	G_s	PI
Soft clay	10±3	71±15	74±14	27±4	16±2	2.64±2	47
Medium stiff clay	4±1	55±9	70±10	26±4	32±8	2.64±3	44
Stiff to very stiff clay	5±3	28±5	50±13	22±5	117±25	2.65±2	28
First sand layer	5±4	21±6	—	—	—	Na	
Very stiff clay	16±4	21±3	48±14	21±4	270±52	Na	27
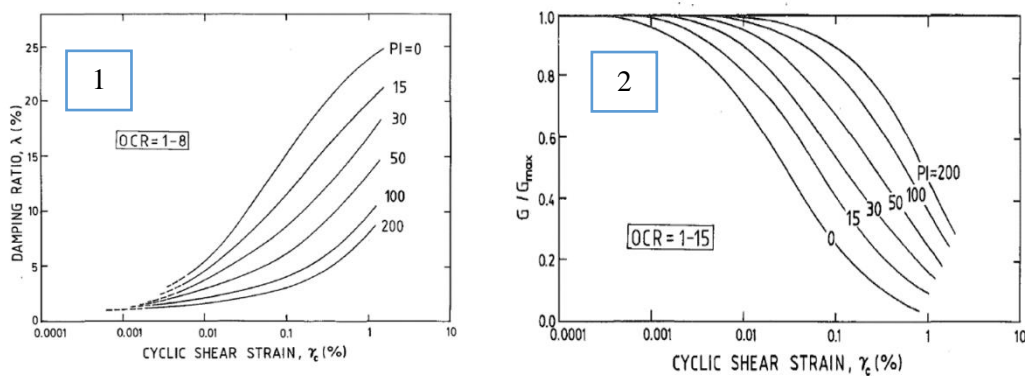
Figure 2.7. (1) Relations damping ratio and cyclic shear strain (2) Relations between G/G_{max} and cyclic shear strain for Normally consolidated soil and Overconsolidated Soils (Vucetic and Dobry, 1991)

2.4.1. Shear Wave Velocity in Bangkok

The shear wave velocity (V_s) in Bangkok have been investigated by several researchers. The velocity increases as deeper layer. Warnitchai et al (2000) has summarized the Bangkok subsoil and shear wave velocity from Ashford et al (1996) and Shibuya (1998) (Figure 2.8). At the first, the shear wave velocity was estimated from specific field and laboratory works, and then they were validated with the V_s measurement by using down-hole method. The general result of shear wave velocity in Bangkok is extremely low (60 to 100 m/s) (Likitlersuang & Kyaw, 2010).

Shear wave velocity in Bangkok is linearly correlated to the depth from the ground surface until reaching the bedrock. Bangkok's bedrock is very deep from the surface. Based on the microtremor observation by Poovarodom & Jirasakjamroonsri (2014), the bedrock was assumed up to 800 meters depth with shear wave velocity value is 2000 m/s. It is shown at Figure 2.9.
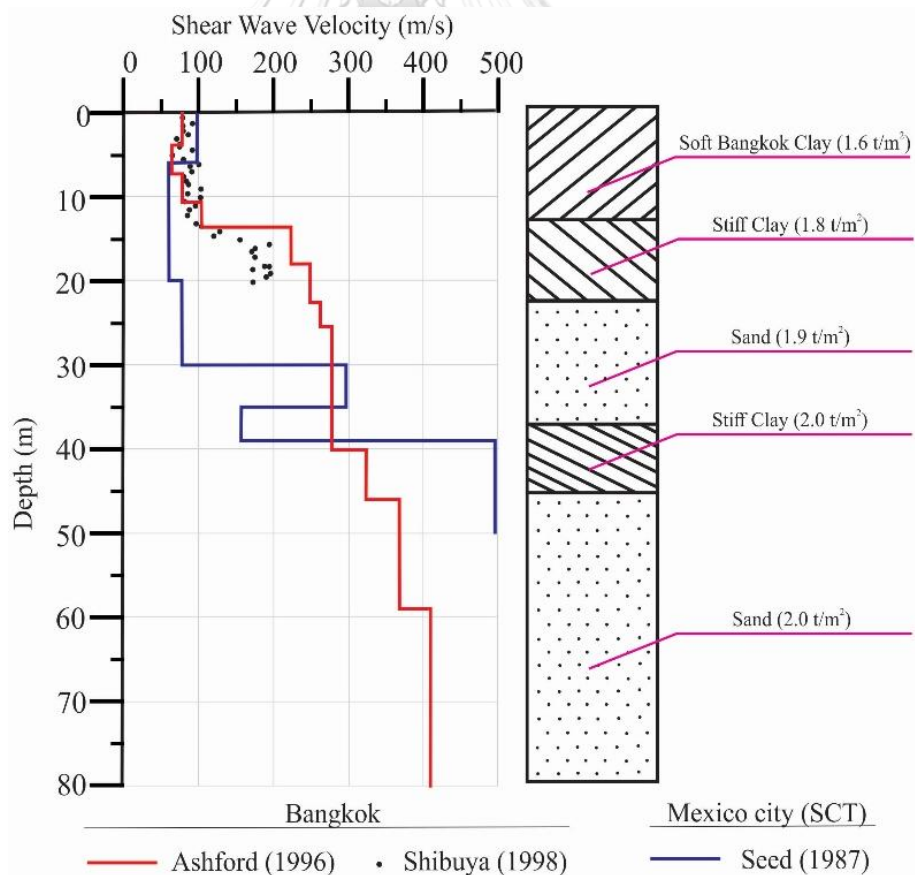
Figure 2.8. Bangkok soil and shear wave velocity (Warnitchai et al., 2000)

Poovarodom & Jirasakjamroonsri, (2014) present the data with two different zones (A and B). The data were separated considering to similarity of spectral acceleration.The bedrock ranges of zone A is from 718 to 791 m and bedrock ranges of zone B is from 410 to 679 .

Considering the result of V_{S30}, The V_S observation at zone B are lower than average V_S from surface until 300 m depth. Beneath of 300 m the, the value of V_{s500} in zone A and zone B are relatively same with the less of V_s influence from the upper deposits.
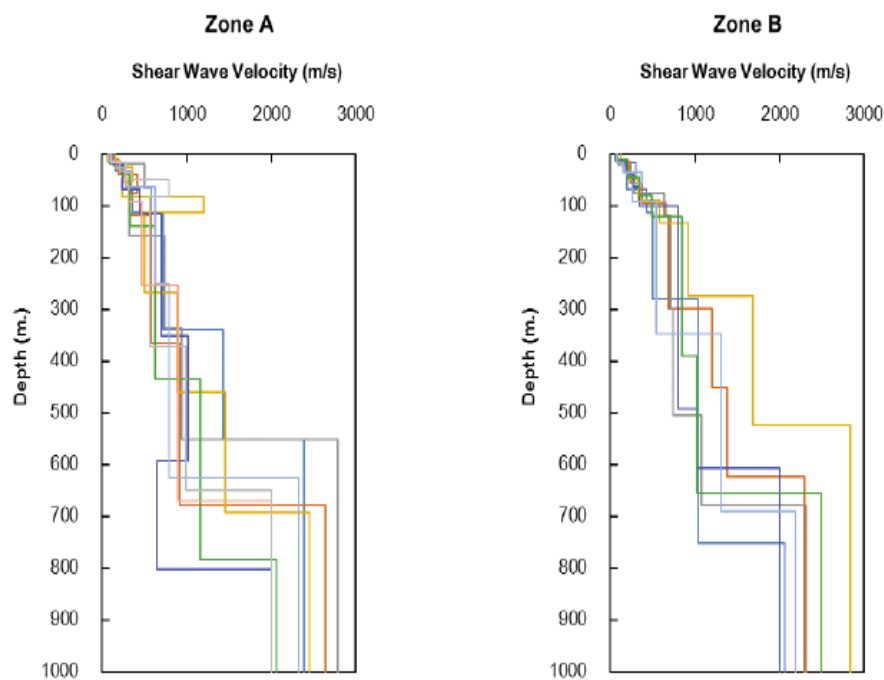
Figure 2.9. Shear wave velocity from array microtremor technics (Poovarodom &
Jirasakjamroonsri, 2014)

Several tests are required to compute shear wave velocity like cross-hole and down-hole seismic, standard penetration (SPT), spectral analysis of surface waves test (SASW) and microtremor test. If the soil is drained, the shear wave velocity in Bangkok city can be calculated by using Equation 2. This equation is derived from down-hole seismic test and multichannel analysis of surface wave (MASW) model with non-drainage shear strength (Imai, 1982). If the soil is undrained, shear wave velocity can be calculated by using Equation 3 and Equation 4 respectively (Likitlersuang & Kyaw, 2010)

$$V_s = 97\ N^{0.310}$$

Equation 2

$$V_s = 228\ \left(\frac{Su}{Pa}\right)^{0.510}$$

Equation 3

$$V_s = 187\ \left(\frac{Su}{Pa}\right)^{0.372}$$

Equation 4

where V_S is shear wave velocity (m/s), N is standard penetration test blow count (SPT-N), Su is undrained shear strength (kPa), and Pa is atmospheric pressure (kPa)

2.4.2. Shear Wave Velocity 30 meter

Earthquake that is related to ground amplifications. That amplification can change ground stiffness at shallow depths relatively. Basically, the most influential factor of the amplifications is V_{S30}. This V_{S30} is also becoming the indicator of soil stiffness. V_{S30} is the average shear wave velocity from soil surface to 30 m depth. The mean V_{S30} in the soil layer can be calculated by using this Equation 5 below

$$V_{s30} = \frac{\sum_{i=1}^{n} d_i}{\sum_{i=1}^{n} \frac{d_i}{V_{si}}}$$

Equation 5

Where d_i = soil layer thickness, i in the first 30 meters, V_{Si} = shear wave velocity in any i layer (m/s) and n = soil layers amount in the first 30 meters

V_{S30} is important criterion for designing the building structures (Boore, 2004). The National Earthquake Hazard Reduction Program (NEHRP) developed by the U.S. Congress in 1997 adopts this criterion and classifies a site into one of several different categories. Table 2.6 shows this classification from United Stated Building Seismic Safety Council (USBSS) in 1991. According to Poovarodom and Plalinyot (2013), Vs30 in Bangkok city are mostly less than 180 m/s and be classified as NEHRP site class E (soft soil and soft to medium clay).

Table 2.6. NEHRP site classification considering on shear wave velocity (V_s) (USBSS, 1991)

Site Class	S-Velocity (V_S) (m/sec)
A (Hard Rock)	>1500
B (Rock)	760 – 1500
C (Very Dense Soil and Soft Rock)	360 – 760
D (Stiff Soil)	180 – 360
E (Soft Clay Soil)	<180
F (Soils requiring additional response)	<180, additional condition

2.5. Geophysical Observation using Microtremor

Geophysical methods have been applied for many purposes. One of the geophysical methods is microtremor. Microtremor is conducted to show the natural vibration of the earth surface. Microtremor represent the seismic frequencies. The amplitude of the microtremor is 10^{-4} to 10^{-2} that is very small and best amplitude to study for seismic (Poovarodom & Jirasakjamroonsri, 2016). Moreover, the microtremor is useful for studying and estimating the effect of seismic motion at the surface, determination of site properties (Kyaw et al., 2014), conducting the model of subsurface and creating the seismic microzonation (Kiyono et al., 2011). The parameters that can be shown from microtremor observation are predominant period, amplification factor, and shear wave velocity (V_s) (Kyaw et al., 2014).

There are several methods that have been proposed to process and analyze data from microtremor observation. The popular method is Horizontal Vertical Spectral Ratio (HVSR) that be analyze by Nakamura in 1989 (Nakamura, 2000). Another analysis is using spectrum method that presented by Tokeshi, et al. (1996). The update analysis is proposed by Almendros, et al (2004) using the modification of HVSR method. The microtremor test is considered that the horizontal motion that consist of shear waves. The horizontal motion spectral reflects the site transfer function. This horizontal motion is required to determine predominant period (T_0), predominant frequency (f_0) and sediment H/V ratio.

2.5.1. Horizontal to Vertical Spectral Ratio Method (H/V spectral ratio)

The method of microtremor analysis that commonly used is Horizontal to Vertical Spectral Ratio Method. HVSR method is used as an guide of subsoil structure that presents the relationship between comparison Fourier Spectral of the microtremor signals at horizontal components to its vertical components (Nakamura, 2000). This method is based by horizontal to vertical spectra ratio of the surface tremor as an approximated transfer function. Microtremor observation consist of three wave components to estimate the dynamic of surface characteristic i.e. (1) Horizontal North-South component (2) Horizontal East-West component, and (3) Vertical Up-Down component.

The HVSR method concept is shown of horizontal and the vertical spectral. The propagation of seismic wave can be stated that the estimation of transfer function of surface layer. That mean the amplification magnitude of horizontal maximum value can be estimated by the fraction of horizontal to maximum value in the surface. Thus, observation the surface tremor can be known by dynamic characteristic of the layer (Nakamura, 2000). The ground motion happens when there is a geological structure on sedimentary basin. This motion has the spectra at on the ground, i.e. horizontal and vertical spectra (H_f, V_f) considering wave content in microtremor. This process is shown in Figure 2.10.
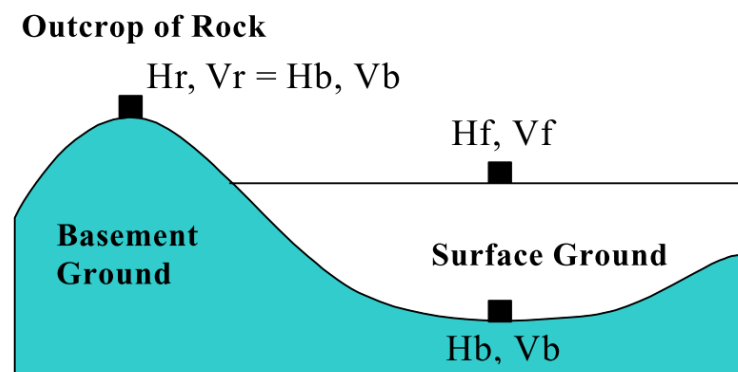
Figure 2.10. Geological structure of sedimentary basin model (Nakamura, 2000)

The horizontal spectra (H_f) and vertical spectra (V_f) on the sedimentary basin can be expressed as Equation 6, 7, 8 and 9 below

$$H_f = A_h * H_b + H_s$$

Equation 6

$$V_f = A_v * V_b + V_s$$

<div align="right">*Equation 7*</div>

$$T_h = \frac{H_f}{H_b}$$

<div align="right">*Equation 8*</div>

$$T_v = \frac{V_f}{V_b}$$

<div align="right">*Equation 9*</div>

where A_h is factor of horizontal motions that amplify from vertically incident body wave, A_v is factor of vertical motions that amplify vertically incident body wave, H_b is horizontal motion spectrum at the base of basin and V_b is vertical motion spectrum in the basement under the basin, H_s is horizontal direction spectrum of Rayleigh waves, and V_s is vertical directions spectrum of Rayleigh waves. T_h is factor of horizontal motion that amplify at the surface, and T_v is factor of vertical motion that amplify at the surface.

2.5.2 Microtremor Observation for Site Response Analysis

The utilization of microtremor has been done by many researchers. Observation of site effect is used the short-period of microtremor. The shear wave velocity is analyzed by horizontal motion assumption. The horizontal motion spectral reflect the ground condition based on transfer function (Mase et al., 2018). The ground transfer function can be assumed predominant period, predominant frequency and H/V ratio (Nakamura, 2000). The ratio of horizontal to vertical is recorded by ambient noise. From ambient noise measurement, shear wave velocity can be expected based on sediment deposits. The H/V calculation can be done by dividing the resultant of Fourier spectra on horizontal section by vertical section, as shown in Equation 10 below.

$$H/V = \sqrt{\frac{H^2(EW) + H^2(NS)}{2V^2}}$$

<div align="right">*Equation 10*</div>

Where, H(EW) and H(NS) are the Fourier amplitude spectra on horizontal component in the EW and NS directions, respectively, and V is the vertical spectral value (Mase et al., 2018)

The European commission had developed guidelines for the implementation of the H/V spectral ratio technique on ambient vibrations called SESAME. SESAME is stand for the Site Effects Assessment using Ambient Excitations (Acerra et al., 2004). The SESAME is required to give the guide related to the field experiment design related recording duration, measurement spacing and equipment (Mase et al., 2018). This guideline is recommended to perform the observation and interpretation to get the best result when combined with geology and geotechnical data. SESAME project classified the H/V curves according the main peak types. The classification gives the suggestion for processing and interpretation of H/V in many situations. Each curve must fulfill the criteria of reliable H/V curve and ideal H/V peak. The standards of reliable H/V curve are

1. $f_0 > 10 / l_w$
2. $n_c (f_0) > 200$
3. $\sigma_A(f) < 2$ for $0.5f_0 < f < 2f_0$ if $f_0 > 0.5$Hz or
   $\sigma_A(f) < 3$ for $0.5f_0 < f < 2f_0$ if $f_0 < 0.5$ Hz

The criteria for a clear H/V peak are

1. $\exists\, f^- \in [f_0/4, f_0] \,|\, A_{H/V}(f^-) < A_0/2$
2. $\exists\, f^+ \in [f_0, 4f_0] \,|\, A_{H/V}(f^+) < A_0/2$
3. $A_0 > 2$
4. $f_{peak} < [A_{H/V}(f) \pm \sigma_A(f)] = f_0 \pm 5\%$
5. $\sigma_f < \varepsilon(f_0)$
6. $\sigma_A(f_0) < \theta(f_0)$

Where l_w is window length, n_w is quantity of windows selected for the average H/V curve, $n_c = l_w \cdot n_w \cdot f_0$, n_c is quantity of major cycles, f is current frequency, f_0 is H/V peak frequency, σ_f is standard deviation of H/V peak frequency $(f_0 \pm \sigma_f)$, $\varepsilon(f_0)$ is limit value for the stability condition $\sigma_f < \varepsilon(f_0)$, A_0 is H/V peak amplitude at frequency f_0, $A_{H/V}(f)$ is H/V curve amplitude at frequency f, f^- is frequency between $f_0/4$ and f_0 which $AH/V(f^-) < A_0/2$, f^+ = frequency between f_0 and $4f_0$

which $A_{H/V}$ $(f^+) < A_0/2$, $\sigma_A(f)$ is "standard deviation" of $A_{H/V}(f)$, and $\sigma_A(f)$ is the factor which the mean $A_{H/V}(f)$ curve should be multiplied or divided.

The classified H/V curve based Acerra et al. (2004) are (a) Clear peak means there are two effects from deep and shallow soil in lower and higher period. (b) Unclear low frequency peak shows low frequency properties on sediment deposits because of either its very soft surface layers or stiff and thick layer. (c) Two peaks Cases ($f_1 > f_0$) shows two large impedance contrast which shear wave velocity is low in the surface and very high in the bedrock. (d) Broad peak or multiple peaks that happen in urban condition that H/V curves shows local narrow peaks (e) Sharp peaks and industrial origin means very bad and must be ignored for characteristics interpretation (f) Flat H/V ratio curves (on sediments) means no available any sharp impedance in the local site. The curve models are shown in Figure 2.11 that reflects the ambient vibration average H/V ratio (thick red line) multiplied/divided by $10^{\sigma(logH/V)}$ (thin red line).
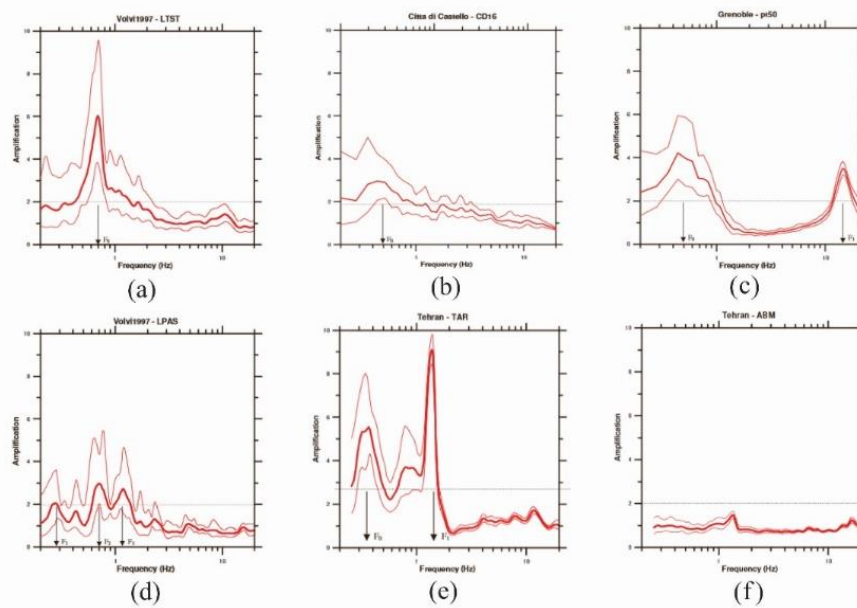
Figure 2.11. H/V Ratio Curves (a) Clear peak (b) Unclear Low Frequency Peak (c) Two Peaks Cases ($f_1 > f_0$) (d) Broad Peak or Multiple Peaks (e) Sharp Peaks and Industrial Origin (f) Flat H/V Ratio Curves [on sediments] (Acerra et al., 2004)

2.6. Seismic Site Response Analysis

Earthquake is one of considering factors that must be understood in geotechnical engineering field. In the last 50 years, the earthquake is demonstrated becoming the part of site effect that related to seismic event. The analysis of site response analysis is required understanding of wave propagation characteristics (Hashash et al., 2010). The site response analysis intends to get soil response from bedrock motion. Soil properties becomes the important thing to determine the ground surface motion (Kramer, 1996). In the seismic design, ground motion propagation cannot be neglected because it would be significant considered the effect of local geology. The site response analysis only consider horizontal ground motion as it is the principal motion factor that causes structural loss (Pruiksma, 2016). The illustration is presented at Figure 2.12 below.

Estimating the soil response use the dynamic equation through the soil column (Phillips & Hashash, 2009). There are two numerical approaches to solve the dynamic equation for site response:

1. Equivalent linear analysis (frequency domain)
2. Nonlinear analysis (time domain)
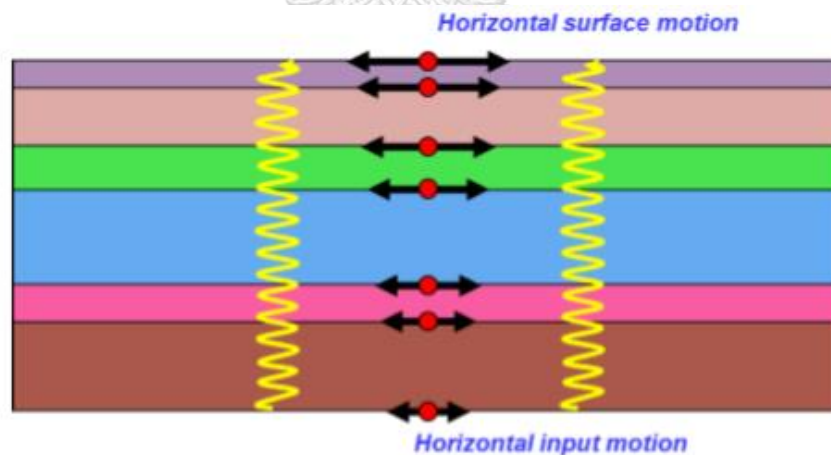
Figure 2.12. Illustration of site response for a horizontal input motion

The equivalent linear analysis is normally used in engineering works because of its simplicity and more conservative in term of spectral acceleration. Basically, this analysis calculates higher spectral acceleration for most spectral periods and considers the soil nonlinearity layers by using strain compatible shear modulus and damping ratio through an iterative process. In the other hand, the nonlinear analysis uses the

integration scheme and stage. The integration scheme is implicit and solved by Newmark β formulation. This method is more accurate and close to the true behavior of soil (Park & Hashash, 2004a).

2.6.1. One-dimensional of Site Response Analysis

In one-dimensional site response analysis, the bedrock and soil surface are assumed that the direction is horizontal infinitely. Figure 2.13 shows the travelling of body waves, when the fault happens beneath the site.
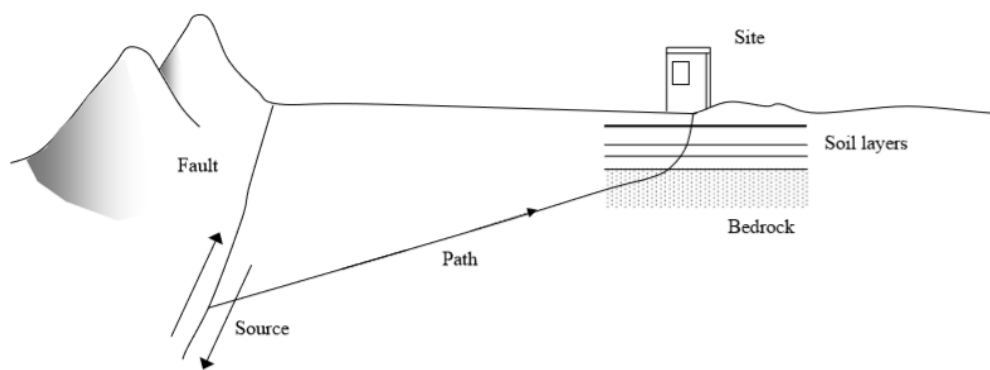
Figure 2.13. Source to site of ground motion propagation

The wave propagation velocity will be decreased along with the shallower depth. Ground response prediction is used the assumption from the procedure. This method as based on the assumption of the horizontal boundaries and the response is depending on the SH-waves that predominantly cause the response on the soil deposit (Kramer, 1996). There are several terms that commonly use in ground motion as shown in Figure 2.14, such as

1. Free surface motion means the soil surface deposit motion
2. Rock outcropping motion means bedrock that motion exposed
3. Bedrock motion means the base of deposit motion
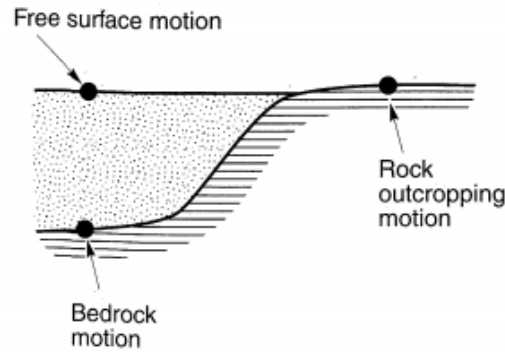
Figure 2.14. Ground motion terms (Kramer, 1996)

The ground motion characteristics are shown by the local site effect through several earthquakes. The response can be shown in term of peak ground acceleration and response spectra. A site response would show the model of fault propagation of stress wave of bedrock in particular site and ground motion propagation the soil column (Park & Hashash, 2004a). This analysis equation which the shear wave propagates vertically trough unbound medium can be expressed by the Equation 11 below

$$\rho \frac{\partial^2 u}{\partial z^2} = \frac{\partial \tau}{\partial z}$$

Equation 11

Where ρ = density, τ = shear stress, u = displacement, z = depth. Soil behavior is estimated as a Kelvin-Voigt solid. The shear stress-shear strain relationship is presented in Equation 11 below:

$$\tau = G\gamma + \eta \frac{\partial \gamma}{\partial z^2}$$

Equation 12

G = shear modulus, γ = shear strain and η = viscosity, from the equation 10 and Equation 11, can be gotten the formulation of one-dimensional site response analysis as Equation 12 below.

$$\rho \frac{\partial^2 u}{\partial t^2} = \frac{\partial u}{\partial z} + \eta \frac{\partial^3 u}{\partial z^2 \partial t}$$

Equation 13

Equation 13 calculate a harmonic wave propagation through a stratigraphic soil as shown in Figure 2.15.
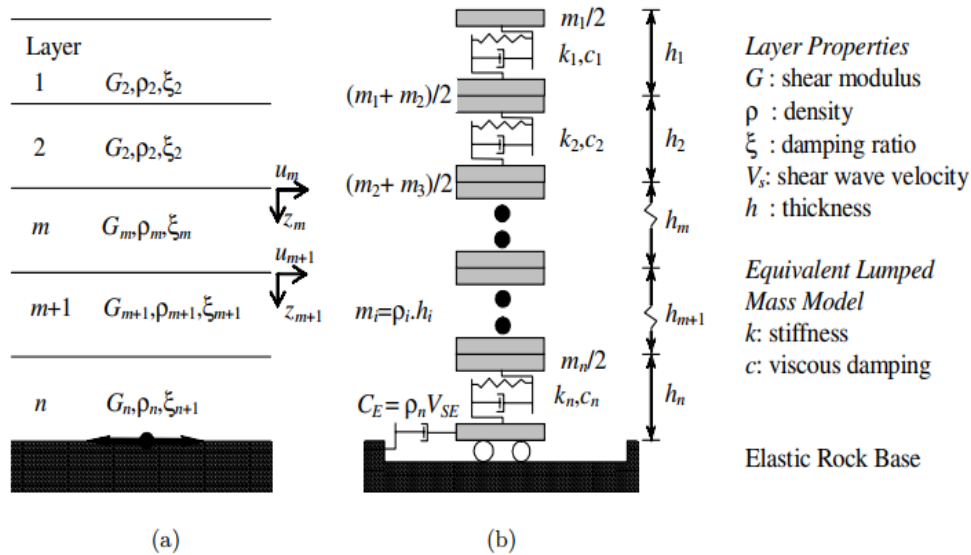
Figure 2.15. Soil stratigraphy (a) Layered soil column (frequency domain solution)
(b) Multi degree of freedom lumped parameter model (time domain solution) (Park &
Hashash, 2004b)

There are three data analysis for site response (1) PGA based on the attenuation model (2) Seismic ground response (3) Spectral acceleration. For one-dimensional seismic response analysis, the computer program application that is known as DEEPSOIL have been developed to analyze both equivalent linear and nonlinear model.

2.6.2. Equivalent Linear Model

The linear and equivalent linear site response model use frequency-domain calculation. This equivalent linear model uses soil properties like linear shear modulus (G), density (ρ), shear-wave velocity (V_s), and damping ratio (ξ). For linear model, the shear modulus (G) and damping ratio (ξ) is assumed be constant in every soil layer. The motion is inputted at the base (bedrock) to assess ground motion at the surface by using the equivalent linear model software. This model approach is modified when the nonlinearity of soil behavior is identified. The nonlinear stress and strain behavior

of cyclically loading soil can be estimated by the equivalent linear soil properties (Kramer, 1996).

Basically, equivalent linear model shows the wave equation for a linear elastic soil. Therefore, the G and ξ of linear model should be constant in every layer. The problem of this model is determining the consistency of value that strain induced in each layer. The solving of the problem is the equivalent linear need the strain level definition that can be obtained with laboratory test (Kramer, 1996). The laboratory test is required the modulus degradation and damping ratio curves (Figure 2.16) that have been advanced using the simple harmonic loading and generated the strain level by peak shear strain amplitude. So equivalent linear method, characterization of strain level based on the effective shear strain is around 50 and 70% of the maximum shear strain.

The equivalent linear model is effective to nonlinearity of soil, inelastic response of soil. Nonlinearity usually located in cohesionless soil but may be negligible in stiff soils. In equivalent linear site response analysis, the soil behavior is usually state in the term of shear strain that derive the shear modulus. The shear modulus is shown in this Equation 14 below

$$G = \frac{\tau}{\gamma}$$

Equation 14

τ is stand for shear stress and γ is stand for shear strain amplitude.

Seismic site response analysis, the data of shear strain is related with shear modulus ratio G/G_{max} and damping ratio are defined as functions of shear strain (%). The damping ratio can be solved with the Equation 15 below

$$\xi = \frac{W_d}{4\pi W_s}$$

Equation 15

W_s is the maximum energy saved in the soil, W_d is the dissipated energy during cycles. The Equation of W_s and W_d can be seen in Equation 16 and Equation 17

$$W_s = \frac{1}{2}G\gamma^2$$

Equation 16

$$W_d = \int \tau d\,\gamma^2$$
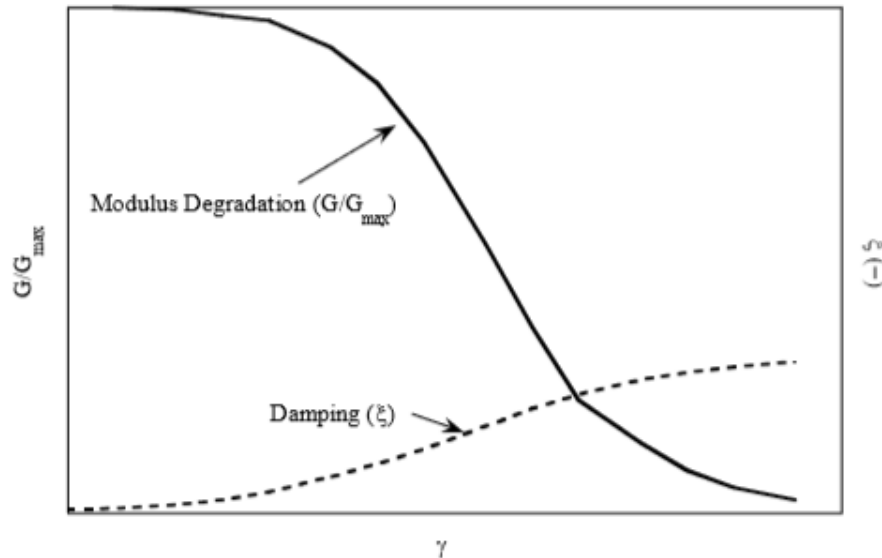
Figure 2.16. The modulus degradation and damping ratio curves (Kramer, 1996)

The iteration process in the equivalent linear approach is reflected in Figure 2.17. The equivalent linear method using shear modulus and damping ratio approximates actual material behavior. Performing the initial shear modulus and damping ratio as an elastic simulation. G (1) and ξ (1) corresponding to a strain zero. After the simulation in every layer, an effective non-zero strain γ_{eff} (1) is calculated corresponding to shear modulus G (2) and damping ratio ξ (2). The new version values of shear modulus and damping are used in the following iteration and generated in an updated effective strain in the layer γ_{eff} (2), corresponding to new values G (3) and ξ (3).

2.6.3. Nonlinear Model

The nonlinear analysis is the time domain using the Newmark β method for solving the equation to estimate the single degree of freedom (SDOF). The soil column is divided into individual layers using a multi-degree-of-freedom lumped parameter model or finite elements (Kramer, 1996). Nonlinear model is an alternative approach that computationally convenient. It remains the actual nonlinear process and

provides results like the real conditions of soil. Nonlinear method can be stated the parameter of effective stress to generate the model, redistribution, and excess pore water pressure along the earthquake.

The nonlinear analysis of soil deposit uses the time domain of direct numerical integration. The correlation of linear and nonlinear model could be done by equation integration of motion. There are several nonlinear features, i.e. soil model, viscous damping formulation, dynamic integration scheme, enlarged numerical accuracy, and user interface. In the site response analysis, nonlinear model is conducted to analyze essential factors such as cyclic behavior of soil. Cyclic soil behavior is nonlinear when the shear strain exceeds about 10^{-5}. When shear of soil exceeds the linear threshold strain, the nonlinear behavior of soil must be calculated because it is the main factor in ground motion propagation. Many computational programs can be used for nonlinear one-dimensional site response analysis. Site response analysis using one-dimensional nonlinear approach is conducted using two types of Rayleigh viscous damping formulations, (a) Rayleigh damping formulation and (b) extended Rayleigh damping formulation. Both Rayleigh and extended Rayleigh formulations are resulted in frequency dependent damping, the thickness of soil profile influences the maximum frequency that can be propagated. It can be expressed in the Equation 18

$$f_{max} = \frac{(V_s)_i}{4h_i}$$

Equation 18

where f_{max} = maximum frequency that layer i can propagate, $(V_s)_i$ = shear velocity, $4h_i$ = thickness of each layer.

Determining constant shear modulus and damping is a method to estimate nonlinear response (Pruiksma, 2016). An iterative process is effective to calculate elastic shear modulus and damping ratio ξ from effective strain γ_{eff} in layer respectively. This effective strain (γ_{eff}) is defined as a fraction α of the maximum strain γmax reached in a layer $\gamma_{eff}= \alpha \gamma max$. Basically, This fraction α is about 0.5 to 0.7, however in the site response software, α is 0.65 as default value (Kramer, 1996). The DEEPSOIL manuals provide the relationship with earthquake magnitude M in Equation 19.

$$\alpha = \frac{M-1}{10}$$

Equation 19
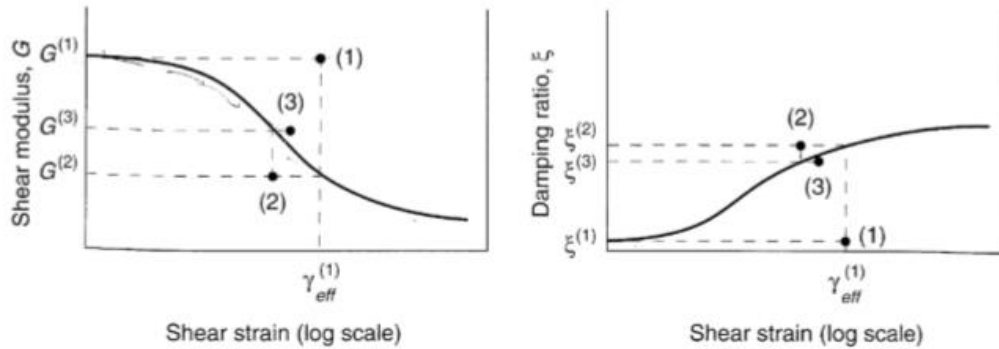
Figure 2.17. Procedure of a strain compatible shear modulus and damping ratio

(Kramer, 1996)

2.6.4. Numerical Computer Program for DEEPSOIL as Site Response Analysis Program

One-dimensional analysis site response analysis is conducted to calculate the effect of ground vibration during the earthquake (Park & Hashash, 2004b). DEEPSOIL is an application that is developed for modelling the site response analysis. The new viscous damping formulation and confining pressure is enhanced in this program over conventional analysis. In a nonlinear analysis the soil damping is representative as hysteretic loading-unloading cycles. (Park & Hashash, 2004a).

The Newmark β average acceleration method is used to calculate the dynamic equation of the motion by Newmark (1959). The dynamic equation of the motion expressed as Equation 20 below

$$[M]\{\ddot{u}\} + [C]\{\dot{u}\} + [K]\{u\} = -[M]\{I\}U_g$$

Equation 20

Where [M] = mass matrix, $[C]$ is viscous damping matrix $[K]$ is stiffness matric, $\{u\}$ is vector of nodal relative velocities and $\{u\}$ is vector of nodal relative displacement and U_g is the acceleration at the soil column base and $\{l\}$ is the unit vector. This numerical can solve the dynamic equation. Earthquake motion for site response analysis uses the Newmark Method or Duhamel integral solutions to estimate the single degree of freedom (SDOF). DEEPSOIL can be used to analyze

one-dimensional nonlinear site response analysis. The essential factors that must be consider for earthquake response are shear wave velocity, unit weight, shear modulus (G), damping ratio, shear strain, bedrock condition. In site response analysis the natural frequency of the selected mode is commonly expressed as this Equation 21 below

$$f_n = \frac{V_s}{4H}(2n - 1)$$

Equation 21

where n is the mode number and f_n is the natural frequency of the corresponding model. The nonlinear soil model is used the pressure dependent (Hashash & Park, 2001). The model for this linear analysis is an extension of the modified hyperbolic model that developed by (Matasovic, 1993). This model can calculate the influence of confining pressure on soil dynamic properties that expressed by Equation 22 and Equation 23

$$\tau = \frac{G_{mo}\gamma}{1 + \beta \left(\frac{\gamma}{\gamma_r}\right)^s}$$

Equation 22

$$\gamma_r = a \left(\frac{\sigma'}{\sigma_{ref}}\right)^b$$

Equation 23

where τ is shear stress, γ is shear strain, G_{mo} is initial shear modulus, b and s is curve fitting parameters that adjust the shape of the backbone curve, γ_r is the reference shear strain, a and b are curve fitting parameters to account for confining pressure dependent soil behavior, and σ_{ref} is a reference confining pressure (Park & Hashash, 2004b).

Site response analysis due to the earthquake using DEEPSOIL have to assume the layer to get the information of the starting of the wave propagation. Hashash et al. (2015) classify the rock properties below

a. Rigid half space

The parameter of rock layer using these properties can be used if only the initial oscillation is analyzed. The rock layer is not slip and located under the ground layer as shown in figure 2.18.
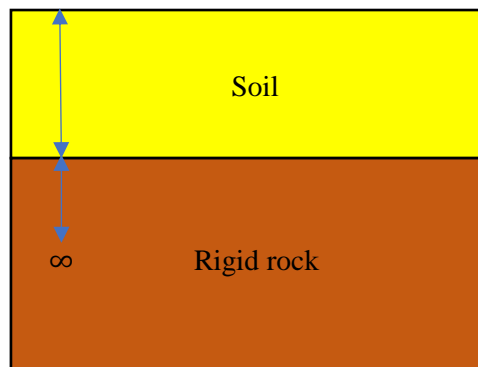
Figure 2.18. Rigid half space illustration

b. Elastic half space

The parameter of rock layer using these properties are used when the motion analyzes at the outcrop of rock. The rock layer is assumed as elastic that can move slightly and have same depth as the rigid half space. In these assumptions, the parameter of soil layer can obtain shear wave velocity in the unit of weight as shown in Figure 2.19.
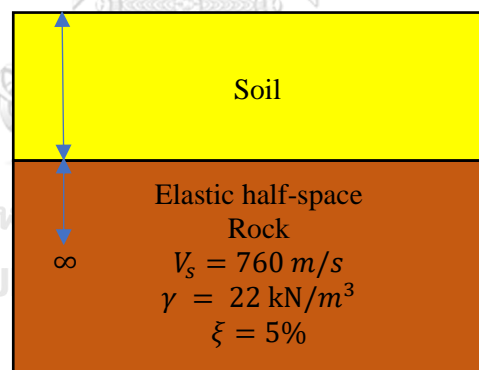
Figure 2.19. Elastic half space rock beneath soil column illustration

CHAPTER 3
RESEARCH METHODOLOGY

3.1. Research Area

Concerning about research location, four sites are investigated to answer the research objectives. Those sites are presented in Figure 3.1. The locations selection is based data availability of Bangkok subsoil properties, such as the number of layers and shear wave velocity. Several test like seismic downhole, boring log, and spectral analysis of surface wave (SASW) had been conducted at those locations. One of these locations is a seismic station of Thai Meteorological Department in Bangkok City.

Figure 3.1. Research Spots

Those 4 sites are namely,

1. Chulalongkorn University (CU), Pathumwan, Bangkok, 10330

   Coordinate: Latitude 13° 44' 17.87" N

   Longitude 100° 31' 56.06" E E

2. Kasetsart University (KU), Chatuchak, Bangkok 10900

   Coordinate: Latitude 13° 54' 1.76" N

   Longitude 100° 22' 56.31" E

3. Asian Institute of Technology (AIT), Khlong Luang, Pathumtani, 12020

   Coordinate: Latitude 14° 5' 0.1" N

   Longitude 100° 37' 5.04" E

4. Meteorological Department of Thailand (TMD), Bangna (BKK), Bangkok. 10260

   Coordinate: Latitude 13° 40' 6.77" N

   Longitude 100° 36' 24.4" E

3.2. Research Analysis Framework

This research is divided into three main steps, i.e.

1. Preliminary studies

   In the first step, the background and objectives are defined. Literature review that related to the whole research are conducted. After that, the hypothesis can be established based on the research objectives.

2. Data collection and elaboration

   In this step, microtremor and geological data are elaborated as the main data collection. Then, H/V spectrum is generated to get the wave and shear wave velocity. Ground motion analysis and bedrock are also conducted to generate the site response.

3. Analysis and reporting.

   In this step, one dimensional analysis is done to get peak ground acceleration and spectral acceleration as the main result of this research. After that, preparing the report. At last, the conclusions are created as summarize of the whole research. The detail methodology of this research is summarized in the flow chart (Figure 3.2).
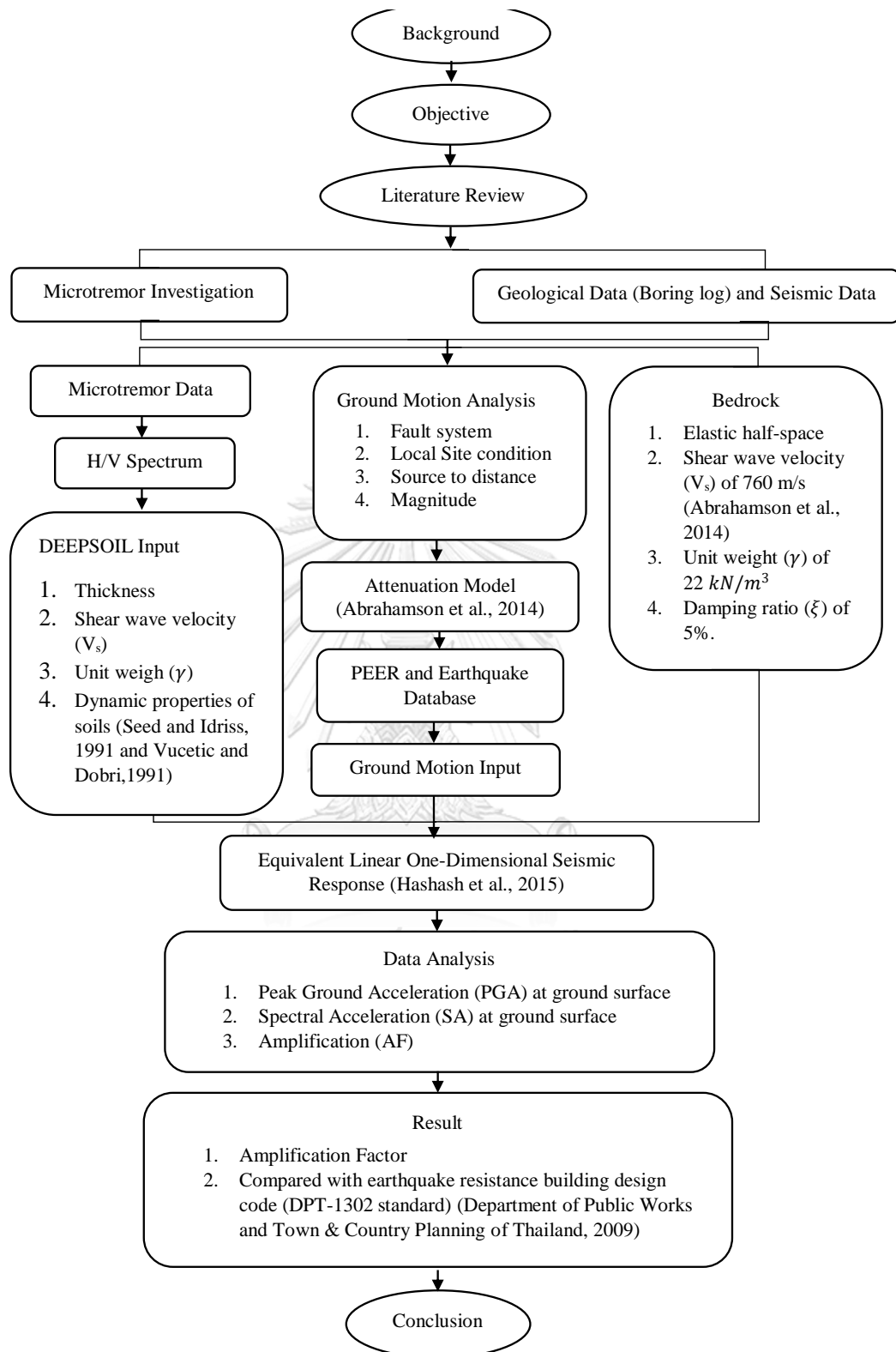
Figure 3.2. Research flow chart

3.3. Data Recording of Microtremor

Recently the microtremor observation method have been evolved as one of the latest approaches to get the data of site response analysis and to determine shear wave velocity and predominant period of the site. In this step, the local site is measured and recorded by using this microtremor. Microtremor observation is conducted using microtremor DATAMARK JU410 that produced by HAKUSAN Co. Ltd. This tool consists of three accelerometer (tri-direction accelerometer) component, i.e., (North-South, East-West, and Up and Down). The sensitivity of this type of microtremor is low because it is developed to record both strong and weak motion. The small noise of the measurement can be ignored. This micrometer can be operated up to 130 dB at 100Hz (wide dynamic range) (Mase et al., 2018).

Figure 3.3. The microtremor tool DATAMARK JU410

The measurement is based on SESAME (Acerra et al., 2004). The observation is suggested and conducted about 1000s (30 minutes). Before doing the measurement, the initializing of the machine will be run about 10 minutes to keep away from the noise problem in low frequency. The spot recorded are selected based on availability of the borehole data that were required before for validating purpose.

3.4. Microtremor Data Extraction and H/V Processing

The second step of the research is data extraction. The result of microtremor machine measurement is transferred to the computer. Data from microtremor is generated using the TremorDataView Application (Naito et al., 2013). In this application, the noised is removed and the best vibrations are picked. The best

sections or the quiet sections of the ambient noises will be used to determine the H/V ratio. The best recorded data is converted from the excel data (time domain data) into H/V spectrum (frequency domain data). Determining, data processing and interpretation of the best H/V spectral ratio technique using ambient vibration is used and consider the SESAME (Acerra et al., 2004). The criteria of SESAME are defined about the reliable curve and clear peak to estimate the sediment thickness and impedance. Reliability shows the actual H/V curve from the recording will characterizes the H/V curve from the other ambient vibrations recording.

The data processing is required to generate Vs profile from the H/V ratio. The program that will be used in this data processing is HV-Inv computer program. HV-Inv is a computer code to analyze the ambient noise and its inversion that developed by Garcia-Jerez et al. (2016). There are three main inversion algorithms that provided by this software as be written in Matlab®

1. Monte Carlo sampling
2. Simulated Annealing method (SA)
3. Interior Point method (IP)

For this research Monte Carlo sampling is used to calculate the H/V spectral ratios inversion. This method is used to compute the H/V spectral ratios inversion in this program. This method is required to find the best model. The model of spectral rations inversion is based on 5 parameters, i.e. thickness, compressional wave velocity (V_P), shear wave velocity (V_S), soil density (ρ), and Poisson's ratio (ν) (García-Jerez et al., 2016). Those parameter at this research are estimated and taken from the previous study and investigation of the site based on boring log test and geological profile. Compressional wave velocity (V_P) is derived the ratios of V_P/V_S model (Tatham, 1982). The profile will be calculated and shown until the estimated H/V is suitable with measured H/V.

H/V spectrum are observed at four sites and then the results were analyzed for the inverse analysis. Several assumptions are used in this the inversion, as follow

1. The depth of soil profile is about 500 m as quaternary geological profile by Sinsakul (2000) and estimated as layered half-space. In this research, only 100 m depth of CU site and 30 m depth of the other sites are known by the boring log data.

2. The amount of the layers is assumed from the boring log data layer and geological aquifer and every site is different each other.

3. The shear wave velocities (V_S) and density (ρ) are predeterminate from the result of boring log and extrapolation until reaching the engineering bedrock. The shear wave velocities that were measured the boring log and the H/V inversion are consistent with each other.

The range value of input parameter is shown in Table 3.1. The bottom layer was assumed as the elastic half space assumption. Physical properties of the materials and soil structure become the first factors that to define the range of minimum and maximum value of each parameter.

3.5. Data analysis response using DEEPSOIL

The last step of this research is data analysis using DEEPSOIL to evaluate the site response. The reasonable analysis for the Bangkok subsoil that consist relatively uniform is one-dimensional site response analysis. Data that is derived from the processing of ambient noise can be used for estimating the shear wave velocity and density. The sediment layer can be elaborated from the measurement using boring log that have been conducted in the site.

DEEPSOIL can generate wave propagation model, and the equivalent linear analysis can be applied in this program. The concept of analysis is running the DEEPSOIL for nonlinear and equivalent linear analysis with many steps below:

1. Analysis definition

In this step, the selection of analysis is required. The analysis method is chosen as frequency domain with linear or equivalent linear and time domain with linear or nonlinear, then the type of inputs for the shear properties, units and pore water pressure control are chosen.

2. Data collection for soil profile properties, i.e. shear wave velocity (V_s) or initial shear modulus (G_{max}), unit weigh, small strain damping ratio (%) (dynamic of soil properties), or another important parameter. In this research, the ground water is ignored so the pore water pressure is not considered. For time domain analysis, the maximum frequency must be chosen for completing the soil and model properties.

Table 3.1. Range value of initial parameter for HV Inv Input at CU sites

Layer	Soil Type (USCS)	Thickness (m)		Vp (m/s)		Vs (m/s)		Density ρ (kg/m3)		Poison ratio (v)	
		Min	Max	Min	Max	Min	Max	Min	Max	Min	Max
Layer 1	CH	1	10	120	300	60	123	1800	2000	0.4000	0.4950
Layer 2	CH	1	10	400	400	100	164	1800	2000	0.4000	0.4950
Layer 3	CH	1	10	600	600	200	245	1800	2000	0.4000	0.4950
Layer 4	CH	1	10	500	700	250	286	1800	2000	0.4000	0.4950
Layer 5	SM-SP	1	10	500	700	250	327	1800	2000	0.3000	0.4000
Layer 6	CH	1	10	600	800	300	327	1800	2000	0.4000	0.4950
Layer 7	CL	1	10	700	900	300	327	1800	2000	0.4000	0.4950
Layer 8	SC	1	10	500	700	300	327	1800	2000	0.3000	0.4000
Layer 9	CH	1	10	600	800	300	327	1800	2000	0.4000	0.4950
Layer 10	SC	10	100	600	800	350	368	1800	2000	0.3000	0.4000
Layer 11	SM-SP	10	100	700	900	350	368	1800	2000	0.3000	0.4000
Layer 12	SC	10	100	700	900	350	368	1800	2000	0.4000	0.4950
Layer 13	CL	10	100	900	1100	450	550	1800	2000	0.3000	0.4000
Layer 14	SC	10	100	900	1100	450	550	1800	2000	0.4000	0.4950
Layer 15	CL	10	100	100	1200	500	600	1800	2000	0.3000	0.4000
Layer 16	SC	10	100	1100	1300	550	650	1800	2000	0.3000	0.4000
Layer 17	SC	10	100	1300	1500	650	750	1800	2400	0.3000	0.4000
Layer 18	SC	10	100	1500	2000	760	1000	1800	2400	0.3000	0.4000
Half Space	Rock	10	100	1500	2000	760	1070	1800	2400	0.3000	0.4000

The material type and target shear modulus ratio-shear strain ($G/G_{max} - \varepsilon$) curve for each layer are selected. For soft clay, medium stiff clay, stiff to very stiff clay and very stiff clay use the $G/G_{max} - \varepsilon$ relationship from Vucetic and Dobry (1991) and for sand use the $G/G_{max} - \varepsilon$ relationship from Seed and Idriss (1971).

3. Inputting and defining the nonlinear parameter

Considering the limitation information of real engineering bedrock, the bedrock is assumed the elastic half-space assumption with shear wave velocity is 760 m/s (Miller et al., 1999), weight unit is 22 kN/m^3 and damping ratio is 5%. Miller et al. (1999) had defined the engineering bedrock value in general about 760 m/s and that value also was used as basic value in several researcher, i.e. Mase (2018), and Adampira et al. (2014).

4. Inputting the motion

The attenuation model is determined for obtaining the earthquake event data. DEEPSOIL has a motion tab to input motions from earthquake event. DEEPSOIL has list of earthquake events that will generate acceleration, velocity, displacement, and time histories. The motion can be added manually using .txt files. In this research, the earthquake motion is derived from the Chichi earthquake, Loma prieta earthquake, Northridge earthquake, and Tarlay earthquake after matched with the attenuation model. The analyzing of the propagation of ground motion, the waves motions are inputted at the bottom of each site (rock layer).

5. Viscous Damping

The differences steps of nonlinear and equivalent linear is for equivalent linear, the Iteration number and Fourier Transfer Type (DFT or FFT), and Complex Shear Modulus is chosen. The transfer function defines the amplification or de-amplification of each frequency in the bedrock (input) motion by the soil layer. For nonlinear model, the features that must be analysis is Soil Model, Viscous Damping Formulation (Damping Matrix Type), and Increased Numerical Accuracy (Fixed or Flexible). The result of the nonlinear soil model will be shown in shear modulus degradation and damping ratio graph.

6. Output (running the analysis)

For one-dimensional non-linear time domain analysis, the outputs are Acceleration (g) vs Time (sec), Response Spectra: PSA (g) vs Period (sec), PGA Profile: Max PGA vs Depth, Strain Profile: Max Strain vs Depth.

3.6. Seismic Hazard Analysis and Ground Motion Input

Considering the two-big earthquake in Thailand, there is only record from Tarlay earthquake for ground motion input but there is no proper record of Mae Lao earthquake. Kusumahadi (2018) had done the identification of uncertainties of Mae Lao earthquake based on magnitude, epicenter location to site distance (11.21 km from the epicenter to White Temple), fault modelling, paleoseismic characteristic, local site condition (shear wave velocity) and ground motion intensity. Kusumahadi (2018) derived the motion from PEER database. The analysis is required by NGA-West2 (PEER, 2011). The parameters from NGA-West2 is conducted to get PGA and SA of the ground motion.
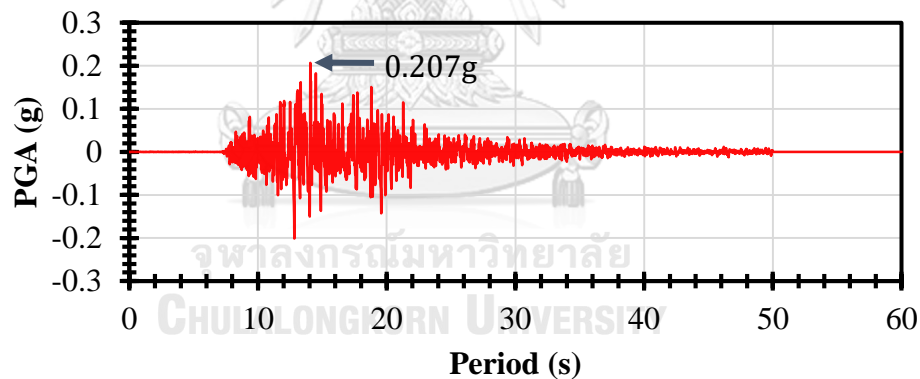
Figure 3.4. Tarlay earthquake Acceleration Record at Mae Sai Station (TMD, 2015)

Designing the motion in Three Pagodas fault can be required and derived from NGA-West2 (PEER, 2011). NGA-West2 is developed to update the NGA-West1 (2008) in 2014. PEER (2011) leads designing of ground motion by using the NGA-West2 2014 attenuation model. Those are considering the magnitude, source-to-site distance, fault modelling, paleoseismic characteristic, local site condition (shear wave velocity) and ground motion intensity. The motion parameter is acquired from the Ground Motion Prediction Equation (GMPEs).

Getting appropriate motion for the site, those GMPEs parameters must be required. There are several requirements that are proposed by NGA-West2 (2014) to analyze the motion in this research as following (1) Defining magnitude of the earthquake. In this research the magnitude is determined from the closest fault and most contributed earthquake to Bangkok city (The Three Pagodas Fault). The magnitude are M_W 5 from Kanchanaburi earthquake in 1982 and M_W 6.2 and M_W 7.5 from maximum credible earthquake magnitude (Palasri & Ruangrassamee, 2010). (2) Determining the paleoseismic characteristic. Three Pagodas Fault is strike slip faulting (F_{SS}) (3) Source-to-site distance is presented in the table 3.1. In this research, Joy Boore distance (R_{JB}) and horizontal distance (R_X) is estimated from the google earth to sites as shown in Figure 3.5. Z_{TOR} is assumed as 0 or inputted as 999 in the GMPEs spread sheet to be unknown parameter and automatically calculated R_{RUP} will be equal to R_{JB} value in case of strike slip faulting model as Three Pagodas Fault. (3) Discovering local site condition. The shear wave velocity depth of 30 is calculated from SPT-N of each site as shown in the table 3.2.
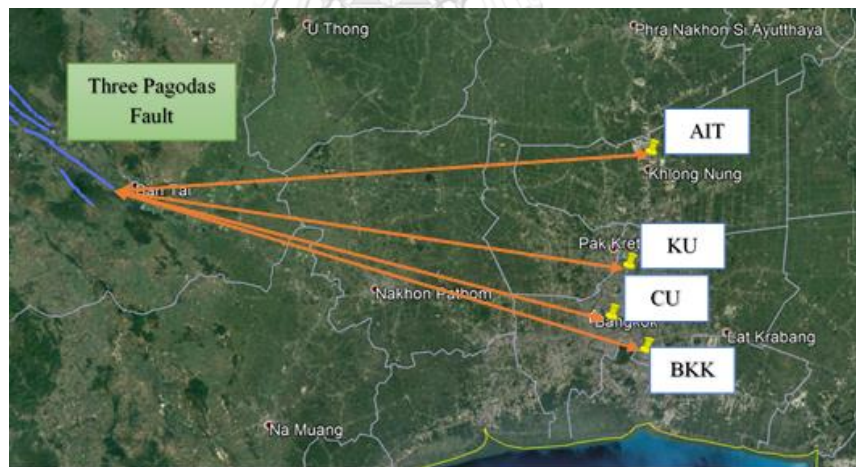
Figure 3.5. The distance of Three Pagoda Fault to Bangkok

Table 3.2. GMPEs requirements at each site

Site	V_{S30} (m/s)	Soil Type	Source to Site Distance (km)
CU	142.0920	E	119
KU	179.3952	E	120
AIT	171.9507	E	123
BKK	152.9823	E	128

3.7. Attenuation Model Analysis

Abrahamson et al (2014) of Next Generation Attenuation (NGA) model is used to define the motion of Three Pagodas Fault as shown on Figure 3.6.
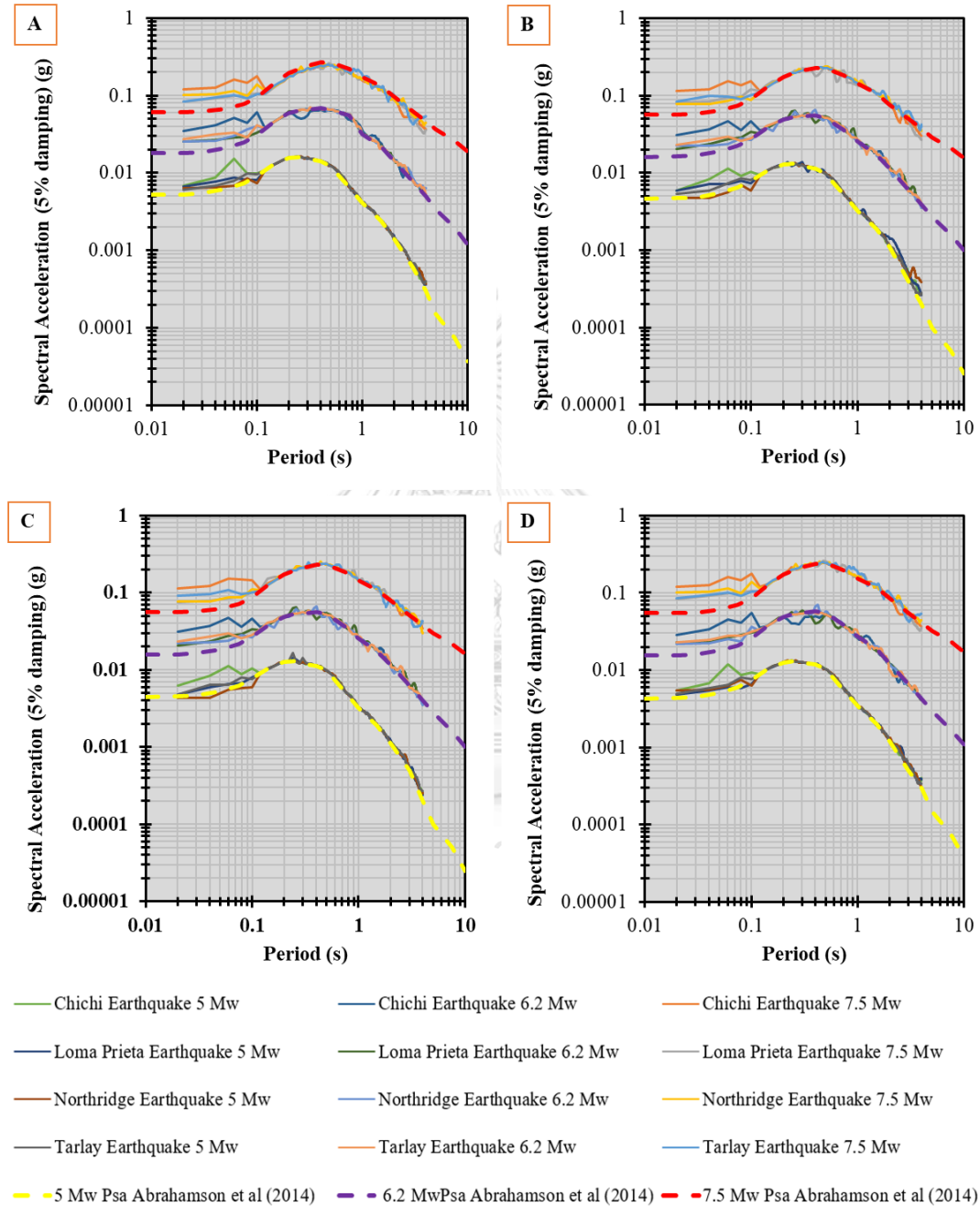
Figure 3.6. Target response spectrum of M_W 5, M_W 6.2, and M_W 7.5 of earthquake with 5% damping (A) CU site (B) KU site (C) AIT site (D) BKK site

Based on the current version database, the most comprehensive set of metadata that is suitable for the far distance of source and site (Abrahamson et al.,

2014). After the attenuation model is selected, the Time-History selection, scaling and matching are conducted. PEER NGA-West2 ground motion database consists the large set ground motion that recorded around the world.

The result of the PEER database shown in Table 3.3. A total three ground motion were recorded at several stations. Those are located on many site conditions during earthquake events with epicentral distances are not over than 150 km and magnitudes with range from 6.20 to 6.92. The V_{s30} are available at all stations. according to the NEHR, Site conditions of sites can be classified into D (stiff soil) and E (soft soil). Those are relatively equivalent with Bangkok condition (USBSS, 1991).

Table 3.3. The Selected Motion from PEER and Tarlay Earthquake TMD

Selected motion from PEER						
Earthquake Name		**Station**	**Year**	**Mw**	**Epicentral Distance**	**V_{s30}**	**Soil Type**
Chi-Chi	"Chi-Chi_ Taiwan-04"	"TCU045"	1999	6.2	119.22	150.18	E
Loma Prieta	Loma Prieta	Alameda Naval Air Stn Hanger	1989	6.93	71	190	D
Northridge	"North-ridge-01"	Hemet - Ryan Airfield	1994	6.69	144.71	290.93	D
Motion from TMD						
Earthquake Name		**Station**	**Year**	**Mw**	**Epicentral Distance**	**V_{s30}**	**Soil Type**
Tarlay		Bangna	2011	6.2	±700	±133	E

In this research, Chichi earthquake, Loma prieta earthquake, Northridge earthquake, and Tarlay earthquake would be basic of the seismic motion to investigate the seismic response in Bangkok at all sites presented in Figure 3.7 - Figure 3.10. The seismic response is considered on wave propagation and attenuation model. The result of the research would be PGA and SA in the investigated area according to the PEER database Earthquake and Tarlay earthquake data.
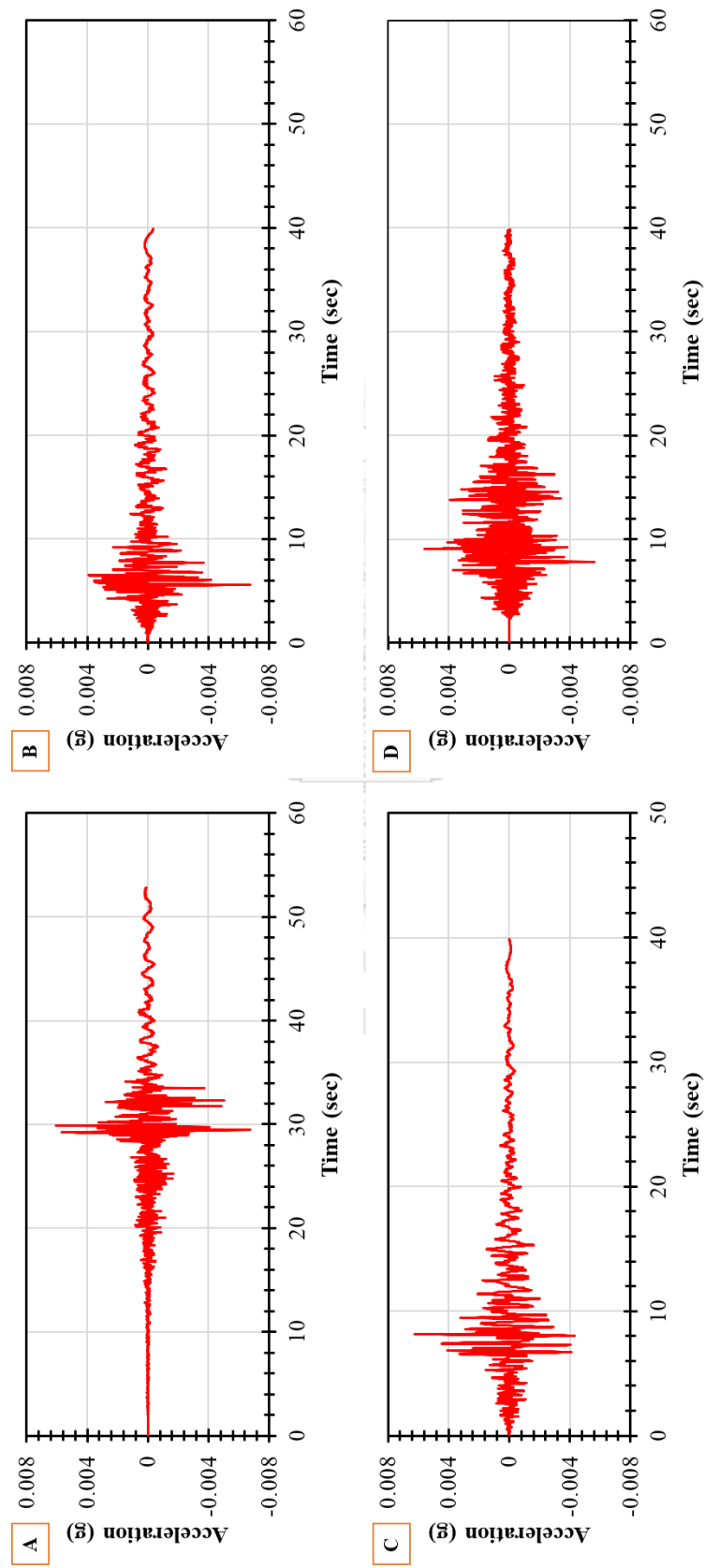
Figure 3.7. The Mw 5 of ground motions resulted from spectral matching for CU site (A) Chichi Earthquake (B) Loma Prieta Earthquake (C) Northridge Earthquake (D) Tarlay Earthquake
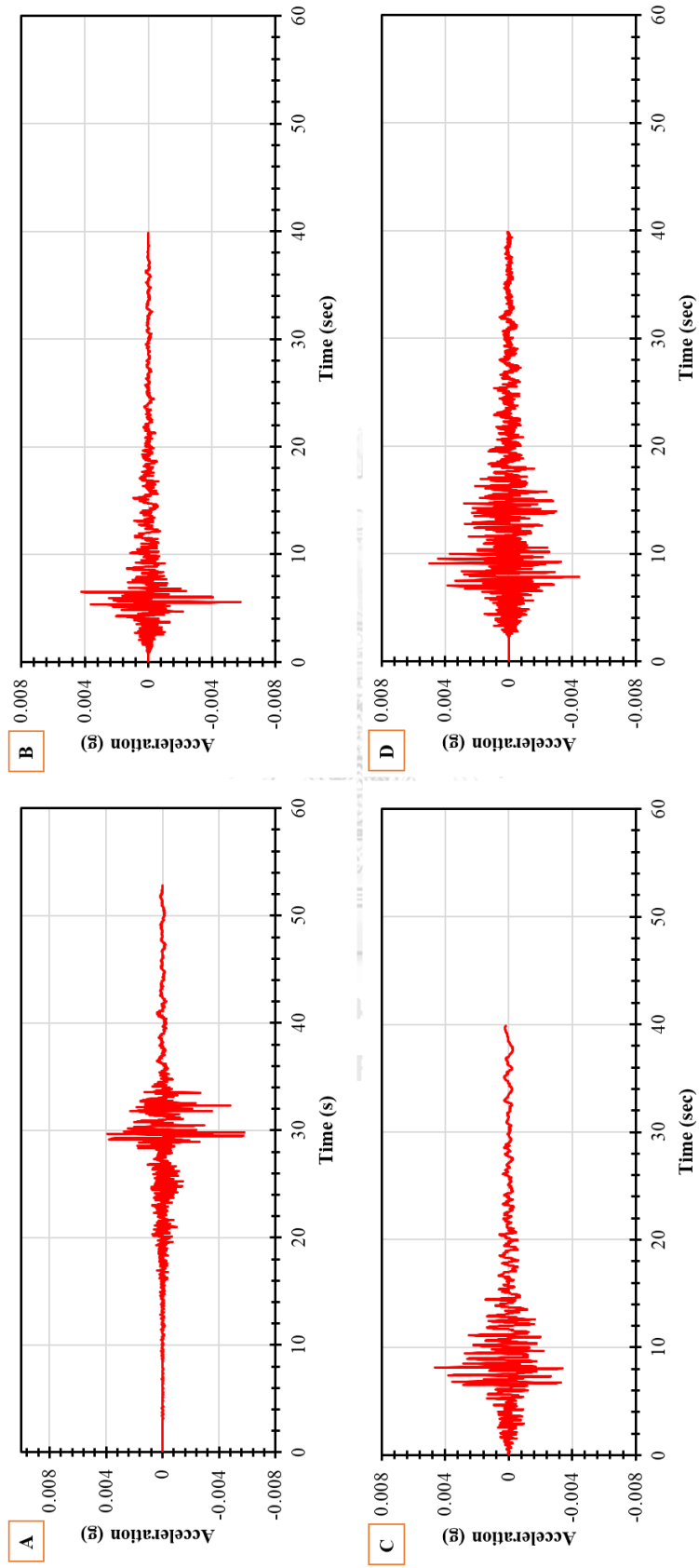
Figure 3.8. The Mw 5 of Ground motions resulted from spectral matching for KU site (A) Chichi Earthquake (B) Loma Prieta Earthquake (C) Northridge Earthquake (D) Tarlay Earthquake
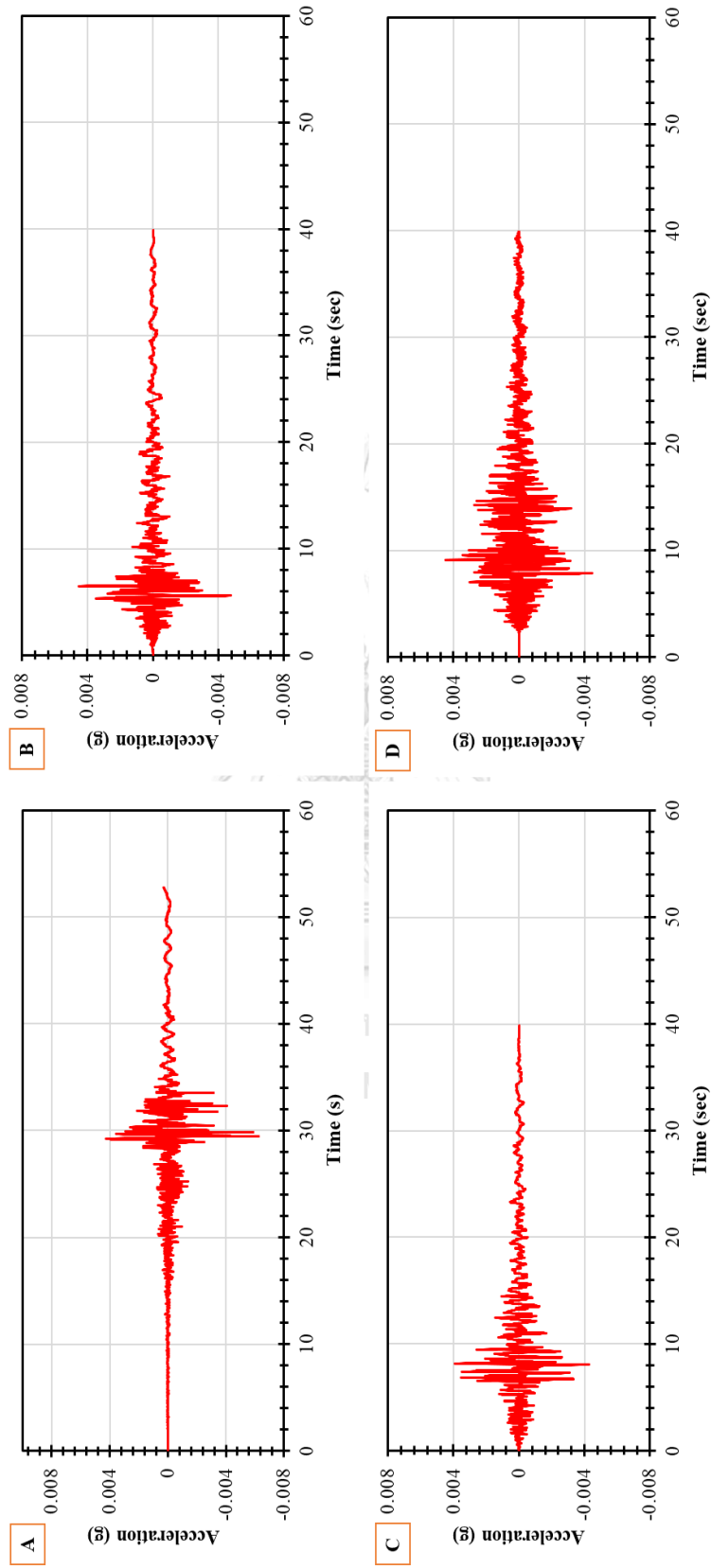
Figure 3.9. The Mw 5 of Ground motions resulted from spectral matching for AIT site (A) Chichi Earthquake (B) Loma Prieta Earthquake (C) Northridge Earthquake (D) Tarlay Earthquake
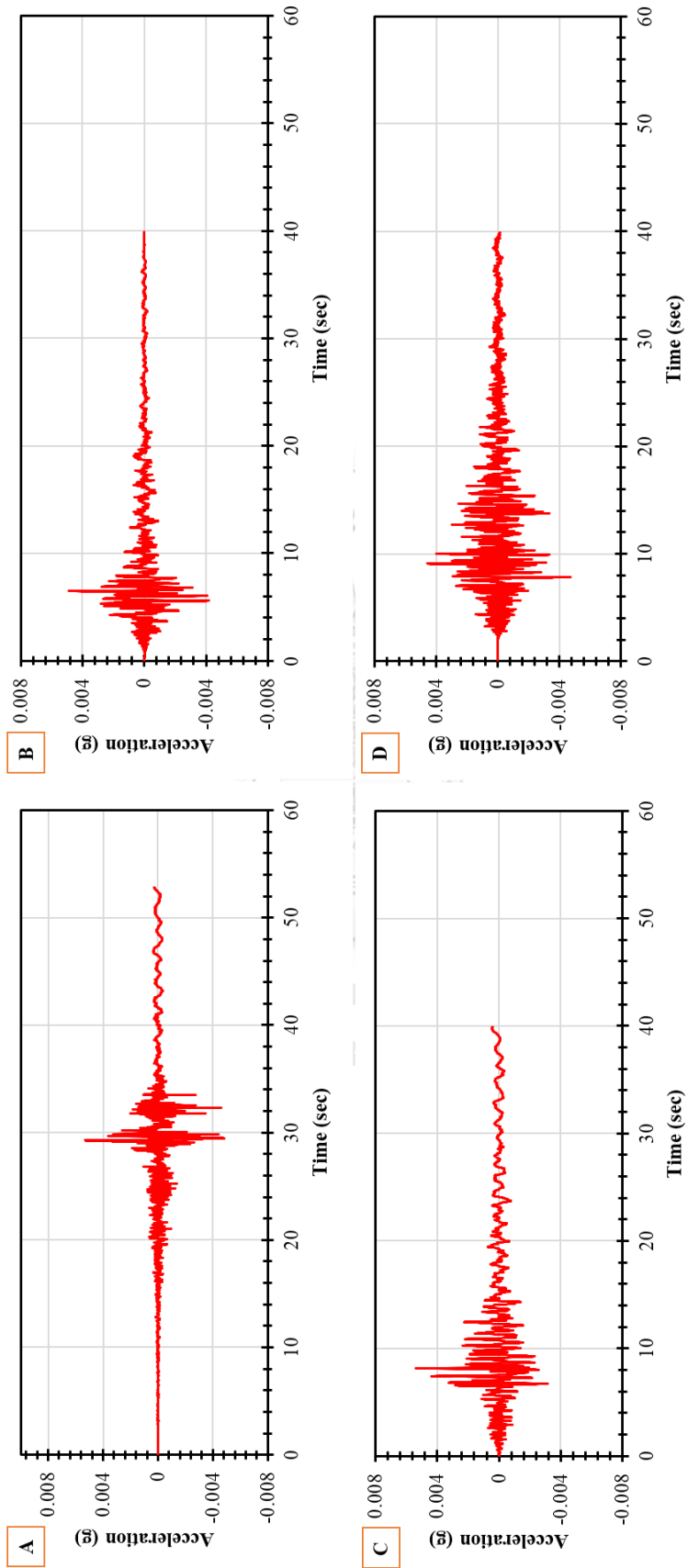
Figure 3.10. The Mw 5 of Ground motions resulted from spectral matching for BKK site (A) Chichi Earthquake (B) Loma Prieta Earthquake (C) Northridge Earthquake (D) Tarlay Earthquake

CHAPTER 4
RESULTS

4.1. Microtremor Measurement

Microtremor investigations were conducted at four sites to interpret the H/V spectral ratios related to geological condition of local sites in Bangkok. For assessing the site effects in Bangkok subsoil, the microtremor is the effective tool. The soil characteristic of shear wave velocity (V_S) is derived from inversion of the record and then this V_S is used to investigate the site response analysis during earthquake that triggered by the fault near the Bangkok city. The result of microtremor is shown in Figure 4.1 after following and fulfilling the criteria from the guideline of SESAME from Acerra (2004).
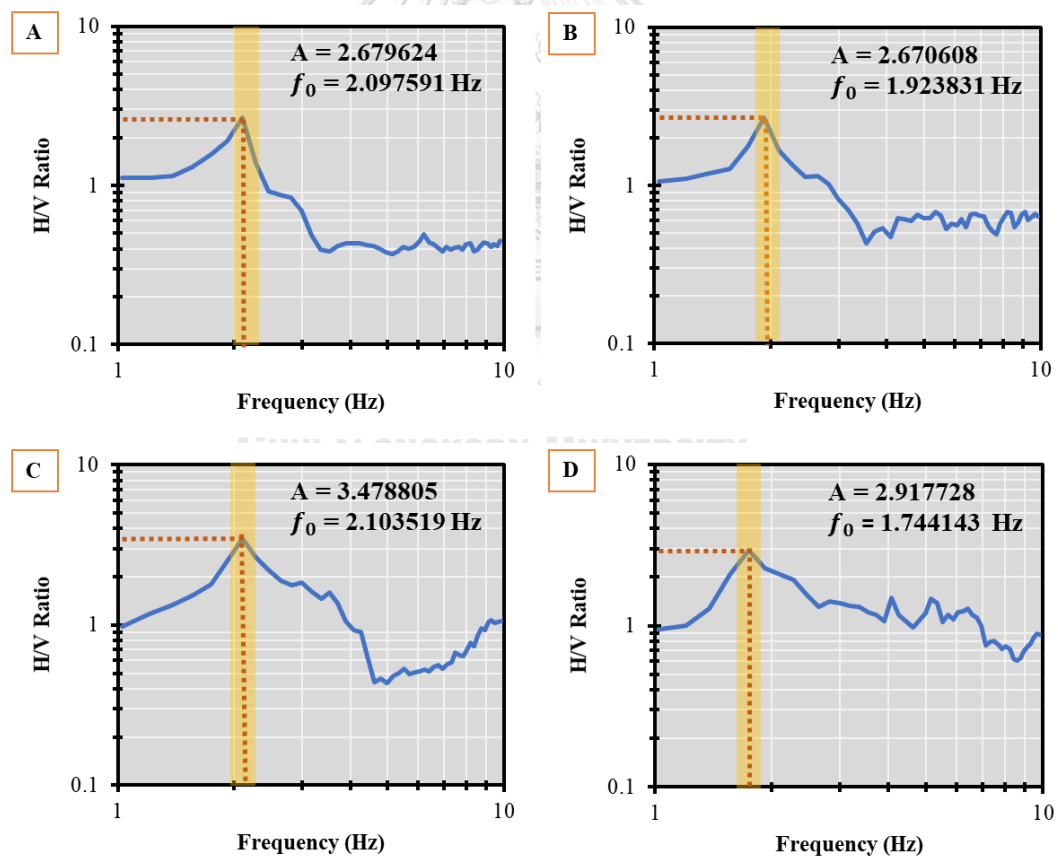
Figure 4.1. The amplitude versus frequency (A) CU site (B) KU site (C) AIT site (D) BKK site

Generally, the results spectra from microtremor have clear peaks which reflects there are two effects from deep and shallow soil in lower and higher period (Acerra et al., 2004). As the shown in Figure 4.1. The microtremor conducted in the Bangkok subsoil resulted narrow variations in the fundamental frequency which is about 1.744 – 2.103 Hz. The result of the predominant frequency of sediments are indicated as medium sediment at investigated area. The peaks of H/V graph produce the predominant periods around 0.477 – 0.573 sec.

According to the HV-Inv program, the result of microtremor observation were compared and matched with the inputted data from geological profile and boring log. Furthermore, the inversion would be done by deriving horizontally layer model by iteration procedure. From the inversion, the result of best-fit model of shear wave velocity will be determined (Poovarodom & Jirasakjamroonsri, 2016). H/V graph of inversion were resulted from the H/V ratio and frequency interpretation. The result of the comparison of H/V Ratio between H/V measurement and H/V inversion from the analysis is shown in Figure 4.2.

Based to inversion analysis in Figure 4.2, the result of H/V measurement graph in all station are not perfectly match with H/V Inversion graph because of the uncertainty of geological profile reaching depth 500 m. However, the trend of the both graphs are relatively same. The graph from the inversion analysis is stronger than the real condition (Souriau et al., 2011). The input of soil profile to generate the shear wave velocity profile is generated according to several data like boring log and geological profile.
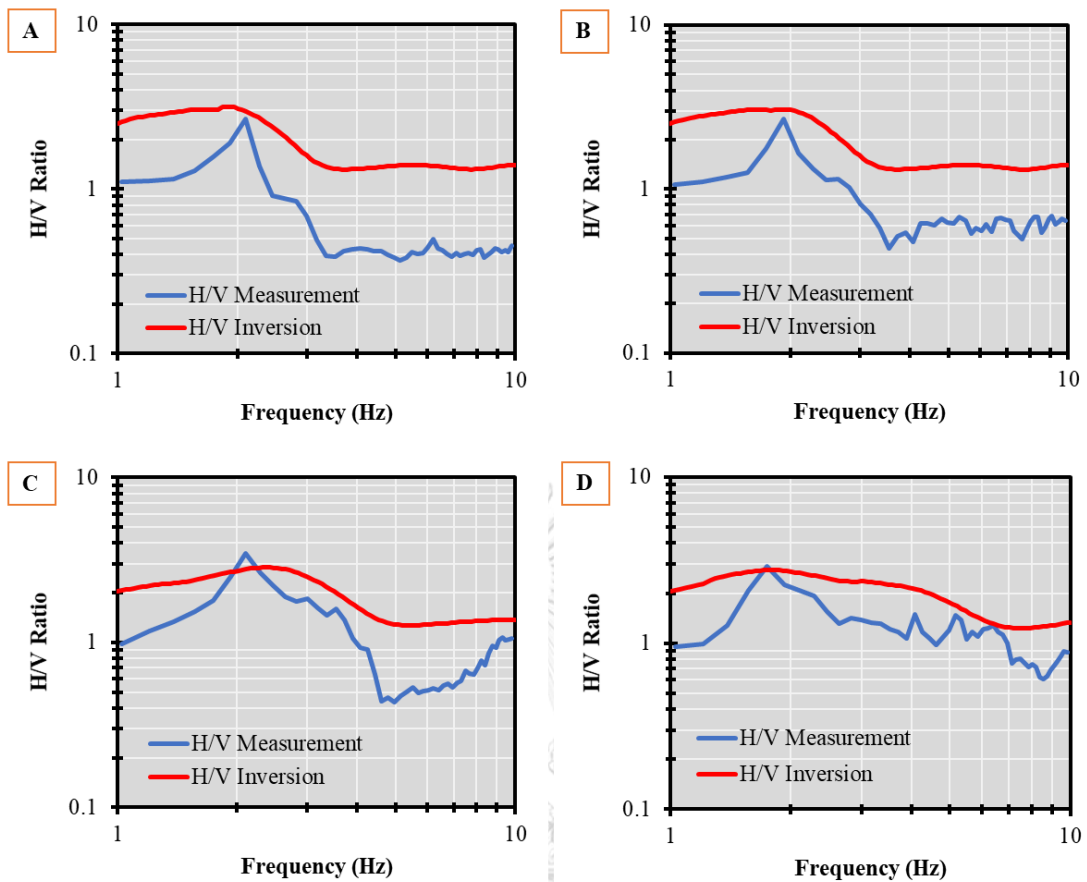
Figure 4.2. The comparison of H/V Ratio between H/V measurement and H/V inversion (A) CU site (B) KU site (C) AIT site (D) BKK site

4.2. Predominant Frequency and Shear Wave Velocity Profile

Nakamura (1989) had been released of his study that the amplification factor of the site probably can be estimated from the vertically incident S-wave. Observation of the site by using the microtremor with the one three-component sensor show the shear wave velocity profile from the HVSR of microtremors. The result of thickness and shear wave velocity is computed from H/V inversion method which are shown in Figure 4.3.
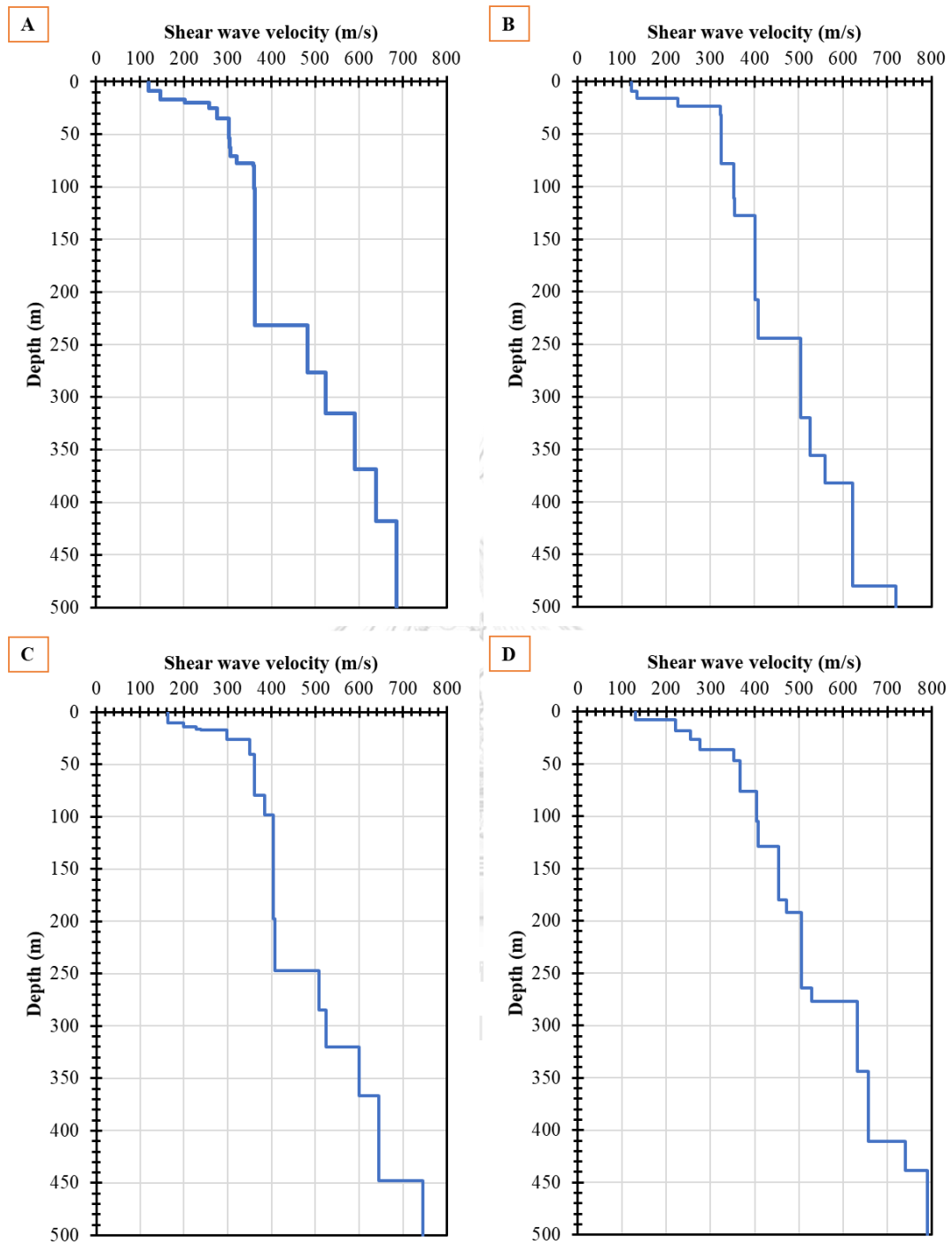
Figure 4.3. Results of Shear Wave Velocity derived from H/V Inversion (A) CU site (B) KU site (C) AIT site (D) BKK site

The Vs profile at CU site is presented in Table 4.1.

Table 4.1. Shear wave velocity from H/V inversion of CU sites

No	Soil Profile	Thickness (m)	Vp (m/s)	Vs (m/s)	Unit Weight (kN/m³)	Vs from boring log
1	Clay, trace fine sand	8.717	299.272	120.176	19.46	77.81
2	Silty clay trace fine sand	8.381	400.000	146.897	18.70	147.55
3	Silty clay trace fine sand	3.026	498.584	202.828	19.91	248.48
4	Silty clay trace fine sand	5.227	673.433	258.764	18.17	280
5	Fine sand and fine to medium sand	9.624	586.434	275.679	18.80	266.51
6	Silty clay trace fine sand	18.811	783.737	302.662	18.30	348.99
7	Fine sandy clay	8.639	793.896	304.870	18.89	401.23
8	Clayey fine sand	8.480	639.646	307.035	19.75	280
9	Silty clay trace fine sand	6.862	794.217	321.468	18.21	348.99
10	Clayey fine sand	1.742	847.872	358.822	19.58	392.82
11	Fine to medium sand and clayey sand	22.194	717.615	360.414	19.68	331.32
12	Sand	93.919	783.666	362.291	18.67	Geological Profile
13	Clay	35.777	892.916	362.889	18.18	Geological Profile
14	Sand	45.066	1019.330	482.143	18.73	Geological Profile
15	Clay	38.820	1019.497	523.203	19.91	Geological Profile
16	Sand	53.037	1148.614	589.799	18.39	Geological Profile
17	Sand	49.687	1228.521	638.634	19.66	Geological Profile
18	Sand	90.089	1443.960	686.233	21.98	Geological Profile

The Vs profile at KU site is presented in Table 4.2.

Table 4.2. Shear wave velocity from H/V inversion of KU sites

No	Soil Profile	Thickness (m)	Vp (m/s)	Vs (m/s)	Unit Weight (kN/m^3)	Vs from boring log
1	Silty clay	8.886	298.160	120.945	19.824	119.9
2	Clay	6.757	393.652	133.913	19.697	152.78
3	Silty clay	7.684	595.890	227.437	19.207	266.51
4	Silty fine sand	8.157	663.012	323.717	19.603	331.31
5	Clay	46.317	796.132	324.992	19.059	Geological Profile
6	Clay	33.426	890.310	352.636	18.450	Geological Profile
7	Sand	16.404	852.876	355.765	18.912	Geological Profile
8	Sand	80.059	943.013	401.210	19.794	Geological Profile
9	Clay	36.176	999.575	408.066	19.495	Geological Profile
10	Sand	76.068	1039.015	504.521	19.731	Geological Profile
11	Clay	35.549	1169.037	525.361	18.805	Geological Profile
12	Sand	26.171	1383.909	560.414	19.190	Geological Profile
13	Sand	98.396	1370.431	622.204	18.479	Geological Profile
14	Sand	22.823	1391.562	696.984	18.363	Geological Profile

The Vs profile at AIT site is presented in Table 4.3.

Table 4.3. Shear wave velocity from H/V inversion of AIT sites

No	Soil Profile	Thickness (m)	Vp (m/s)	Vs (m/s)	Unit Weight (kN/m³)	Vs from Boring log
1	Silty clay	9.999	399.932	163.182	19.860	104.12
2	Silty clay	4.258	540.336	200.093	18.150	239.55
3	Silty sand	2.128	462.136	228.689	18.248	370.7
4	Silty clay	1.019	588.302	238.702	19.331	257.48
5	Clayey fine sand	8.487	578.175	298.178	19.266	236.11
6	Dense sand	14.565	719.058	351.029	18.929	331.32
7	Clay	39.247	883.538	360.595	18.605	363.426
8	Sand	18.380	869.233	384.928	18.253	Geological Profile
9	Sand	99.552	953.495	403.844	19.253	Geological Profile
10	Clay	49.810	998.740	407.691	19.653	Geological Profile
11	Sand	37.198	1212.110	507.963	20.000	Geological Profile
12	Clay	35.364	1299.446	523.620	18.458	Geological Profile
13	Sand	46.406	1286.460	600.504	19.503	Geological Profile
14	Sand	81.526	1321.475	644.245	18.236	Geological Profile
15	Sand	85.271	1415.737	745.826	21.686	Geological Profile

The Vs profile at BKK site is presented in Table 4.4.

Table 4.4. Shear wave velocity from H/V inversion of BKK sites

No	Soil Profile	Thickness (m)	Vp (m/s)	Vs (m/s)	Unit Weight (kN/m³)	Vs from Boring log
1	soft silty clay, trace of shell bits	8.166	318.510	129.542	19.897	110.11
2	stiff silty clay	9.912	586.985	221.598	19.204	250.03
3	Dense clayey sand	8.577	605.390	254.797	18.231	359.24
4	Hard silty clay, gravel	10.000	691.775	276.150	19.516	272.71
5	Dense sand	10.000	837.943	353.363	19.048	365.73
6	Clay	29.570	880.473	366.673	20.000	Geological Profile
7	Clay	28.210	997.700	403.599	18.439	Geological Profile
8	Sand	24.571	903.738	407.853	18.817	Geological Profile
9	Sand	50.956	1021.927	454.784	18.116	Geological Profile
10	Clay	12.237	1179.861	472.644	19.078	Geological Profile
11	Sand	72.120	1180.951	505.873	19.785	Geological Profile
12	Clay	12.747	1297.683	529.760	18.041	Geological Profile
13	Sand	66.825	1249.252	632.288	18.297	Geological Profile
14	Sand	66.798	1296.824	656.707	19.233	Geological Profile
15	Sand	27.555	1395.230	741.474	20.737	Geological Profile
16	Sand	61.985	1952.805	813.631	19.364	Geological Profile

The result of predominant period and shear wave velocity in 30 m depth are fit with the predominant period and shear wave velocity in 30 m depth result of Bangkok from Poovarodom and Plalinyot (2015) about 0.2 – 1.1 sec as shown in Table 4.1 and Figure 4.4. In term of dynamic properties of sediment, shear wave velocity and predominant period are the main factor that influence the ground motion at the site. Furthermore, shear wave velocity at 30 m depth (V_{S30}) is calculated because amplification is happened in this depth most of the time.

Table 4.5. The result of shear-wave velocity (V_S) in the top 30 m depth and predominant period

Site	V_{S30} from boring log (m/s)	V_{S30} from H/V Inversion (m/s)	Predominant Period (s)	Class Site (NEHRP)
Bangkok Metropolitan (Poovarodom and Playinyot, 2015)		70-220	0.2-1.1	D-E
CU	142.092	167.4005	0.476737	E
KU	179.3952	164.0107	0.519796	E
AIT	171.9507	173.8116	0.475394	E
BKK	152.9823	168.8778	0.573347	E
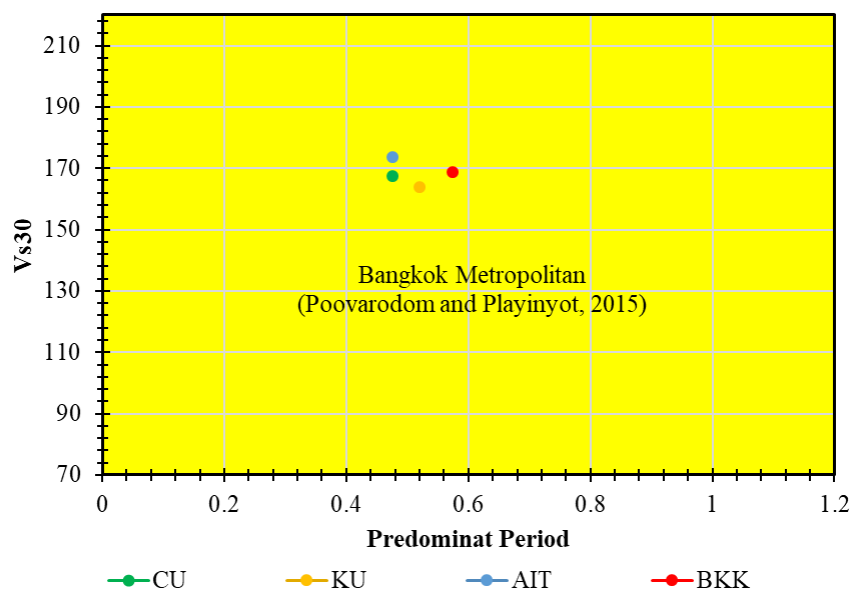
Figure 4.4. Comparison shear wave velocity vs predominant period results to Bangkok Metropolitan in general (Poovarodom and Playinyot, 2015)

4.3. Equivalent Linear Site response analysis

4.3.1. Spectral Acceleration of seismic response analysis

The result of spectral accelerations of soil surface due to the earthquake on each site are presented in Figure 4.5 for M_W 5 of earthquake, Figure 4.6 for M_W 6.2 of earthquake and Figure 4.7 of M_W 7.5 of earthquake.
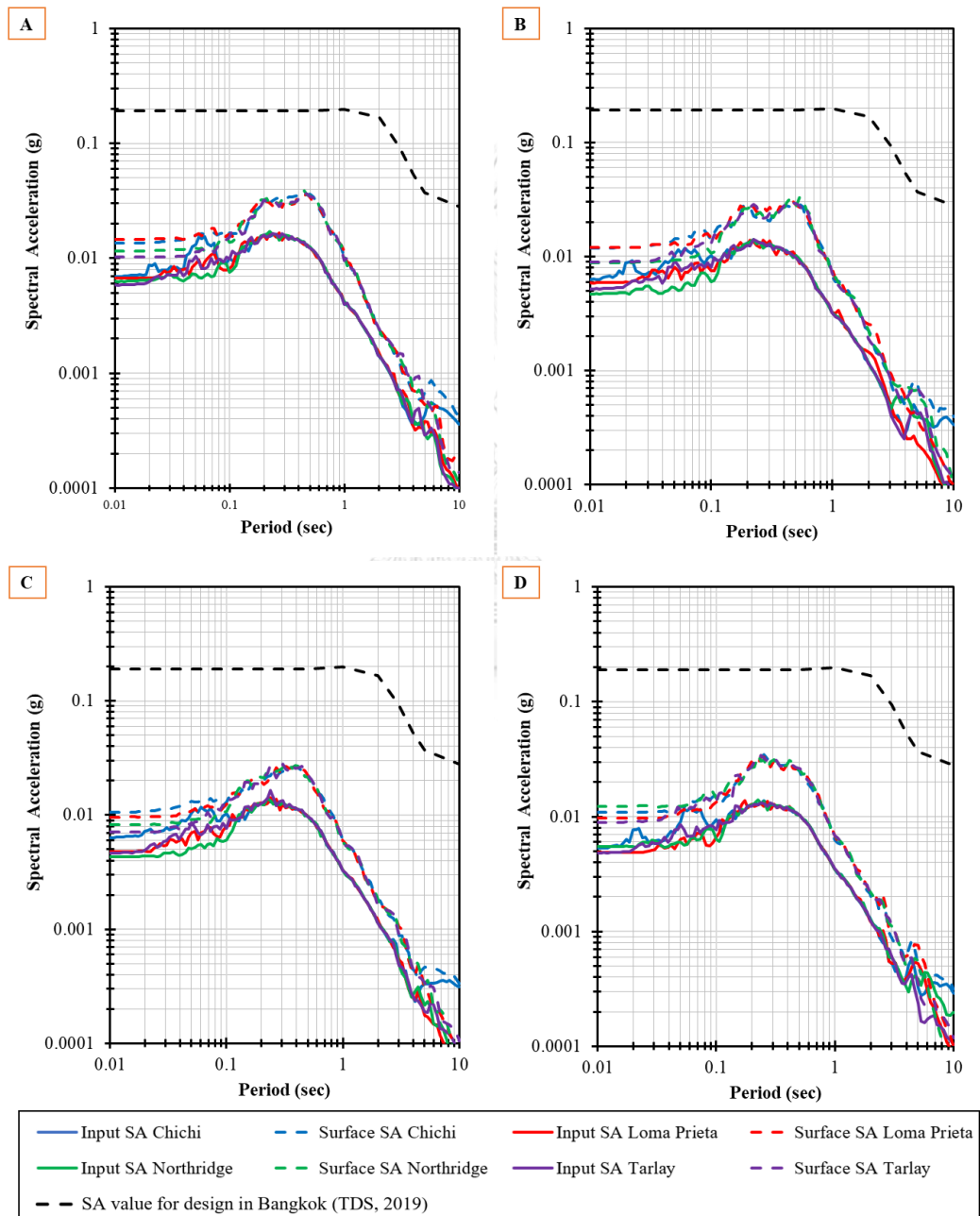
Figure 4.5. Spectral acceleration of M_W 5 of earthquake comparison on each site (A) CU site (B) KU site (C) AIT site (D) BKK site
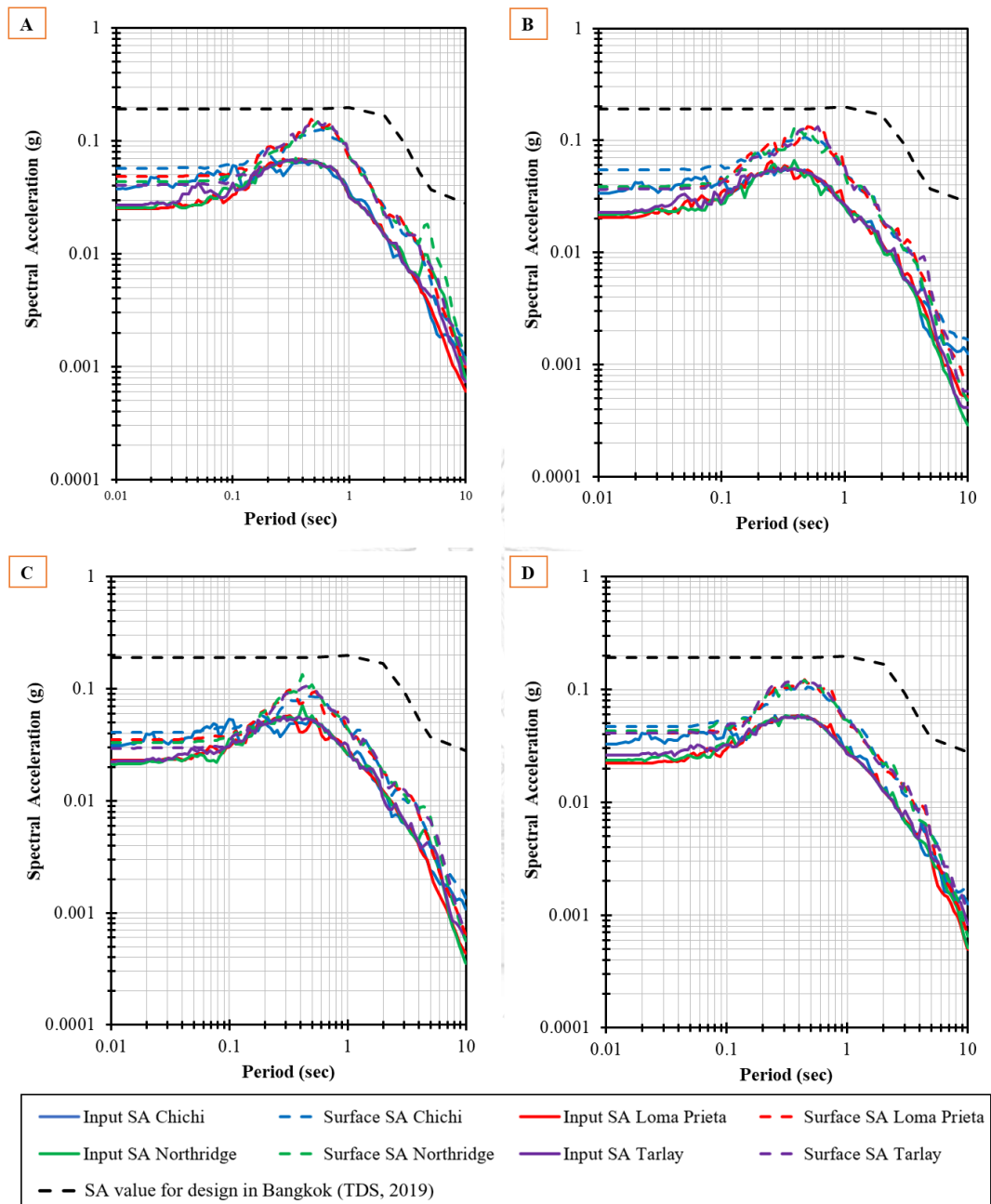
*Figure 4.6. Spectral acceleration of M$_W$ 6.2 of earthquake comparison on each site
(A) CU site (B) KU site (C) AIT site (D) BKK site*
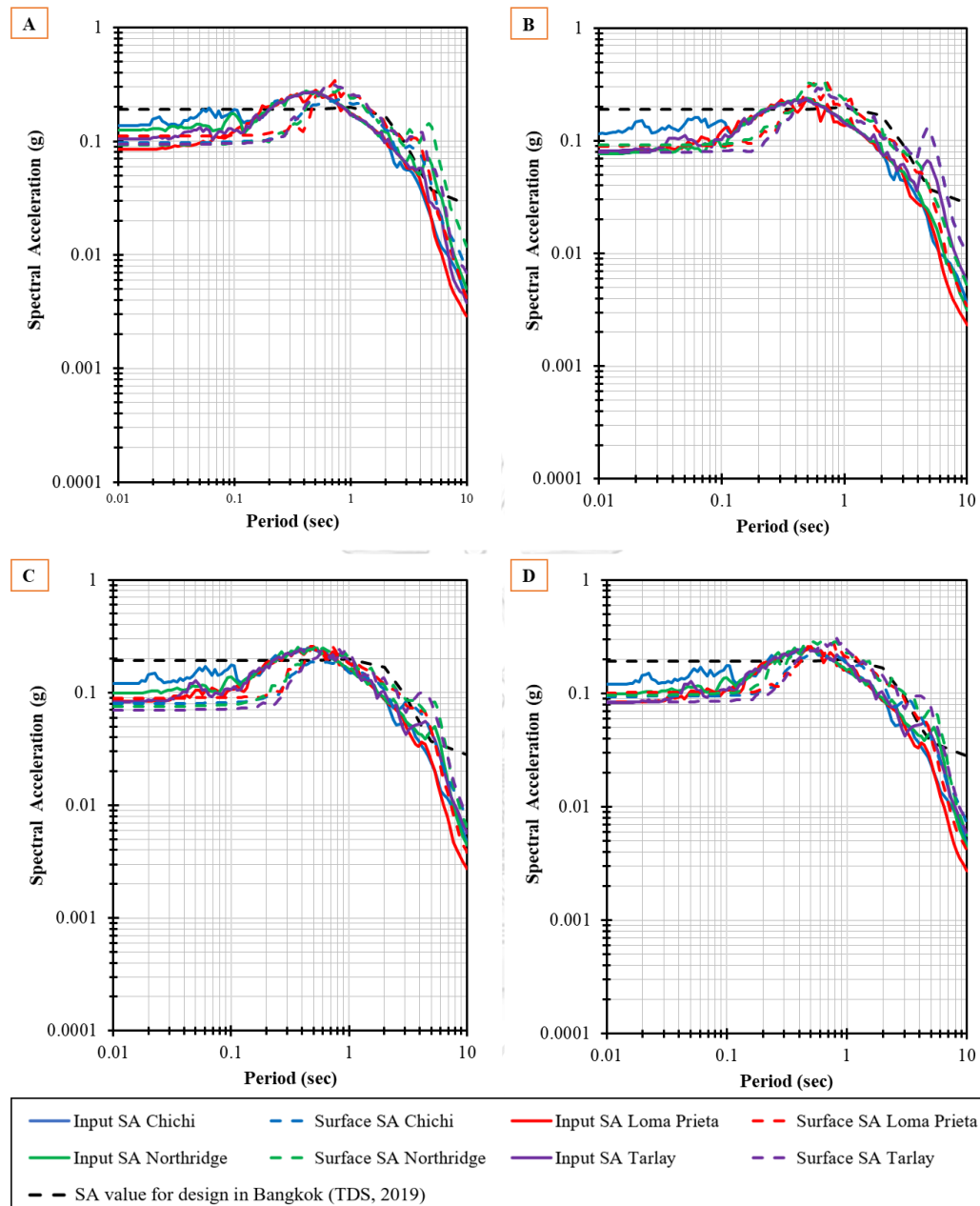
Figure 4.7. Spectral acceleration of M$_W$ 7.5 of earthquake comparison on each site (A) CU site (B) KU site (C) AIT site (D) BKK site

In general, the spectral acceleration at the surface of AIT site has the highest value. The spectral acceleration of the motions at ground surface reaches the maximum spectral acceleration for M$_W$ 5 of earthquake at period of 0.2 to 0.6 sec, for M$_W$ 5 of earthquake at period of 0.4 to 0.6 sec, and for M$_W$ 5 of earthquake at period of 0.6 to 0.8 sec. Based on increasing of the magnitude, the results of spectral acceleration are increasing followed with the increasing of period.

The detailed explanation of the result of spectral acceleration is presented in Table 4.6 for M_W 5 of earthquake, Table 4.7 for M_W 6.2 of earthquake and Table 4.8 for M_W 7.5 of earthquake and explained following below

1. CU sites

   The peak spectral acceleration of CU sites M_W 5-7.5 of earthquake is 0.2–0.8 s period. The peak spectral accelerations occur at the minimum period of 0.416 s of M_W 5 Loma Prieta Earthquake and maximum period of 0.825 s of 7.5 M_W Northridge Earthquake. The peak of spectral acceleration is 0.342 g of 7.5 M_W Loma Prieta Earthquake.

2. KU sites

   The peak spectral acceleration of KU sites M_W 5-7.5 of earthquake is 0.2–0.7 s period. The peak spectral accelerations occur at the minimum period of 0.443 s of 5 M_W Tarlay Earthquake and maximum period of 0.728 s of 7.5 M_W Loma Prieta Earthquake. The peak of spectral acceleration is 0.344 g of 7.5 M_W Northridge Earthquake.

3. AIT sites

   The peak spectral acceleration of AIT sites M_W 5-7.5 of earthquake is 0.2–0.8 s period. The peak spectral accelerations at M_W 5 occur at the minimum period of 0.305 s of 5 M_W Loma Prieta and Tarlay Earthquake and maximum period of 0.825 s of 7.5 M_W Tarlay Earthquake. The peak of spectral acceleration is 0.267 g of 7.5 M_W Northridge Earthquake.

4. BKK sites

   The peak spectral acceleration of BKK sites with M_W 5-7.5 of earthquake is 0.2–0.8 s period. The peak spectral accelerations occur at the minimum period of 0.224 s of 5 M_W Northridge Earthquake and maximum period of 0.824 s of 7.5 M_W Tarlay Earthquake. The peak of spectral acceleration is 0. 0.308 g of 7.5 M_W Tarlay Earthquake.

Table 4.6. The result of maximum spectral acceleration on natural period at M_w 5 of earthquake

CU							
Chichi		Loma Prieta		Northridge		Tarlay	
Period (s)	Sa (g)	Period (s)	Sa (g)	Period (s)	Sa (g)	Period (s)	Sa (g)
0.2	0.0302	0.2	0.0327	0.2	0.03219	0.2	0.03197
0.5	0.0364	0.4	0.0363	0.4	0.03909	0.4	0.0375
1.0	0.0103	1.0	0.0116	1.0	0.01059	1.0	0.00955
KU							
Chichi		Loma Prieta		Northridge		Tarlay	
Period (s)	Sa (g)	Period (s)	Sa (g)	Period (s)	Sa (g)	Period (s)	Sa (g)
0.2	0.028	0.2	0.029	0.2	0.026	0.2	0.026
0.5	0.0290	0.5	0.03062	0.5	0.03344	0.4	0.03019
1.0	0.007	1.0	0.008	1.0	0.007	1.0	0.007
AIT							
Chichi		Loma Prieta		Northridge		Tarlay	
Period (s)	Sa (g)	Period (s)	Sa (g)	Period (s)	Sa (g)	Period (s)	Sa (g)
0.2	0.021	0.2	0.02003	0.2	0.02147	0.2	0.0206
0.3	0.027	0.3	0.028	0.3	0.028	0.3	0.028
1.0	0.006	1.0	0.006	1.0	0.006	1.0	0.006
BKK							
Chichi		Loma Prieta		Northridge		Tarlay	
Period (s)	Sa (g)	Period (s)	Sa (g)	Period (s)	Sa (g)	Period (s)	Sa (g)
0.2	0.027	0.2	0.029	0.2	0.027	0.2	0.027
0.3	0.035	0.3	0.034	0.3	0.034	0.3	0.034
1.0	0.006	1.0	0.007	1.0	0.007	1.0	0.007

Table 4.7. The result of maximum spectral acceleration on natural period at M_W 6.2 of earthquake

CU							
Chichi		Loma Prieta		Northridge		Tarlay	
Period (s)	Sa (g)	Period (s)	Sa (g)	Period (s)	Sa (g)	Period (s)	Sa (g)
0.2	0.082	0.2	0.088	0.2	0.074	0.2	0.084
0.6	0.125	0.5	0.156	0.5	0.147	0.4	0.149
1.0	0.073	1.0	0.071	1.0	0.073	1.0	0.074
KU							
Chichi		Loma Prieta		Northridge		Tarlay	
Period (s)	Sa (g)	Period (s)	Sa (g)	Period (s)	Sa (g)	Period (s)	Sa (g)
0.2	0.077	0.2	0.076	0.2	0.081	0.2	0.071
0.5	0.107	0.5	0.132	0.4	0.129	0.6	0.132
1.0	0.049	1.0	0.052	1.0	0.051	1.0	0.059
AIT							
Chichi		Loma Prieta		Northridge		Tarlay	
Period (s)	Sa (g)	Period (s)	Sa (g)	Period (s)	Sa (g)	Period (s)	Sa (g)
0.2	0.056	0.2	0.064	0.2	0.062	0.2	0.051
0.5	0.085	0.3	0.097	0.4	0.133	0.4	0.105
1.0	0.042	1.0	0.043	1.0	0.044	1.0	0.053
BKK							
Chichi		Loma Prieta		Northridge		Tarlay	
Period (s)	Sa (g)	Period (s)	Sa (g)	Period (s)	Sa (g)	Period (s)	Sa (g)
0.2	0.071	0.2	0.074	0.2	0.075	0.2	0.083
0.5	0.105	0.24	0.122	0.4	0.121	0.4	0.118
1.0	0.051	1.0	0.049	1.0	0.053	1.0	0.049

Table 4.8. The result of maximum spectral acceleration on natural period at M$_W$ 7.5 of earthquake

CU							
Chichi		Loma Prieta		Northridge		Tarlay	
Period (s)	Sa (g)	Period (s)	Sa (g)	Period (s)	Sa (g)	Period (s)	Sa (g)
0.2	0.104	0.2	0.118	0.2	0.098	0.2	0.101
0.8	0.232	0.7	0.342	0.8	0.294	0.7	0.313
1.0	0.217	1.0	0.244	1.0	0.237	1.0	0.253
KU							
Chichi		Loma Prieta		Northridge		Tarlay	
Period (s)	Sa (g)	Period (s)	Sa (g)	Period (s)	Sa (g)	Period (s)	Sa (g)
0.2	0.083	0.2	0.101	0.2	0.119	0.2	0.083
0.7	0.299	0.7	0.325	0.7	0.344	0.7	0.299
1.0	0.223	1.0	0.202	1.0	0.231	1.0	0.223
AIT							
Chichi		Loma Prieta		Northridge		Tarlay	
Period (s)	Sa (g)	Period (s)	Sa (g)	Period (s)	Sa (g)	Period (s)	Sa (g)
0.2	0.092	0.2	0.094	0.2	0.088	0.2	0.079
0.6	0.186	0.7	0.255	0.6	0.266	0.8	0.241
1.0	0.151	1.0	0.182	1.0	0.201	1.0	0.212
BKK							
Chichi		Loma Prieta		Northridge		Tarlay	
Period (s)	Sa (g)	Period (s)	Sa (g)	Period (s)	Sa (g)	Period (s)	Sa (g)
0.2	0.107	0.2	0.111	0.2	0.118	0.2	0.099
0.6	0.217	0.7	0.276	0.6	0.286	0.8	0.307
1.0	0.183	1.0	0.211	1.0	0.225	1.0	0.245

In general, the result ranges reflect the natural period of 2 to 5 stories of concrete building for M_W 5 of earthquake, 4 to 6 stories of concrete building for M_W 6.2 earthquake, and 6 to 8 stories of concrete building for M_W 7.5 earthquake, based on this following equation below

$$Tn = 0.1n$$

Equation 24

Where n is the stories number. According to that results, the ground motion can make serious damage to the medium stories building in Bangkok for M_W 7.5 of earthquake. Figure 4.5, Figure 4.6, and Figure 4.7 also compare the results spectral acceleration to the spectral acceleration design for Bangkok by TDS (2019). The results show the spectral acceleration at the M_W 5 and M_W 6.2 of ground motion are not exceeding the spectral acceleration design for Bangkok at both the short and long period. In the other hand, the spectral acceleration M_W 7.5 of ground motion is exceeding the spectral acceleration design for Bangkok at both the short and long period. The Bangkok soft clay filter the predominant period of ground shaking about 1 sec. The shaking period matches with the natural period of 10-20 stories buildings. Due to the resonance effect, the building of Bangkok about 2-8 stories will tent to respond. The low-medium rise building in Bangkok are more susceptible to damages compared to the high rises building.

According to the previous research by Warnitchai et al. (2000), the result spectral acceleration in Bangkok Metropolitan subsoil is about 0.005 – 0.09. That is consistent with the result in this research about 0.028 g – 0.039 g. The detail of comparison is shown in Table 4.9 and Figure 4.8.

Table 4.9. The comparison of spectral acceleration result with previous research

Magnitude (M$_W$)	Source to Site Distance (km)	Total soil thickness (m)	Rock Vs (m/s)	Spectral Acceleration (g)	Predominant Period (s)	Site
7-8	80-350	80-300	900	0.005 - 0.09	0.5 - 2	Bangkok (Warnitchai et al., 2000)
7-8	Input 0.2g	80-300	900	0.2 – 0.4	0.5-4	Bangkok (Poovarodom et al., 2016)
6.8	700	30	1100	0.008-0.01	0.2-0.8	Bangkok (Plengsiri, 2018)
5-7.5	119	500	760	0.039-0.342	0.502-0.824	CU
5-7.5	120	500	760	0.033-0.344	0.534-0.728	KU
5-7.5	123	500	760	0.028-0.266	0.253-0.824	AIT
5-7.5	128	500	760	0.034-0.307	0.253-0.824	BKK
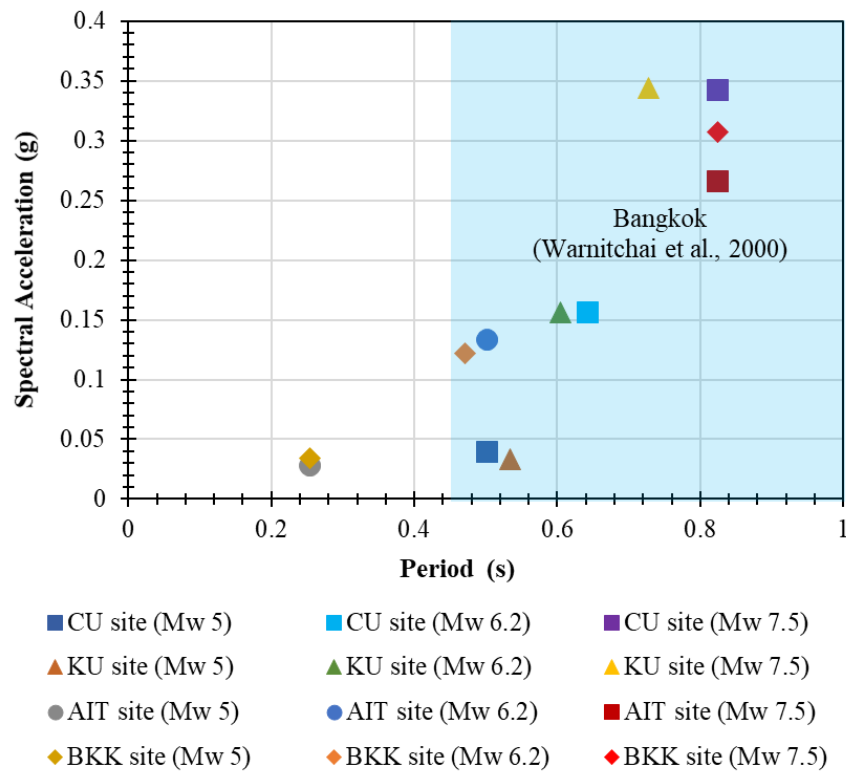
Figure 4.8. Spectral acceleration vs period results compared to Bangkok Metropolitan in general

4.3.2. PGA of seismic response analysis

Table 4.10, Table 4.11, and Table 4.12 show the results of PGA input and PGA at ground surface in each site in different input motion and different magnitude of earthquake M_W 5, M_W 6.2, and M_W 7.3 respectively. Those can be calculated of the amplification factor (AF) with the following formula of Equation 24.

$$\frac{\text{PGA at ground surface}}{\text{PGA input}} = AF$$

Equation 25

The highest amplification among all ground surface is CU site and the lowest amplification among all ground surface is AIT site in all input motions of M_W 5 and M_W 6.2 applied. The amplification factor in all the sites research are about 1.5372 - 2.5220 for M_W 5 of earthquake, 1.318 – 1.920 for M_W 6.2 of earthquake and 0.750 – 1.306 for M_W 7.5 of earthquake. Some of sites of that were inputted M_W 7.5 of earthquake occur de-amplification.

The detailed explanation of the result of peak ground acceleration is shown in following below

1. CU sites

   The example result of ground acceleration versus time as the comparison of input motion and ground surface motion for M_W 5 of earthquake at CU sites is shown in Figure 4.9. The result of PGA at ground surface at CU sites from M_W 5 and M_W 6.2 of earthquake are amplified in all earthquake input with amplification factor range is 1.577 - 2.155. The highest amplification comes from the Loma Prieta earthquake. The results of PGA at ground surface at CU sites from M_W 7.5 are occurred de-amplification on Chichi earthquake, Northridge earthquake and Tarlay earthquake.

2. KU sites

   The result of ground acceleration versus time as the comparison of input motion and ground surface motion M_W 5 of earthquake at KU sites is shown in Figure 4.10. The result of PGA at ground surface at KU sites from M_W 5 and M_W 6.2 of earthquake are amplified in all earthquake input with amplification factor range is 1.636 - 2.065. The highest amplification comes from the Loma Prieta earthquake.

The results of PGA at ground surface at KU sites from M_W 7.5 are occurred de-amplification on Chichi earthquake, Northridge earthquake and Tarlay earthquake.

3. AIT sites

The result of ground acceleration versus time as the comparison of input motion and ground surface motion M_W 5 of earthquake at AIT sites is shown in Figure 4.11. The result of PGA at ground surface at AIT sites from M_W 5 and M_W 6.2 of earthquake are amplified in all earthquake input with amplification factor range is 1.318- 2.021. The highest amplification comes from the Loma Prieta earthquake. The results of PGA at ground surface at AIT sites from M_W 7.5 are occurred de-amplification on Chichi earthquake, Northridge earthquake and Tarlay earthquake

4. BKK sites

The result of ground acceleration versus time as the comparison of input motion and ground surface motion M_W 5 of earthquake at BKK sites is shown in Figure 4.12. The result of PGA at ground surface at BKK sites from M_W 5 and M_W 6.2 of earthquake are amplified in all earthquake input with amplification factor range is 1.640 - 2.065. The highest amplification comes from the Northridge earthquake. The results of PGA at ground surface at BKK sites from M_W 7.5 are occurred de-amplification on Chichi earthquake, Northridge earthquake and Tarlay earthquake

Table 4.10. The results of PGA_{max} and amplification factor on each site with $M_W 5$ of earthquake

Chichi Earthquake

Site	V_{S30} (m/s)	PGA input (g)	PGA at ground surface (g)	AF
CU	167.401	0.0067	0.0135	2.003
KU	164.011	0.0058	0.0118	2.035
AIT	173.812	0.0062	0.0102	1.653
BKK	168.879	0.0053	0.0108	2.044

Loma Prieta

Site	V_{S30} (m/s)	PGA input (g)	PGA at ground surface (g)	AF
CU	167.401	0.0068	0.0147	2.155
KU	164.011	0.0058	0.0120	2.065
AIT	173.812	0.0048	0.0096	2.021
BKK	168.879	0.0049	0.0096	1.975

Northridge Earthquake

Site	V_{S30} (m/s)	PGA input (g)	PGA at ground surface (g)	AF
CU	167.401	0.0063	0.0115	1.837
KU	164.011	0.0047	0.0088	1.890
AIT	173.812	0.0042	0.0082	1.961
BKK	168.879	0.0054	0.0122	2.253

Tarlay Earthquake

Site	V_{S30} (m/s)	PGA input (g)	PGA at ground surface (g)	AF
CU	167.401	0.0056	0.011	1.836
KU	164.011	0.0050	0.008	1.789
AIT	173.812	0.0045	0.007	1.581
BKK	168.879	0.0047	0.009	1.896

Table 4.11. The results of PGA$_{max}$ and amplification factor on each site with M$_W$ 6.2 of earthquake

Chichi Earthquake

Site	V$_{S30}$ (m/s)	PGA input (g)	PGA at ground surface (g)	AF
CU	167.401	0.035	0.057	1.629
KU	164.011	0.031	0.054	1.742
AIT	173.812	0.028	0.041	1.464
TMD	168.879	0.026	0.046	1.769

Loma Prieta

Site	V$_{S30}$ (m/s)	PGA input (g)	PGA at ground surface (g)	AF
CU	167.401	0.025	0.048	1.920
KU	164.011	0.021	0.037	1.762
AIT	173.812	0.023	0.035	1.522
TMD	168.879	0.022	0.041	1.864

Northridge Earthquake

Site	V$_{S30}$ (m/s)	PGA input (g)	PGA at ground surface (g)	AF
CU	167.401	0.025	0.043	1.720
KU	164.011	0.022	0.038	1.751
AIT	173.812	0.018	0.029	1.611
TMD	168.879	0.023	0.042	1.826

Tarlay Earthquake

Site	V$_{S30}$ (m/s)	PGA input (g)	PGA at ground surface (g)	AF
CU	167.401	0.026	0.041	1.577
KU	164.011	0.022	0.036	1.636
AIT	173.812	0.022	0.029	1.318
TMD	168.879	0.025	0.041	1.640

Table 4.12. The results of PGA_{max} and amplification factor on each site with M_W 7.5 of earthquake

Chichi Earthquake						Loma Prieta				
Site	V_{S30} (m/s)	PGA input (g)	PGA at ground surface (g)	AF		**Site**	V_{S30} (m/s)	PGA input (g)	PGA at ground surface (g)	AF
CU	167.401	0.137	0.097	0.708		CU	167.401	0.085	0.111	1.306
KU	164.011	0.115	0.105	0.913		KU	164.011	0.081	0.089	1.099
AIT	173.812	0.109	0.080	0.734		AIT	173.812	0.083	0.089	1.072
TMD	168.879	0.120	0.093	0.775		TMD	168.879	0.083	0.101	1.217

Northridge Earthquake						Tarlay Earthquake				
Site	V_{S30} (m/s)	PGA input (g)	PGA at ground surface (g)	AF		**Site**	V_{S30} (m/s)	PGA input (g)	PGA at ground surface (g)	AF
CU	167.401	0.124	0.093	0.750		CU	167.401	0.102	0.093	0.912
KU	164.011	0.076	0.091	1.197		KU	164.011	0.081	0.078	0.963
AIT	173.812	0.085	0.075	0.882		AIT	173.812	0.081	0.071	0.877
TMD	168.879	0.097	0.096	0.990		TMD	168.879	0.081	0.080	0.988

Figure 4.9. The comparison of input ground motion and surface ground motion of M_W 5 earthquake at CU site (A) Chichi Earthquake (B) Loma Prieta Earthquake (C) Northridge Earthquake (D) Tarlay Earthquake

Figure 4.10. The comparison of input ground motion and surface ground motion M_W 5 earthquake at TU site (A) Chichi Earthquake (B) Loma Prieta Earthquake (C) Northridge Earthquake (D) Tarlay Earthquake

Figure 4.11. The comparison of input ground motion and surface ground motion $M_W 5$ earthquake at AIT site (A) Chichi Earthquake (B) Loma Prieta Earthquake (C) Northridge Earthquake (D) Tarlay Earthquake
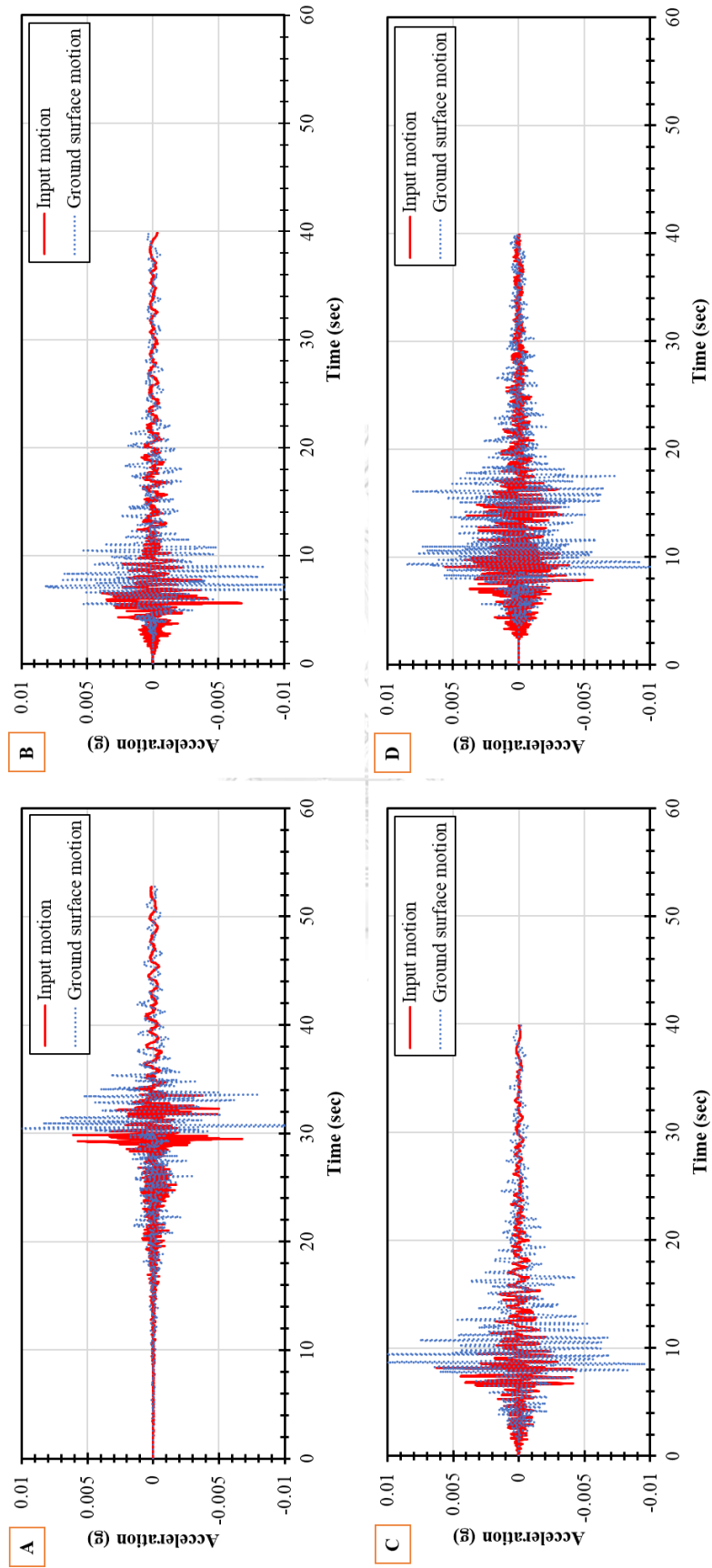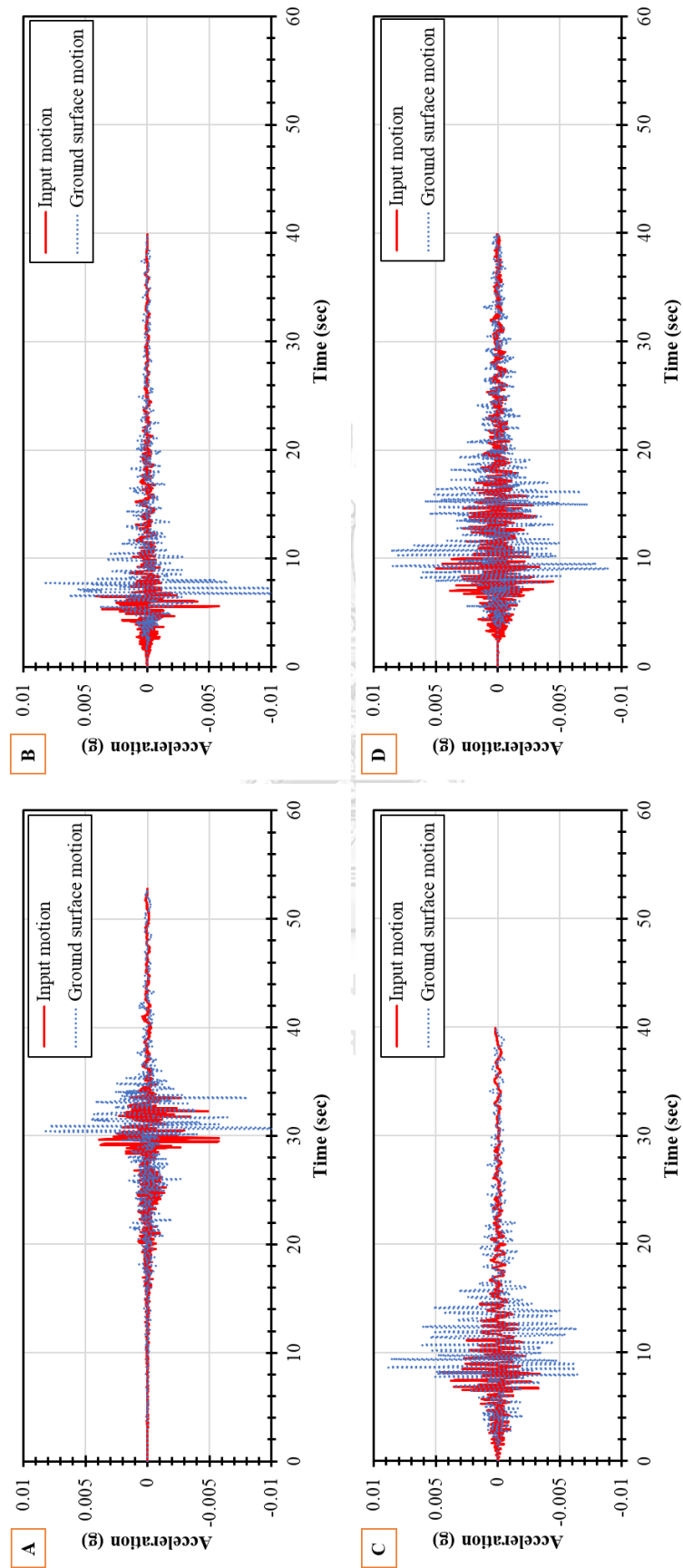
Figure 4.12. The comparison of input ground motion and surface ground motion Mw 5 earthquake at BKK site (A) Chichi Earthquake (B) Loma Prieta Earthquake (C) Northridge Earthquake (D) Tarlay Earthquake
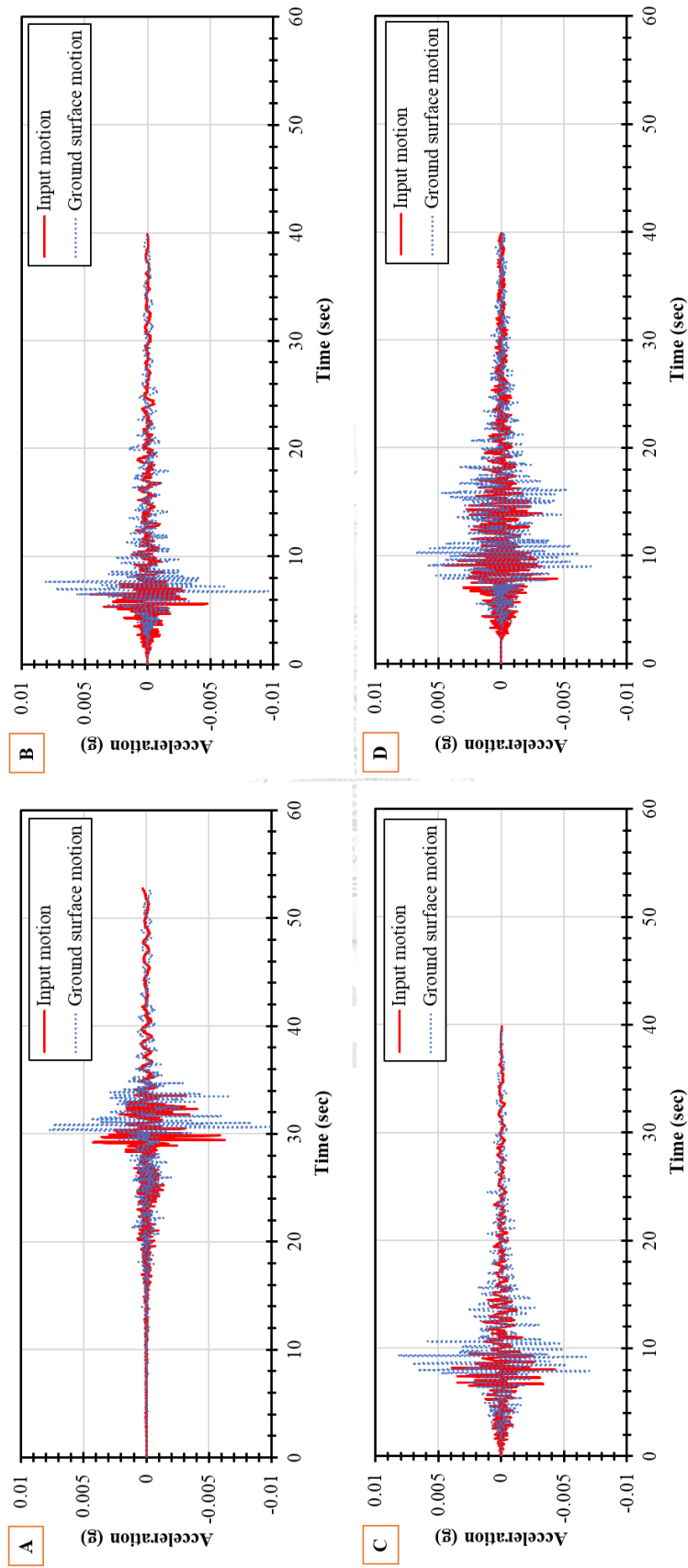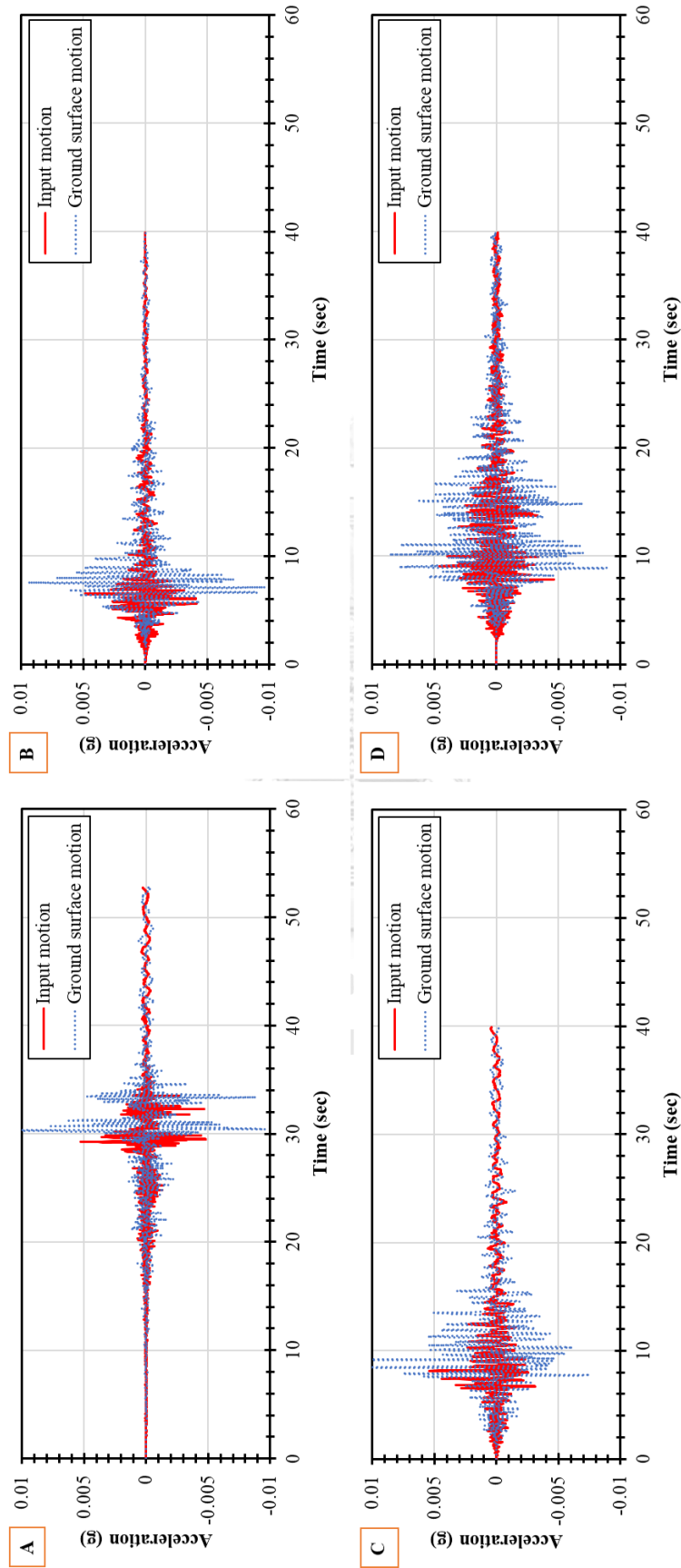
In general, the motions that inputted and analyzed in the sites show higher at the ground surface especially in the sites with M_W 5 and M_W 6.2 of earthquake applied. Those indicate that amplification of motion on the site. Among all ground motions, the Chichi earthquake motions undergo the largest amplification with M_W 5. According to the increasing of earthquake magnitude, the amplification result would decrease and some of sites occur de-amplification. Basically, amplification factor results in this research are quite low due to the earthquake magnitude for input motion and depth and shear wave velocity of bedrock assumption.

Based on the previous research by Warnitchai et al. (2000), the amplification factor range in Bangkok Metropolitan subsoil is 2.8-3.9. The same statement also coming from Choi and Stewart (2005) that the soil layer with $V_{S30}<180$ m/s can increase the earthquake power. The results of the research are corresponding with the previous study that Bangkok Metropolitan area that Bangkok subsoil could amplify for low intensity input motion about 3-6 times from input motion. The amplification results are quite similar to amplification factor in Mexico City due to Michoacan earthquake and San Francisco Bay Area due to Loma Prieta earthquake reaching 2-5 times. It confirmed that the amplification factor will be variative with input motion. During the 1985 Michoachan earthquake, the wave propagated upward from the bedrock and showed the significant amplification in soft clay layer. Those places have similarity of site condition with Bangkok city that has thick soft clay.

Figure 4.13. shows that the result of the peak ground acceleration controls the weak layer. It means the shear-strength the layer influences the acceleration at the ground surface. According to Yoshida (2015), the existence of soft soil is the main role that control the amplification. Considering the different V_{S30} on each station, V_{S30} is not always consistent with the amplification factor as shown in Figure 4.14 with the comparison from previous research as mention in Table 4.13. The different trend between the result of amplification and V_{S30} is caused by differences the thickness and abundance of soft soil in every site. Warnitchai et al. (2000) have been explained that the bedrock depth and shear wave velocity effect on the results amplification factor. In the other hand, the amplification had been observed in Bangkok city based on the variation of shear wave velocity (Plengsiri, 2018). The result show that there is variation shear wave velocity give the significant effect of amplification factor.
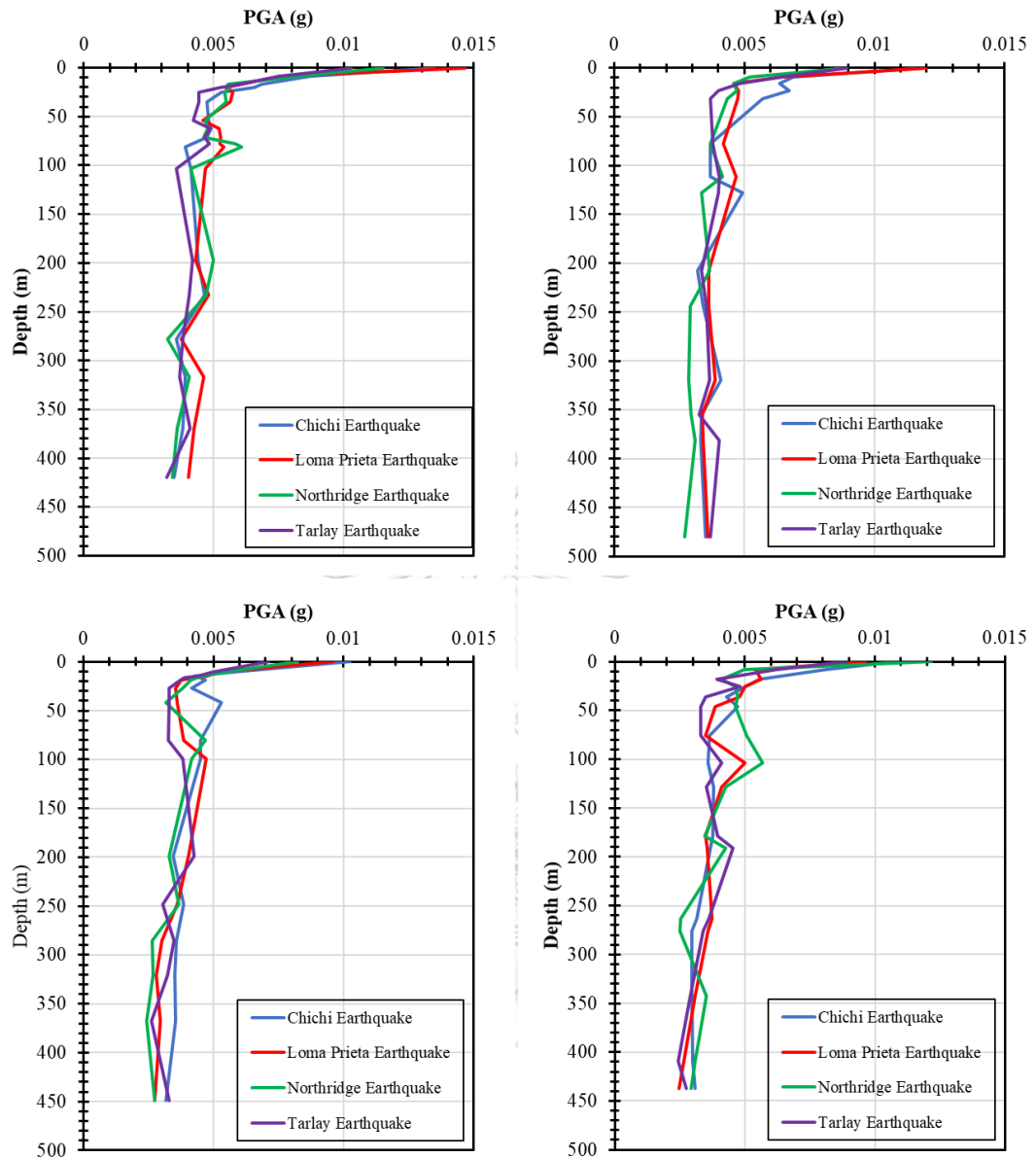
Figure 4.13. The example of peak ground acceleration versus depth from M_W 5 of earthquake at (A) CU site (B) KU site (C) AIT site (D) BKK site

Table 4.13. The amplification factor results from previous research

Magnitude (Mw)	Site	Input PGA (g)	Output PGA (g)	AF	V$_{S30}$ (m/s)	Model
7-8	Bangkok (Ashford et al., 2000)	0.02-0.1	0.05 - 0.3	2-4.2	110-170	EQL
7-8	Bangkok (Warnichai et al., 2000)	0.015-0.1	0.056-0.26	2.8 - 3.9	110-170	EQL
6.8	Bangkok (Plengsiri, 2018)	0.00089g	0.0020-0.0045	2.3 – 5.1	107-169	NL
5-7.5	CU	0.006-0.137	0.014-0.111	1.306-2.154	167.401	EQL
5-7.5	KU	0.005-0.115	0.009-0.105	1.197 - 2.064	164.011	EQL
5-7.5	AIT	0.004-0.089	0.010-0.089	1.072-2.021	173.812	EQL
5-7.5	BKK	0.005-0.121	0.011-0.101	1.217-2.254	168.879	EQL
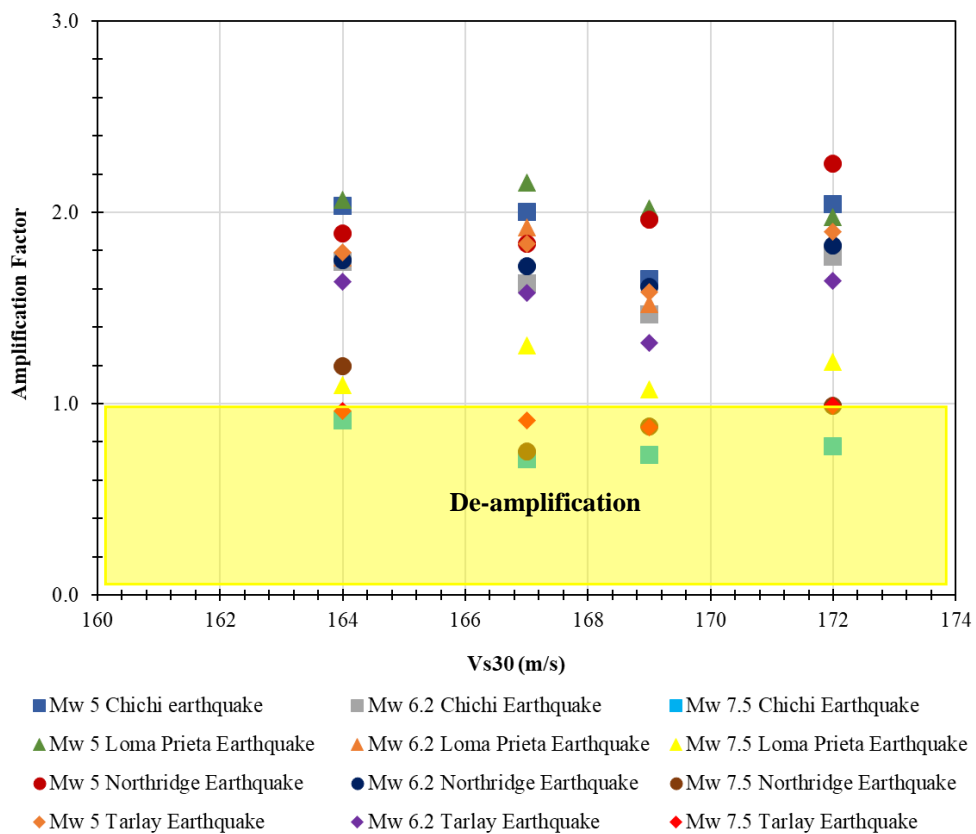
Figure 4.14. The comparison of amplification factor and V$_{S30}$ on each site

CHAPTER 5
CONCLUSIONS AND RECOMENDATIONS

5.1. Conclusions

This research presents the one-dimensional site response analysis on several sites in Bangkok due to the seismic activity from the Three Pagodas Fault in the western Thailand. An equivalent linear site response analysis combined with seismic hazard concept is performed to the site.

1. This study was performed the site response of the Bangkok city during the earthquake that triggered by the Three Pagodas Fault. The microtremor is conducted to obtain the shear wave velocity profile underlaying of Bangkok subsoil reaching the bedrock (around 500 m) based on the model of H/V inversion. In general, the investigated sites are dominated by soft clay layer with Site Class E.

2. The results of the one-dimensional site response analysis of spectral acceleration at the ground surface are larger than the input motion of M_W 5, M_W 6.2 and M_W 7.5 of earthquake. It reflects that Bangkok subsoil that dominated by soft clay has potential to amplify the ground motion. In general, the amplification factor of the investigated sites is about 1.072 to 2.254. Those values are consistent with the study of Warnitchai et al. (2000). According to the increasing of earthquake magnitude, the amplification result would decrease and some of sites occur de-amplification especially 7.5 M_W of earthquake.

3. According to spectral acceleration design of Thailand (TDS, 2019), the spectral acceleration from the result seismic ground response analysis is not exceeding for M_W 5 and M_W 6.2 of earthquake but it is exceeding for M_W 7.5 of earthquake. This indicates that the lower and medium magnitude of earthquake triggering by the Three Pagodas Fault would not result structural damage at the study area but for maximum credible earthquake which is M_W 7.5 would happen structural damage in Bangkok. Based on this case, the attention should be addressed to the medium high-rise building if the strong earthquake of M_W 7.5 from Three Pagodas Fault occurring of Bangkok. Generally, the results of this study warn the local engineer to consider earthquake as the main parameter on the structural design in Bangkok.

5.2. Recommendations

   This research is presented about local site investigation in Bangkok subsoil due to the earthquake. The potential earthquake is determined from the closest fault in Bangkok. Some improvement can be made regarding this research. The researcher made some recommendations that can be applied in the future:

1. Microtremor is only one tools as additional method to investigate the site and clarify the geological data and boring log. The limitation about deep basin of Bangkok area would be challenging. Therefore, another geophysical test like seismic reflectance with large amplitude of the excitation could be performed to measure Bangkok subsoil deeper.

2. The seismic hazard analysis in this research is considered the one of closest active fault in Bangkok. For further study, another potential earthquake from another active fault in Thailand and its surrounding area must be reviewed detailly.

3. This study is performed in limited local sites in Bangkok. In the future, the investigation can be spread at whole Bangkok area so the seismic hazard map in Bangkok can be updated with another method.

REFERENCES

Abrahamson, N. A., Silva, W. J., & Kamai, R. (2014). Summary of the ASK14 ground motion relation for active crustal regions. *Earthquake Spectra, 30*(3), 1025-1055.

Acerra, C., Aguacil, G., Anastasiadis, A., Atakan, K., Azzara, R., Bard, P.-Y., . . . Blarel, F. (2004). Guidelines for the implementation of the H/V spectral ratio technique on ambient vibrations measurements, processing and interpretation.

Ancheta, T. D., Darragh, R. B., Stewart, J. P., Seyhan, E., Silva, W. J., Chiou, B. S.-J., . . . Boore, D. M. (2014). NGA-West2 database. *Earthquake Spectra, 30*(3), 989-1005.

Baker, J. W. (2013). An introduction to probabilistic seismic hazard analysis. *White paper version, 2*(1), 79.

Boore, D. M. (2004). Estimating V s (30)(or NEHRP site classes) from shallow velocity models (depths< 30 m). *Bulletin of the Seismological Society of America, 94*(2), 591-597.

DMR. (2006). Active Fault Maps In Thailand. *Department of Mineral Resources, Thailand*.

García-Jerez, A., Piña-Flores, J., Sánchez-Sesma, F. J., Luzón, F., & Perton, M. (2016). A computer code for forward calculation and inversion of the H/V spectral ratio under the diffuse field assumption. *Computers & Geosciences, 97*, 67-78.

Gregor, N., Abrahamson, N. A., Atkinson, G. M., Boore, D. M., Bozorgnia, Y., Campbell, K. W., . . . Seyhan, E. (2014). Comparison of NGA-West2 GMPEs. *Earthquake Spectra, 30*(3), 1179-1197.

Hashash, Y., Phillips, C., & Groholski, D. R. (2010). Recent advances in non-linear site response analysis.

Hashash, Y. M. (2015). DEEPSOIL 6.1. User Manual. *Department of Civil and Environmental Engineering University of Illinois at Urbana-Champaign*.

Hashash, Y. M., & Park, D. (2001). Non-linear one-dimensional seismic ground motion propagation in the Mississippi embayment. *Engineering Geology, 62*(1-3), 185-206.

Horpibulsuk, S., Shibuya, S., Fuenkajorn, K., & Katkan, W. (2007). Assessment of engineering properties of Bangkok clay. *Canadian Geotechnical Journal, 44*(2), 173-187.

Imai, T. (1982). *Correlation of N-value with S-wave velocity and shear modulus.* Paper presented at the Proceedings of the 2nd European Symposium of Penetration Testing, Amsterdam, 1982.

Kiyono, J., Ono, Y., Sato, A., Noguchi, T., & Putra, R. R. (2011). Estimation of subsurface structure based on Microtremor observations at Padang, Indonesia. *ASEAN Engineering Journal, 1*(3), 66-81.

Kramer, S. L. (1996). Geotechnical earthquake engineering. in prentice–Hall international series in civil engineering and engineering mechanics. *Prentice-Hall, New Jersey.*

Kyaw, Z. L., Pramumijoyo, S., Husein, S., Faisal Fathani, T., Kiyono, J., & Rahmat Putra, R. (2014). Estimation of Subsurface Soil Layers using H/V Spectrum of Densely Measured Microtremor Observations (Case Study: Yogyakarta City, Central Java-Indonesia). *International Journal of Sustainable Future for Human Security, 2*(1), 13-20. doi:10.24910/jsustain/2.1/1320

Likitlersuang, S., & Kyaw, K. (2010). A study of shear wave velocity correlations of Bangkok subsoil. *Obras y proyectos, 7*, 27-33.

Mase, L. Z., Likitlersuang, S., Tobita, T., Chaiprakaikeow, S., & Soralump, S. (2018). Local Site Investigation of Liquefied Soils Caused by Earthquake in Northern Thailand. *Journal of earthquake engineering*, 1-24.

Matasovic, N. (1993). Seismic Response of Composite Horizontally-Layered Soil Deposits. *Ph.D. Thesis*(Los Angeles, California).

Miller, R. D., Xia, J., Park, C. B., Ivanov, J., & Williams, E. (1999). Using MASW to map bedrock in Olathe, Kansas. In *SEG Technical Program Expanded Abstracts 1999* (pp. 433-436): Society of Exploration Geophysicists.

Naito, S., Azuma, H., Senna, S., Yoshizawa, M., Nakamura, H., Hao, K. X., . . . Yoshida, M. (2013). Development and testing of a mobile application for recording and analyzing seismic data. *Journal of Disaster Research, 8*(5).

Nakamura, Y. (2000). *Clear identification of fundamental idea of Nakamura's technique and its applications.* Paper presented at the Proceedings of the 12th world conference on earthquake engineering.

Ornthammarath, T. (2013). A note on the strong ground motion recorded during the Mw 6.8 earthquake in Myanmar on 24 March 2011. *Bulletin of Earthquake Engineering, 11*(1), 241-254.

Ornthammarath, T., & Warnitchai, P. (2016). 5 May 2014 MW 6.1 Mae Lao (Northern Thailand) Earthquake: Interpretations of Recorded Ground Motion and Structural Damage. *Earthquake Spectra, 32*(2), 1209-1238.

Palasri, C., & Ruangrassamee, A. (2010). Probabilistic seismic hazard maps of Thailand. *Journal of Earthquake and Tsunami, 4*(04), 369-386.

Park, D., & Hashash, Y. (2004a). Estimation of non-linear seismic site effects for deep deposits of the Mississippi embayment. *MAE Center Report 04-06*.

Park, D., & Hashash, Y. M. (2004b). Soil damping formulation in nonlinear time domain site response analysis. *Journal of earthquake engineering, 8*(02), 249-274.

PEER. (2011). PEER ground motion database. In: Univ. of California Berkeley, CA.

Phillips, C., & Hashash, Y. M. (2009). Damping formulation for nonlinear 1D site response analyses. *Soil Dynamics and Earthquake Engineering, 29*(7), 1143-1158.

Plengsiri, P. (2018). *Site Response Analysis of Bangkok considering Variation of Shear Wave Velocity.* Chulalongkorn University, Department of Civil Engineering,

Poovarodom, N., & Jirasakjamroonsri, A. (2014). *Evaluation of seismic site effects for Bangkok deep basin.* Paper presented at the Proceedings of the Second European Conference on Earthquake Engineering and Seismology, Istanbul, Turkey.

Poovarodom, N., & Jirasakjamroonsri, A. (2016). Seismic Site Effects of Soil Amplifications in Bangkok. *Science & Technology Asia, 21*(3), 59-69.

Poovarodom, N., & Plalinyot, N. (2015). Evaluation of Site Effects in the Greater Bangkok by Microtremor Observations. *WCEE 2015*.

Pruiksma, J. (2016). Nonlinear and Equivalent Linear Site response analysis for the Groningen area. In: TNO report.

Shibuya, S., Tamrakar, S., & Manakul, W. (2003). Geotechnical hazards in Bangkok—present and future. *Lowland Technology International, 5*(1), 1-13.

Sinsakul, S. (2000). Late quaternary geology of the lower central plain, Thailand. *Journal of Asian Earth Sciences, 18*(4), 415-426.

Souriau, A., Chaljub, E., Cornou, C., Margerin, L., Calvet, M., Maury, J., . . . Péquegnat, C. (2011). Multimethod characterization of the French-Pyrenean valley of Bagnères-de-Bigorre for seismic-hazard evaluation: observations and models. *Bulletin of the Seismological Society of America, 101*(4), 1912-1937.

Tatham, R. H. (1982). V p/V s and lithology. *Geophysics, 47*(3), 336-344.

TDS. (2019). Building Design Standard for Earthquake Resistance. Department of Public Works and Town-Country Planning, Ministry of Interior, Thailand (in Thai).

TMD. (2015). Earthquake Data of March 24, 2011 Earthquake. *Thai Meteorogical Department*.

USBSS. (1991). NEHRP recommended provisions for the development of seismic regulations for new buildings: Part 2: Commentary. In *Earthquake Hazard Reductions Series* (Vol. 65): US Federal Emergency Management Agency (FEMA).

USGS. (2011). https://earthquake.usgs.gov/earthquakes/shakemap/global/shake/c0002aes/. *United States Geological Survey, 14/08/2018*.

USGS. (2014). https://earthquake.usgs.gov/product/shakemap/usb000qack/us/1399289290694/download/intensity.jpg. *United States Geological Survey, 14/08/2018*

Vucetic, M., & Dobry, R. (1991). Effect of soil plasticity on cyclic response. *Journal of Geotechnical Engineering, 117*(1), 89-107.

Warnitchai, P., Sangarayakul, C., & Ashford, S. A. (2000). *Seismic hazard in Bangkok due to long-distance earthquakes.* Paper presented at the Proc. 12th World Conference on Earthquake Engineering, Auckland, New Zealand, Paper.

APPENDICES

Appendix 1 Soil profile at CU site

Soil type	USCS	Depth (m)	Thickness (m)	(kN/m2)	s_u (t/sq.m)	SPT-N (blows/ft)	Vs (m/s)	Source
Clay, trace fine sand	CH	12	12	16.1	1.3		77.81	Boring Log
Silty clay, trace fine sand	CH	14.5	2.5	16.5	5		147.55	Boring Log
Silty clay, trace fine sand	CH	20.5	6	19.7		20	248.48	Boring Log
Silty clay, trace fine sand	CH	29.5	9	20.1		36	280	Boring Log
Fine sand and fine to medium sand	SM-SP	37	7.5	19.7		25	266.51	Boring Log
Silty clay, trace fine sand	CH	63	26	20.1		55	348.99	Boring Log
Fine sandy clay	CL	67	4	21.9		92	401.23	Boring Log
Clayey fine sand	SC	71	4	21.9		88	280	Boring Log
Silty clay, trace fine sand	CH	75	4	21		59	348.99	Boring Log
Clayey fine sand	SC	80	5	19.5		86	392.82	Boring Log
Fine to medium sand and clayey sand	SM-SP	100	20	19.5		50	331.32	Boring Log
Sand	SC	160	60	20			395.35	Geological Profile
Clay	CL	170	10	20			406.075	Geological Profile
Sand	SC	230	60	20			470.425	Geological Profile
Clay	CL	240	10	20			481.15	Geological Profile
Sand	SC	300	60	20			545.5	Geological Profile
Sand	SC	350	50	20			599.125	Geological Profile
Sand	SC	425	75	20			679.563	Geological Profile
Sand	SC	500	75	20			760	Geological Profile

Appendix 2 Soil profile at KU site

Soil type	USCS	Depth (m)	Thickness (m)	(kN/m2)	s_u (t/sq.m)	SPT-N (blows/ft)	Vs (m/s)	Source
Silty clay trace fine sand	CH	4	4	18	3.23		119.9	Boring Log
Clay, trace fine sand	CH	13	9	15.7	5.38		152.78	Boring Log
Silty clay, trace fine sand	CH	20	7	19.2		25	266.51	Boring Log
Silty fine sand	SM	25	5	19.2		50	331.32	Boring Log
Clay	CL	55	30				353.824	Geological Profile
Clay	CL	80	25				376.644	Geological Profile
Sand	SC	100	20				394.9	Geological Profile
Sand	SC	160	60	20			449.668	Geological Profile
Clay	CL	170	10	20			458.796	Geological Profile
Sand	SC	230	60	20			513.564	Geological Profile
Clay	CL	240	10	20			522.692	Geological Profile
Sand	SC	300	60	20			577.46	Geological Profile
Sand	SC	350	50	20			623.1	Geological Profile
Sand	SC	425	75	20			691.56	Geological Profile
Sand	SC	500	75	20			760.02	Geological Profile

Appendix 3 Soil profile at AIT site

| Soil type	USCS	Depth (m)	Thickness (m)	(kN/m2)	s_u (t/sq.m)	SPT-N (blows/ft)	Vs (m/s)	Source
Silty clay	CH	9	9	18	2.4		104.12	Boring Log
Silty clay	CL	17	8	18		17.8	239.55	Boring Log
Silty sand	SM	23	6	18		71.5	370.7	Boring Log
Silty clay	CL	27	4	18		22.4	257.48	Boring Log
Clayey fine sand	SC	30	3	18		17	236.11	Boring Log
Dense sand	SM	46	16	19		50	331.32	Boring Log
Clay	CL	80	34	20			363.426	Boring Log
Sand	SC	100	20	20			382.31	Geological Profile
Sand	SC	160	60	20			438.962	Geological Profile
Clay	CL	170	10	20			448.404	Geological Profile
Sand	SC	230	60	20			505.056	Geological Profile
Clay	CL	240	10	20			514.498	Geological Profile
Sand	SC	300	60	20			571.15	Geological Profile
Sand	SC	350	50	20			618.36	Geological Profile
Sand	SC	425	75	20			689.175	Geological Profile
Sand	SC	500	75	20			759.99	Geological Profile

Appendix 4 Soil profile at BKK site

Soil type	USCS	Depth (m)	Thickness (m)	(kN/m2)	s_u (t/sq.m)	SPT-N (blows/ft)	Vs (m/s)	Source
soft silty clay, trace of shell bits	CH	15	15	18	2.7		110.11	Boring Log
stiff silty clay	CH	21	6	18		20.4	250.03	Boring Log
Dense clayey sand	SM/SC	27	6	18		64.7	359.24	Boring Log
Hard silty clay, gravel	CH	36	9	19		26.8	272.71	Boring Log
Dense sand	SM/ML	39	3	19		68.1	365.73	Boring Log
Clay	CL	55	16	20			378.704	Geological Profile
Clay	CL	80	25	20			400.124	Geological Profile
Sand	SC	100	20	20			417.26	Geological Profile
Sand	SC	160	60	20			468.668	Geological Profile
Clay	CL	170	10	20			477.236	Geological Profile
Sand	SC	230	60	20			528.644	Geological Profile
Clay	CL	240	10	20			537.212	Geological Profile
Sand	SC	300	60	20			588.62	Geological Profile
Sand	SC	350	50	20			631.46	Geological Profile
Sand	SC	425	75	20			695.72	Geological Profile
Sand	SC	500	75	20			759.98	Geological Profile

Appendix 4 Spectral Acceleration for Design in Bangkok and its surrounding area
(TDS, 2019)

ตารางที่ 1.4-5 ค่าความเร่งตอบสนองเชิงสเปกตรัมสำหรับการออกแบบ ด้วยวิธีแรงสถิตเทียบเท่าสำหรับ
พื้นที่ในโซนต่าง ๆ (อัตราส่วนความหน่วง 5.0%) ของพื้นที่ในแอ่งกรุงเทพ

S_a โซน	S_a (0.01s)	S_{DS} (0.2 s)	S_a (0.5 s)	S_{D1} (1.0s)	S_a (2.0 s)	S_a (3.0 s)	S_a (4.0 s)	S_a (5.0 s)	S_a (6.0 s)
1	0.360	0.360	0.360	0.181	0.085	0.041	0.034	0.024	0.022
2	0.352	0.352	0.352	0.193	0.151	0.084	0.047	0.030	0.024
3	0.262	0.262	0.262	0.265	0.166	0.085	0.052	0.035	0.026
4	0.287	0.287	0.287	0.207	0.163	0.078	0.032	0.023	0.020
5	0.191	0.191	0.191	0.199	0.168	0.094	0.053	0.037	0.028
6	0.272	0.272	0.272	0.154	0.150	0.077	0.042	0.031	0.026
7	0.246	0.246	0.246	0.181	0.132	0.084	0.051	0.036	0.030
8	0.162	0.162	0.162	0.075	0.041	0.025	0.015	0.010	0.008
9	0.214	0.214	0.214	0.156	0.107	0.048	0.022	0.014	0.011
10	0.179	0.179	0.179	0.049	0.035	0.023	0.014	0.010	0.008
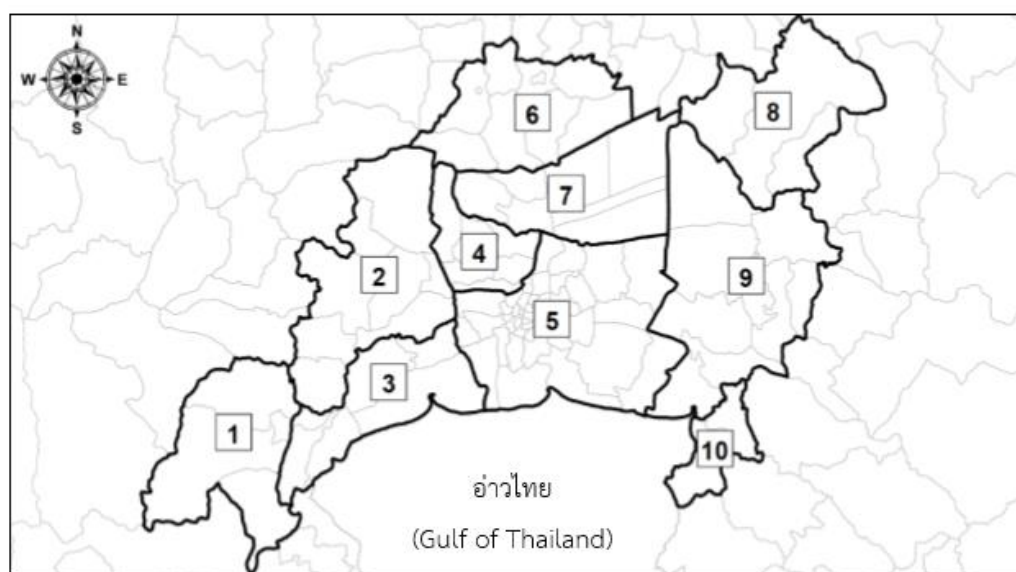
แผนที่แสดงการแบ่งโซนพื้นที่แอ่งกรุงเทพฯ เพื่อการออกแบบ อาคารต้านทานแผ่นดินไหว

VITA

NAME   Muhammad Fatih Qodri

DATE OF BIRTH   11 July 1993

PLACE OF BIRTH   Klaten, Central Java

INSTITUTIONS   UNIVERSITAS GADJAH MADA, Indonesia
ATTENDED

HOME ADDRESS   Piyungan Prambanan KM 1 Street, Piyungan, Srimartani,
                        Piyungan, Bantul, D.I. Yogyakarta

PUBLICATION   The 24th National Convention on Civil Engineering,
                        Thailand